

**UNIVERSIDADE DO VALE DO RIO DOS SINOS - UNISINOS
UNIDADE ACADÊMICA DE PESQUISA E PÓS-GRADUAÇÃO
PROGRAMA DE PÓS-GRADUAÇÃO EM GEOLOGIA
NÍVEL MESTRADO**

CARLA GIMENA PUIGDOMENECH NEGRE

**The relationship between Deltaic and Turbidite Succession at Cerro Bola (LR - Argentina)
and Vidal Ramos (SC - Brazil)**

SÃO LEOPOLDO

2014

Carla Gimena Puigdomenech Negre

**The relationship between Deltaic and Turbidite Succession at Cerro Bola (LR- Argentina)
and Vidal Ramos (SC- Brazil)**

Dissertação de Mestrado apresentada como parte das exigências para a obtenção do título de Mestre, pelo Programa de Pós-Graduação em Geologia da Universidade do Vale do Rio dos Sinos (UNISINOS).

Área de Concentração: Geologia Sedimentar

Linha de Pesquisa: Estratigrafia e Evolução de Bacias

Orientador: Prof. Dr. Ubiratan Ferrucio Faccini

Co-orientador: Prof. Dr. Benjamin C. Kneller

São Leopoldo

2014

N385r Negre, Carla Gimena Puigdomenech
 The relationship between Deltaic and Turbidite Succession at
 Cerro Bola (LR- Argentina) and Vidal Ramos (SC- Brazil) / Carla
 Gimena Puigdomenech Negre. – 2014.
 116 f. : il.

 Dissertação (mestrado) – Universidade do Vale do Rio dos Sinos,
 Programa de Pós-graduação em Geologia, São Leopoldo, RS, 2014.

 “Orientador: Prof. Dr. Ubiratan Ferrucio Faccini”

 1. Geologia. 2. Sedimentos (Geologia) - Cerro Bola (LR,
 Argentina) 3. Sedimentos (Geologia) - Vidal Ramos (SC) I. Título.

CDU 55

Catálogo na fonte:

Mariana Dornelles Vargas – CRB 10/2145

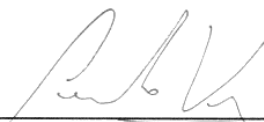
A dissertação de Mestrado

**“THE RELATIONSHIP BETWEEN DELTAIC AND TURBIDITE SUCCESSION AT CERRO BOLA (LR-
ARGENTINA) AND VIDAL RAMOS (SC-BRAZIL)”**


apresentada por **CARLA GIMENA PUIGDOMENECH NEGRE**

foi aceita e aprovada como atendimento parcial aos requisitos para a obtenção do grau de

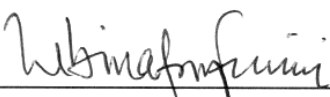
MESTRE EM GEOLOGIA pela seguinte banca examinadora:



Prof. Dr. Fernando Farias Vesely
Universidade Federal do Paraná



Prof. Dr. Ricardo da Cunha Lopes
Universidade do Vale do Rio dos Sinos



Prof. Dr. Ubiratan Ferrucio Faccini
Presidente da Banca Examinadora
Universidade do Vale do Rio dos Sinos

São Leopoldo, 20 de fevereiro de 2014.

INDEX

ACKNOWLEDGEMENTS	VII
ABSTRACT	VIII
1. INTRODUCTION	1
2. OBJECTIVE	3
3. METHODOLOGY	3
3.1 Cerro Bola (Paganzo Basin)	3
3.2 Vidal Ramos (Paraná Basin)	3
4. GEOLOGICAL SETTING	4
4.1 Gondwana Glaciation	4
4.2 Paganzo Basin	9
4.3 Paraná Basin	13
5. RESULTS	18
5.1 Cerro Bola	18
5.1.1 Log Description	21
5.1.2 Provenance Analysis	63
5.1.3 Depositional Model	69
5.2 Vidal Ramos	74
5.2.1 Log Description	76
5.2.2 TOC Analysis	87
5.2.3 Depositional Model	88
6 CONCLUSION	91
7 REFERENCES	93
8 ATTACH	104
8.1 Log Correlation- Cerro Bola	
8.2 Photointerpretation of Cerro Bola Outcrop	

FIGURES INDEX

Fig. 1: Location Map of Cerro Bola	2
Fig. 2: Location Map of Vidal Ramos	2
Fig. 3: Reconstruction of Gondwana glaciation	5
Fig. 4: Polar wander path for the Carboniferous and Permian relative to Gondwana	6
Fig. 5: Paleogeography and distribution of the Late Paleozoic South American basins	7
Fig. 6: Stratigraphy of the late Paleozoic basins in Southern South America	9
Fig. 7: Palaeogeography of Paganzo Basin	10
Fig. 8: Schematic evolution of Paganzo Basin	11
Fig. 9: Chronostratigraphy of the Paganzo and Groups	12
Fig. 10: Geological map of the Paraná Basin	13
Fig. 11: Stratigraphic column of Paraná Basin	14
Fig. 12: Geological map of Cerro Bola	20
Fig. 13: Upper Turbidites Stages (Log CB 1)	22
Fig. 14: Common features Stage IV (Log CB 1)	22
Fig. 15: Upper Turbidites, Stage V (Log CB 1)	23
Fig. 16: Contact between the Upper Turbidites and Fluviodeltaic 3. (Log CB 1)	23
Fig. 17: Units of the Fluviodeltaic 3 (Log CB 1)	24
Fig. 18: Characteristics of Unit 2 (Log CB 1)	25
Fig. 19: Principal characteristics of Unit 3 (Log CB 1)	26
Fig. 20: Unit 4 (Log CB 1)	27
Fig. 21: Green Unit (Log CB 1)	27
Fig. 22: Outcrop view of the log CB 2	28
Fig. 23: Stage IV (log CB 2)	29
Fig. 24: Stage V (log CB 2)	29
Fig. 25: Units of Fluviodeltaic 3 (log CB 2)	30

Fig. 26: Fluviodeltaic 3, Unit 1 (Log CB 2)	31
Fig. 27: Unit 2 (Log CB 2)	31
Fig. 28: Unit 3 (Log CB 2)	32
Fig. 29: Unit 4 (Log CB 2)	33
Fig. 30: Green Unit (Log CB 2)	33
Fig. 31: General view of outcrop of log CB 3	34
Fig. 32: Stage IV (log CB 3)	35
Fig. 33: Stage V (log CB 3)	35
Fig. 34: Unit 1 (log CB 3)	36
Fig. 35: Unit 2 (log CB 3)	37
Fig. 36: Unit 3 (log CB 3)	38
Fig. 37: Unit 4 (log CB 3)	38
Fig. 38: Green Unit (log CB 3)	39
Fig. 39: Stage IV (log CB 4)	40
Fig. 40: Stage V (log CB 4)	40
Fig. 41: Contact between Upper Turbidites and Fluviodeltaic 3 (log CB 4)	41
Fig. 42: Unit 1 (Log CB 4)	42
Fig. 43: Unit 2 (Log CB 4)	42
Fig. 44: Green Unit (Log CB 4)	43
Fig. 45: General view Log CB 5	44
Fig. 46: Stage V (Log CB 5)	44
Fig. 47: Contact between Upper Turbidites and Fluviodeltaic 3 (log CB 5)	45
Fig. 48: Unit 1 (Log CB 5)	45
Fig. 49: Unit 2 (Log CB 5)	46
Fig. 50: Unit 3 (Log CB 5)	47
Fig. 51: Green Unit (Log CB 5)	47

Fig. 52: Outcrop view of Log CB 6	48
Fig. 53: Stage IV (log CB 6)	49
Fig. 54: Stage V (log CB 6)	49
Fig. 55: Contact between Upper Turbidites and Fluviodeltaic 3 (log CB 6)	50
Fig. 56: Unit 1 (Log CB 6)	51
Fig. 57: Unit 2 (Log CB 6)	51
Fig. 58: Unit 3 (Log CB 6)	52
Fig. 59: Unit 4 (Log CB 6)	53
Fig. 60: Green Unit (Log CB 6)	53
Fig. 61: Stage IV (log CB 7)	54
Fig. 62: Stage V (log CB 7)	55
Fig. 63: Contact between Upper Turbidites and Fluviodeltaic 3 (log CB 7)	55
Fig. 64: Unit 1 (Log CB 7)	56
Fig. 65: Unit 2 (Log CB 7)	57
Fig. 66: Unit 3 (Log CB 7)	57
Fig. 67: Unit 4 (Log CB 7)	58
Fig. 68: Green Unit (Log CB 7)	59
Fig. 69: Stages IV (Log CB 8)	60
Fig. 70: Stages V (Log CB 8)	60
Fig. 71: Contact between Upper Turbidites and Fluviodeltaic 3 (log CB 8)	61
Fig. 72: Unit 2 (Log CB 8)	62
Fig. 73: Unit 4 (Log CB 8)	62
Fig. 74: Green Unit (Log CB 8)	63
Fig. 75: Sampling intervals	65
Fig. 76: QFL) and QmFLt diagrams	66
Fig 77: Provenance diagrams from Net & Limarino (2006)	67

Fig. 78: Thin sections photomicrographs of the samples analysed of Upper Turbidites	68
Fig. 79: Microphotography of the sandstones analysed at Log CB 1	68
Fig. 80: Microphotography of the sandstones analysed at Log CB	69
Fig. 81: Block diagram of sand-rich submarine fan	71
Fig. 82: Plan view of coalescing submarine fans regular curved	73
Fig. 83: Geological Map of Vidal Ramos	75
Fig. 83: Sedimentary log of Deltaic deposits (VR- 1)	78
Fig. 84: Facies Sd (VR- 1)	78
Fig. 85: Facies Fd (VR- 1)	78
Fig. 86: Facies Fd, Slump (VR- 1)	78
Fig. 87: Facies Sm (VR-1)	79
Fig. 88: Facies Sr (VR-1)	79
Fig. 89: Sedimentary log (VR-2)	81
Fig. 90: Facies Fl (VR-2)	81
Fig. 91: Facies Sg (VR-2)	81
Fig. 92: Facies Sm (VR-2)	82
Fig. 89: Facies Sd (VR-2)	82
Fig. 94: Facies Sr (VR-2)	82
Fig. 95: Log VR-3	84
Fig. 96: Sedimentary facies (VR-3)	84
Fig. 97: Rippled sandstones (VR-3)	84
Fig. 98: Log VR-4	86
Fig. 99: Facies Fd (VR-4)	86
Fig. 100: Facies Sl (VR-4)	86
Fig. 101: Facies Sr (VR-4)	87
Fig. 102: Stratigraphy location of the sample analysed for TOC	88

Fig. 103: Log correlation

89

Fig. 104: Schematic model of the deposition of the Deltaic Unit

90

ACKNOWLEDGEMENTS

Thanks to BG Brazil for financed this research and ANP for approval the collaborative Research Project: “Late Paleozoic De-glacial Deposits in the Paraná Basin (Brazil) and their analogue in the Paganzo Basin (Argentina): Impacts on Reservoir Prediction”.

Many thanks to the staff of UNISINOS and the people involve in this project for their support during these two years, especially to my field panthers Bruno, Victoria, Claus, Matehus, Fabiano, João, Carolina, Guilherme and Luke.

To my supervisors Prof. Ben Kneller and PhD. Bira Faccini thanks for your critical review and advice.

I want to thanks to Victoria Valdez for presented me this opportunity; I learned a lot of about geology and life.

All my thanks go to Bruno Carvalho, for his affection, support and friendship especially during tough moments.

To my family thanks for be my cornerstone, for always believe in me. I love you.

ABSTRACT

The transport mechanism and deposition of sediments in deep water environments and their relationship with deltaic systems have captured the attention of sedimentologists during the last decades due its importance as hydrocarbon reservoir. This work presents a comparative study of this kind of related deposits in two distinct areas with significant records of the Late Paleozoic glaciation of western Gondwana: (i) the well exposed deposits of Cerro Bola that belong to the Paganzo Group and (ii) the not so well exposed (but with potential economic interest) deposits of Rio do Sul Formation (Itararé Group) in Vidal Ramos, Paraná basin. Cerro Bola records 1000 m of sediment corresponding to five glacial/deglacial cycles; this work focuses on the relationship between the upper part of Cycle 3 and 4, corresponding to Upper Turbidites and Fluviodeltaic 3, respectively. Based on the sedimentary features here presented, the Fluviodeltaic 3 is re-interpreted as a sand-rich submarine fan in which the high sedimentation rates are interpreted as related to tectonic activity. The area of Vidal Ramos exposes ~400 m of the Itararé Group. This research focuses on the upper part of Rio do Sul Formation, which records deltaic sediments dominated by gravity flows in the lower part. The upper part is characterized by a sandy delta front progradation associated with an increased sediment supply. The data presented in this work shows that the delta front deposits under conditions of slope instability generated gravity flows which are deposited as turbidites in the distal delta front/prodelta and is related to the effects of deglacial conditions and phases of increased sediment supply to deep water environments. The results indicate that the two areas are not directly comparable due to distinct depositional processes and paleogeographic configurations. The thick succession of sandstones in Cerro Bola is interpreted as turbidite fan controlled by tectonic activities in a deep basin context, while in Vidal Ramos the identified progradational sandy delta front is produced by a phase of increased sediment supply related to deglacial processes.

1. INTRODUCTION

In last decades the study of turbidite deposits has grown due their importance as hydrocarbon reservoirs. However, the relationship between this kind of deposits and the deltaic environment, which indirectly or directly affects deposition in deep water settings, is a recent topic of debate among sedimentologists and remains poorly understood. Due to this, the present research tries to give some light to this issue with the objective of understanding the link between these two depositional settings and the processes involved in the transport of sediment basinward.

For this reason it was chosen the well exposed outcrops of Cerro Bola, located at 30 km to southeast of Villa Union (La Rioja-Argentina) (Fig. 1), that present approximately 300m of turbidites overlaid by 180 m of deltaic deposits along 8 km of the Paganzo Group, and the compared the results obtained with the not so well exposed (but with potentially economic interesting) deposits of Itararé Group in Vidal Ramos (Santa Catarina-Brazil) (Fig. 2). Both areas are part of the Late Palaeozoic basins, Paganzo and Paraná Basin respectively, affected by the Gondwana glaciation. The idea of comparing these two localities is to try to understand the behaviour of deltaic and turbidite deposits under the equivalent environmental conditions, since the deposits in both areas are related to deglaciation cycles.

This work is part of the collaborative Research Project: "Late Paleozoic De-glacial Deposits in the Paraná Basin (Brazil) and their analogue in the Paganzo Basin (Argentina): Impacts on Reservoir Prediction", funded by BG Group under Brazilian Government Law 999.1/2000.



Fig. 1: Location map of the Cerro Bola outcrops. Note the sparse vegetation in the area favouring a good rock exposure.

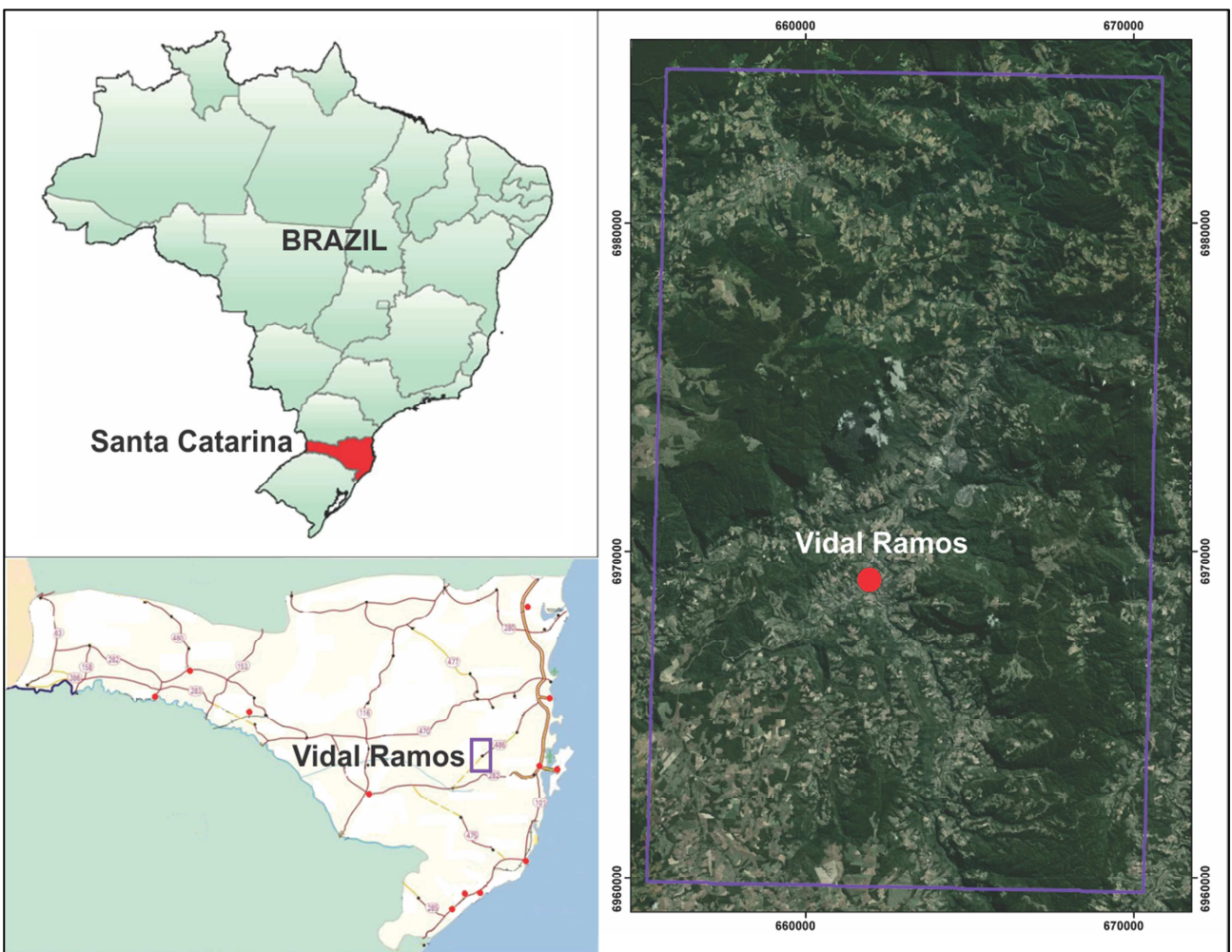


Fig. 2: Location map of Vidal Ramos. Note that the exposure is almost none due the abundant vegetation.

2. OBJECTIVE

The aim of this research is to establish the stratigraphic relations between deltaic successions and the underlying (and laterally equivalent?) pro-deltaic turbidite sequences in Cerro Bola (Paganzo Basin) and compare the results with data from Vidal Ramos of in Paraná Basin.

3. METHODOLOGY

The areas of study, Cerro Bola and Vidal Ramos, present different characteristics in terms of outcrop exposures. The first corresponds to 11 km² of well exposed Carboniferous rocks in contrast to approximately 336 km² almost entirely covered by vegetation. For that reason the methodology for each area is described separately.

3.1 Cerro Bola (Paganzo Basin)

- Bibliographic review.
- Photointerpretation of aerial photomosaics to see the geometry of the deposits.
- Detailed logs at scale 1/100 to record internal sedimentary structures and bed thickness.
- Palaeocurrent analysis of the sedimentary structures using the software Georient.
- Petrographic samples taken at the different intervals to make provenance analysis using thin sections.
- Point counting of the samples (50 points per sample).
- Porosity analysis of the thin sections to see reservoir characteristics of the deposit.
- Creation of an ArcGis project to storage all the information (1/20,000).

3.2 Vidal Ramos (Paraná Basin)

- Bibliographic review.
- Mapping of the area using Trimble GPS to record and describe all the outcrops and photointerpretation of high resolution IKONOS images to recognize regional structures.
- Sedimentary logs at scale 1/100 in outcrops that present at least 15 m of continuously exposed rock to record sedimentary structures and bed thickness.
- Palaeocurrent analysis of the sedimentary structures using the software Georient.

- TOC analysis of black shale intervals to analyse the hydrocarbon potential of the deposit.
- Creation of a geological map (1/10,000) in an ArcGis project and printed in scale 1/60,000.

4. GEOLOGICAL SETTING

4.1 Gondwana Glaciation

During the Late Paleozoic Gondwana was affected by multiple glaciation that waxed and waned across the supercontinent, known as "The Late Paleozoic Ice Age" (LPIA) (Isbell et al., 2011). This period represents the longest glacial interval recorded during the Phanerozoic (Frakes et al., 1992) beginning in the Viséan (Mississippian) to the Capitanian/earliest Wuchiapingian (Middle-earliest Late Permian) and lasted for approximately 72 Myr. The LPIA was characterized by an extensive south polar landmass; low atmospheric partial pressure of CO₂ (pCO₂); and multiple, possibly bipolar, glacial events (Isbell et al., 2003; Fielding et al., 2008a).

These conditions led to the formation of glacial deposits in much of South America, South Africa, India, Antarctica, Australia and several basins of the Perigondwanic region (López Gamundí et al., 1992; López Gamundí, 1997; Visser, 1997; Isbell et al., 2003 a,b, 2008b; Rocha-Campos et al., 2008).

Recent works have identified evidence of numerous small ice centres that advanced and retreated diachronously across Gondwana through multiple glacial intervals of 1–8 million years in duration, alternating with non-glacial periods of approximately equal duration (Fig. 3; Crowell and Frakes, 1970; Caputo and Crowell, 1985; Dickins, 1997; López-Gamundí, 1997; Isbell et al., 2003; Fielding et al., 2008a, 2008c, 2008d; Gulbranson et al., 2010).



Fig. 3: Reconstruction of the maximum glaciation during the LPIA. (A) Reconstruction of Gondwana during maximum glaciation during the Gzhelian to early Sakmarian (Pennsylvanian–Early Permian) based on recent data and ice flow directions. Ice flow directions are from Frakes et al. (1975), Hand (1993), Veevers and Tewari (1995), López-Gamundí (1997), Visser (1997a, 1997b), Visser et al. (1997), Fielding et al. (2008a), Isbell et al. (2008c), Mory et al. (2008), Rocha-Campos et al. (2008) and Isbell (2010). (B) Location map for selected Gondwana basins and highlands for the Carboniferous and Permian. Modified from Isbell et al. (2011)

The LPIA began in western South America during the Viséan (Caputo et al., 2008; Pérez Loinaze et al., 2010) and concluded in eastern Australia during the Middle to earliest Late Permian, Capitanian/earliest Wuchiapingian (Fielding et al., 2008a, 2008c, 2008d). The reason of the glaciation's diachronism has been attributed to the drift of Gondwana across the South Pole during the Late Paleozoic (Fig. 4). Although this pole path roughly follows the general trend of glacier occurrence (i.e. older glaciation in South America, younger in Australia), it cannot explain by itself the patterns of glaciation and deglaciation in Gondwana. If the paleolatitudinal position of the

different parts of Gondwana is taken as the only criterion to explain the occurrence and expansion of glacial centres, it is not clear what the origin of the climatic shift from glacial to non-glacial stages was in South America, as the paleolatitudinal position in both climatic stages was essentially the same (Limarino et al., 2013). Therefore, it is clear that the glaciation that affected Gondwana requires additional factors than paleolatitude, to explain fluctuating cooling conditions that produced periods of expansion and contraction of the ice masses (Isbell et al., 2003a; Fielding et al., 2008b; among others). Recently, Isbell et al. (2012) discussed how the balance between the ELA (equilibrium-line altitude) position and the land surface could be influenced by tectonism, promoting or suppressing the formation and nucleation of glaciers.

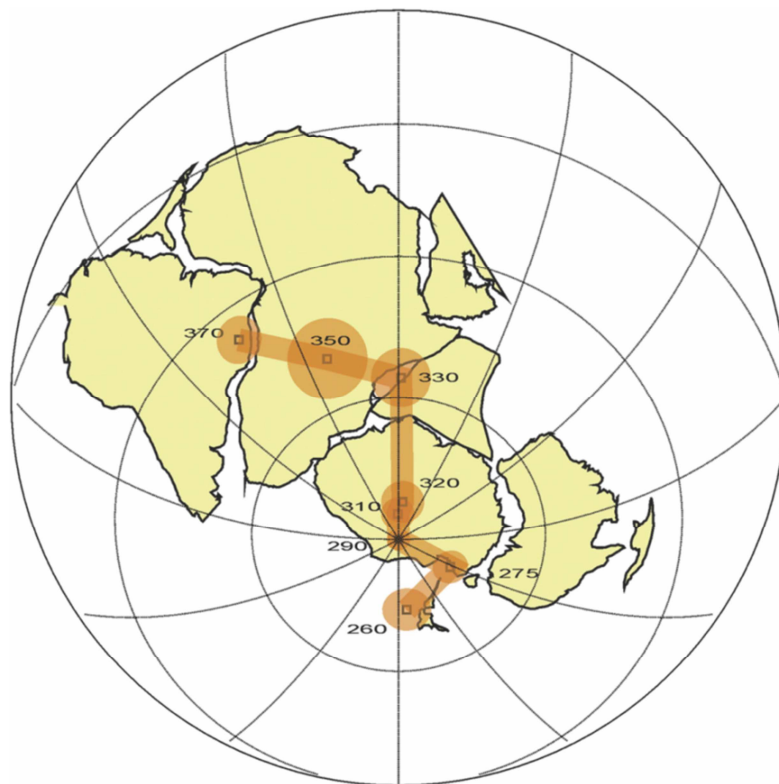


Fig. 4: Polar wander path for the Carboniferous and Permian relative to Gondwana based on the Gondwana paleomagnetic poles selected by Geuna et al. (2010). Schmidt projection, south hemisphere (Limarino et al., 2013)

The LPIA is recorded in several southern South America basins which can be grouped into three major types in terms of stratigraphy, tectonism and magmatism: 1. Eastern intraplate basins, 2. Western retroarc basins and 3. Western arc-related basins (Limarino and Spalletti, 2006).

The eastern intraplate basins were separated from western basins by a large upland area known as the Pampean Arch, composed of crystalline late Precambrian and early Paleozoic rocks. To the

west of the Pampean Arch, a discontinuous orogenic belt, known as the Protoprecordillera, was formed by the accretion of Chilenia to South America during the Late Devonian–early Carboniferous. The Protoprecordillera acted as a barrier that separated a large foreland area (Paganzo Basin) from a more tectonically and magmatically active region located in the present day Andean Cordillera (Río Blanco and Calingasta–Uspallata basins) (Limarino et al., 2013) (Fig. 5).

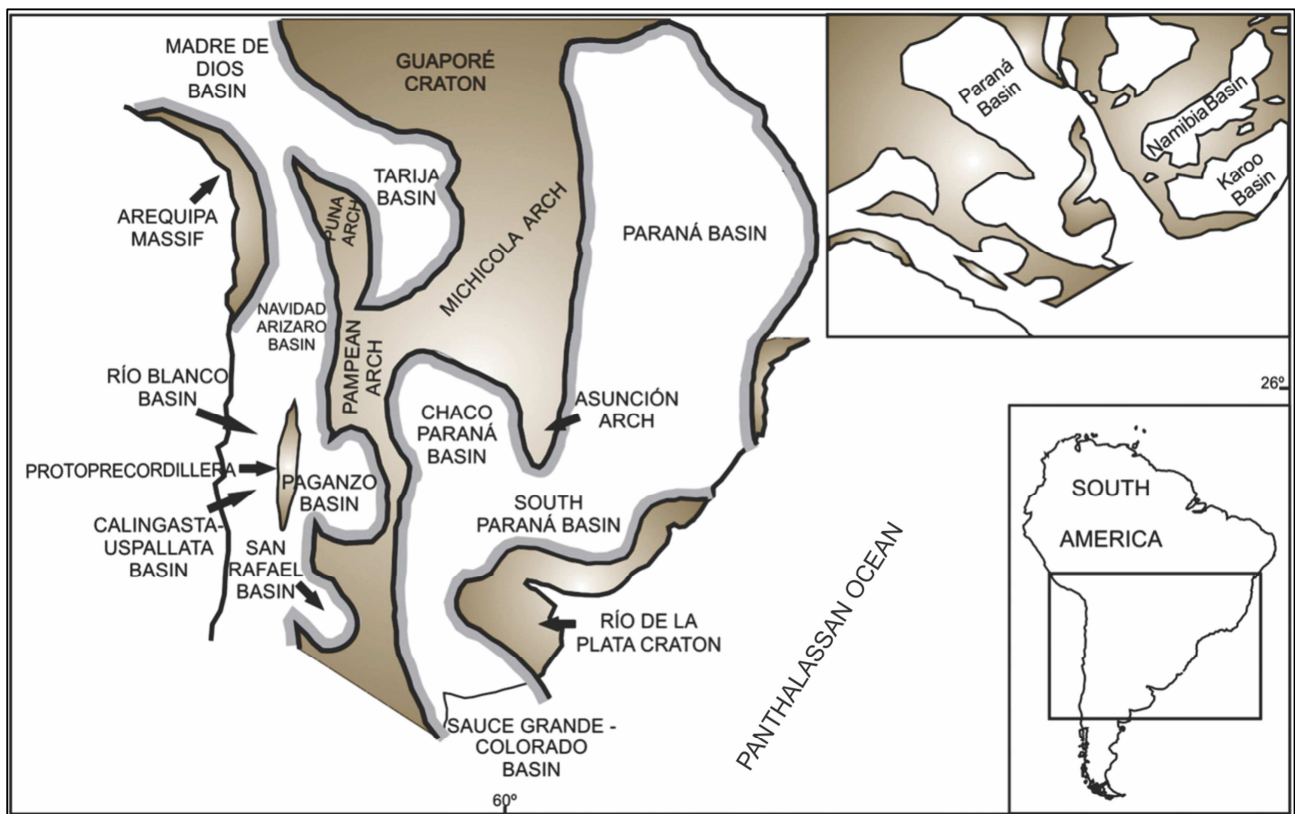


Fig. 5: Paleogeography and distribution of the Late Paleozoic South American basins. Shaded areas indicate positive regions (modified from Limarino et al., 2013).

The intraplate basins in southern South America, comprising the Paraná, the Chaco–Paraná, and the Sauce Grande–Colorado basins, began to subside during the Early Pennsylvanian. The arc-related basins correspond to Navidad–Arizaro, Río Blanco, Calingasta–Uspallata, San Rafael and Madre de Dios basins (Fig. 5). These depositional areas suffered deformation in the high late Paleozoic, extensive magmatism and local metamorphism of Carboniferous sediments (Sempere, 1996; Limarino and Spalletti, 2006). On the other hand, the retroarc basins (including the Tarija, Paganzo and eastern San Rafael basins, Fig. 5) experienced little deformation during the late Paleozoic, less magmatic activity, and are characterized by a complete lack of metamorphism of the Carboniferous–Permian successions.

Limarino et al. (2013), based on lithologic indicators, biostratigraphic information, and chronostratigraphic data, recognized four major types of paleoclimatic stages in these basins: 1. glacial (late Viséan–early Bashkirian), 2. terminal glacial (Bashkirian–earliest Cisuralian) 3. postglacial (Cisuralian–early Guadalupian), and 4. semiarid–arid (late Guadalupian–Lopingian)(Fig.6).

According with Limarino et al. (2013) the glacial stage began in the late Viséan and continued until the latest Serpukhovian or early Bashkirian in almost all of the basins in southern South America. During the Bashkirian–earliest Cisuralian (terminal glacial stage), glacial deposits disappeared almost completely in the western retroarc basins (e.g., Paganzo Basin) but glaciation persisted in the eastern basins (e.g., Paraná and Sauce Grande Basins). A gradual climatic amelioration (postglacial stage) began to occur during the earliest Permian when glacial deposits almost disappeared across all of South America. During this interval, glacial diamictites were replaced by thick coal beds in the Paraná Basin while north–south climatic belts began to be delineated in the western basins, which were likely controlled by the distribution of mountain belts along the Panthalassan Margin of South America. Towards the late Permian, climatic belts became less evident and semiarid or arid conditions dominated in the southern South America basins. Eolian dunes, playa lake deposits, and mixed eolian–fluvial sequences occur in the Paraná Basin and in the western retroarc basins. Volcanism and volcanoclastic sedimentation dominated along the western margin of South America at that time (Fig. 6; Limarino et al., 2013).

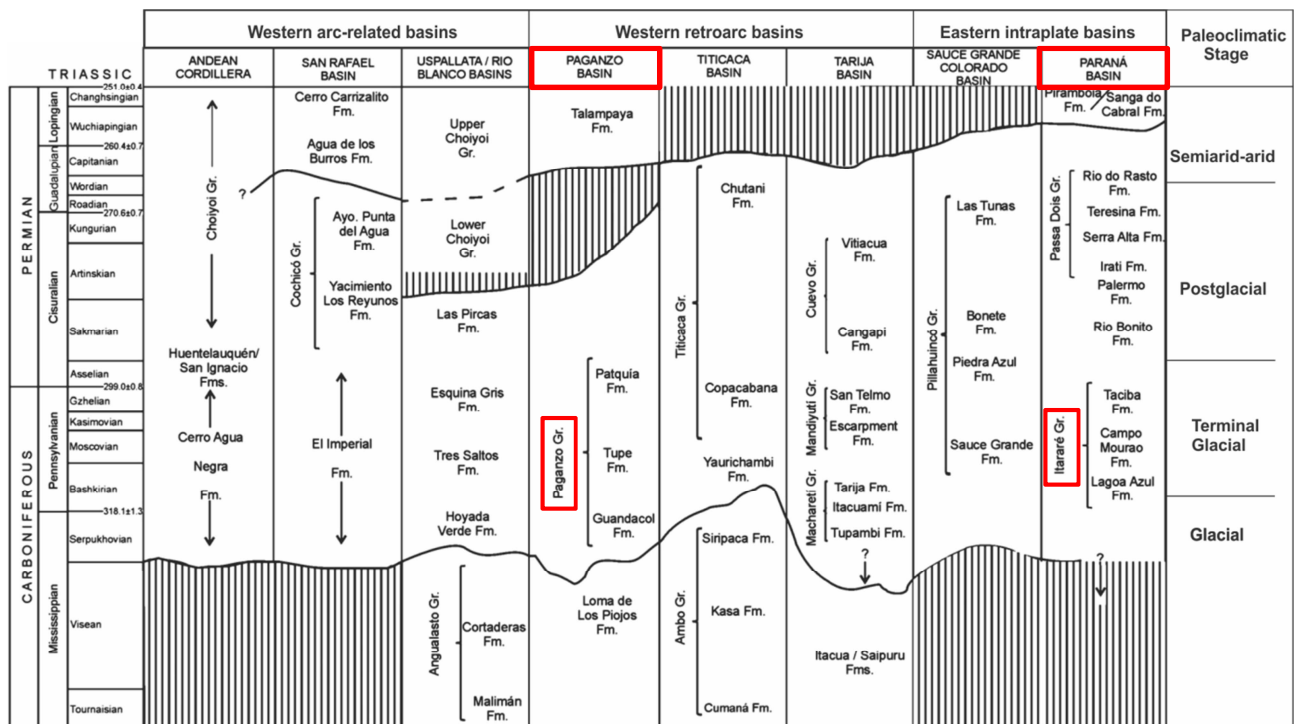


Fig. 6: Stratigraphy of the late Paleozoic basins in Southern South America. The basins studied in this research are indicated by red boxes. Modified from Limarino et al., 2013.

4.2 Paganzo Basin

The Upper Carboniferous-Upper Permian Paganzo basin covers ~ 150,000 km² of western Argentina (Fig. 7), and hosts a sedimentary succession up to 3,000 m thick (Buatois et al., 2010). The tectonic setting is controversial, defined as a strike slip basin by Fernández Seveso & Tankard (1995), and as a foreland basin by Ramos (1988) related to subduction of the Pacific plate beneath the western margin of Gondwana, which probably evolved into a rift system by the Permian.

The Protoprecordillera was uplifted during the Late Devonian-Early Mississippian and constituted a north-south-trending topographic high that separates mostly marine deposits of the Calingasta-Uspallata and Rio Blanco Basins on the west from mostly continental deposits of Paganzo Basin on the east. During the Early Pennsylvanian, the Protoprecordillera became unstable and began to collapse until the range lost its topographic significance at the beginning of the Permian (Fig. 8) (Net & Limarino, 2006; Limarino et al., 2006). The Paganzo Basin was limited to the east and south by the Pampean and Pie de Palo topographic highs, whereas the Puna high represents its northern boundary.

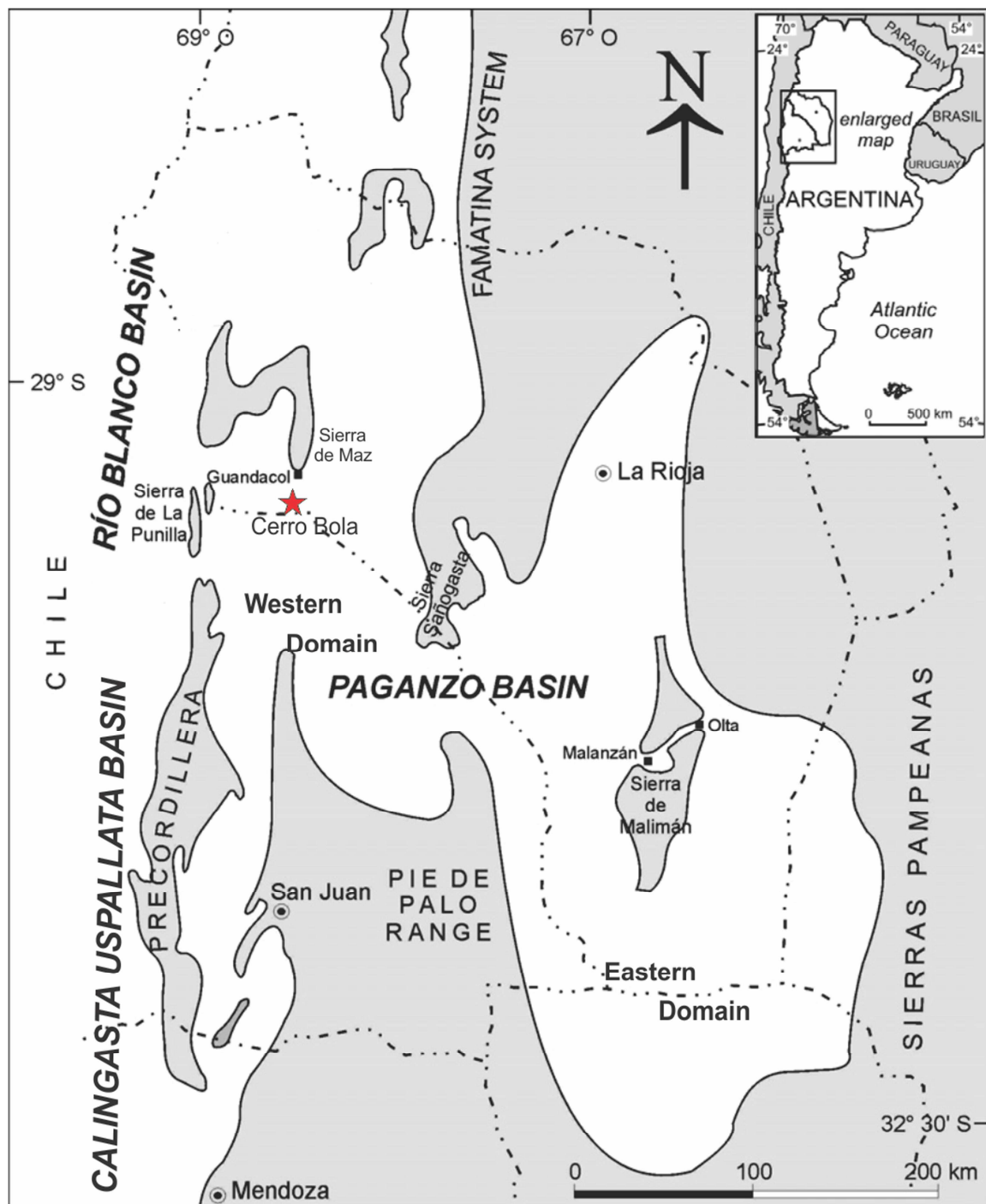


Fig. 7: Paleogeography and main morphostructural elements of the Paganzo Basin in north-western Argentina. The study area is shown with a red star (modified from Limarino et al., 2006; Net & Limarino, 2006)

Sedimentation in the Paganzo Basin occurred in sub-basins separated by internal basement highs. Overall, two major areas can be distinguished within the basin: an eastern zone dominated by continental environments, and a western one with increase marine influence (Fig. 7) (Limarino et al., 2002).

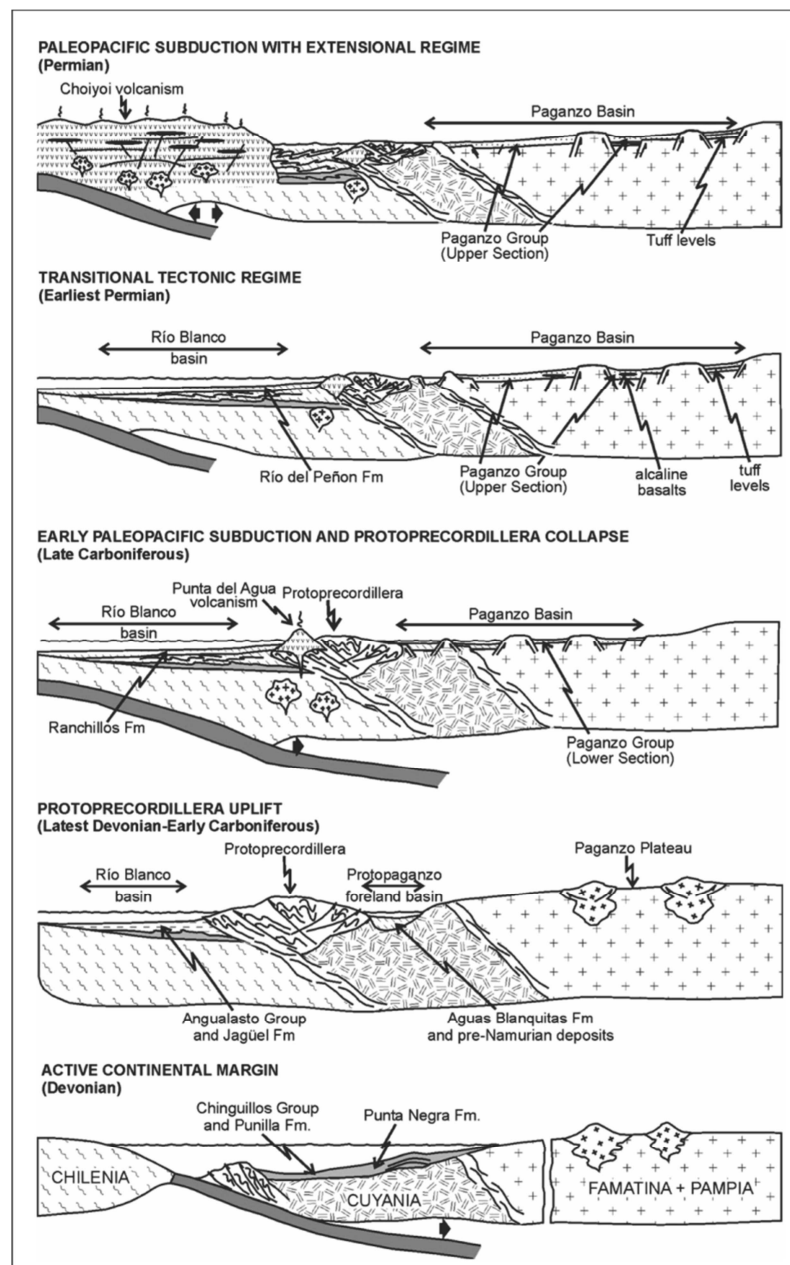


Fig. 8: Schematic stratigraphic cross-sections at 29° 31' S latitude showing the evolution of the Paganzo Basin (Limarino et al., 2006)

The strata of the Paganzo Basin constitute the upper Paleozoic Paganzo Group (Fig. 9), although different nomenclatures have been established in various areas of the basin (Azcuy & Morelli 1970). The sedimentation began during the lower Upper Carboniferous Guandacol Fm. (Limarino & Gutierrez, 1990; Césari & Gutierrez, 2000) with coarse-grained alluvial fan deposits, braided fluvial deposits and tillite that gave way rapidly to transgressive mudstones and sandstones (Limarino & Césari, 1988; Buatois & Mángano, 1995, López Gamundí & Martínez, 2000; Limarino et al., 2002; Pazos, 2002a; Marensi et al., 2005).

During the Permian relative sea level dropped and the sedimentation was dominated by arid or semiarid climates including eolian deposits (Limarino et al., 2013; Limarino and Spalletti, 1986; López Gamundí et al., 1992).

Gulbranson et al. (2011), based on U-Pb data, redefined the chronostratigraphy of the Paganzo Group, and identified three pulses of Carboniferous glaciation in the mid-Viséan, the late Serpukhovian to earliest Bashkirian, and between the latest Bashkirian to early Moscovian (Fig. 9).

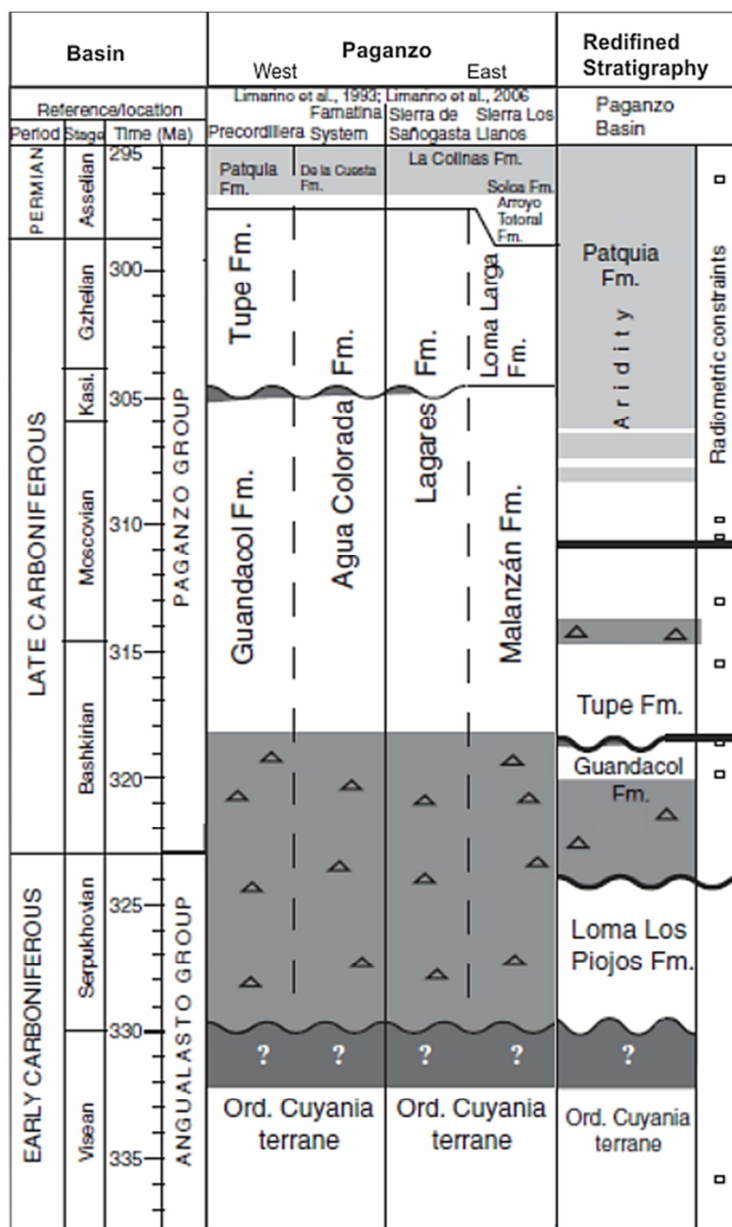


Fig. 9: Chronostratigraphy of the Angualasto and Paganzo Groups from the modern Andean Precordilleran region to the Sierra Pampeanas. The rightmost column represents the redefined stratigraphy by Gulbranson (2010). Dark-gray shading denotes unconformities; question mark indicates an unknown temporal extent of an unconformity. Medium-gray shading with triangle symbols indicates the temporal extent of glacigenic deposits. Light-gray shading denotes sedimentary evidence of aridity (e.g., eolianites, playa-lake deposits). Wavy lines indicate erosional contacts. Radiometric constraints are shown in the rightmost column.

4.3 Paraná Basin

The Paraná Basin is a widespread intracratonic depression with an approximate extent of 1,600,000 km², covering the entire southern portion of Brazil, as well as south-eastern Paraguay, north-eastern Argentina and northern Uruguay (Fig. 10). It was formed during the Ordovician, being completely filled by the Late Cretaceous (Buatois et al., 2010). Due the presence of hydrocarbons the basin has been extensively studied since 1892 when the oil exploration started (Schneider et al., 1974; França & Potter, 1988; Eyles et al., 1993; Milani & Zalán, 1999; Holz, 2003; Holz et al., 2006; Vesely y Assine, 2006, among others).

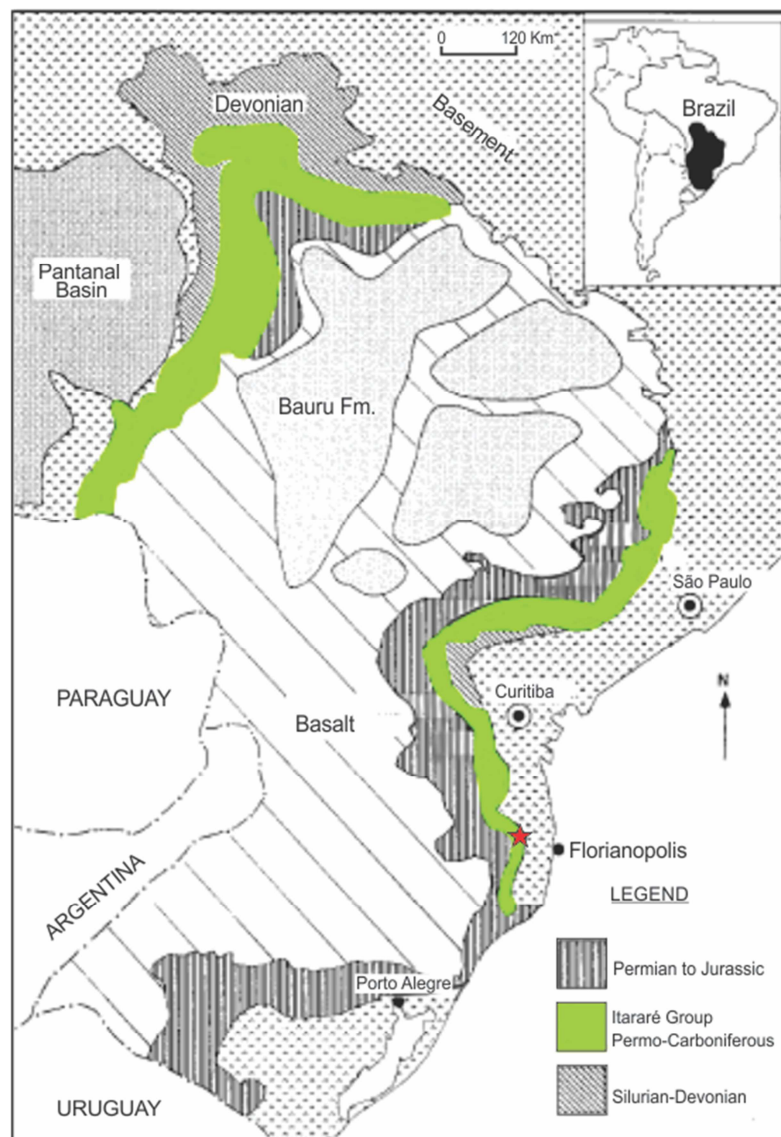


Fig. 10: Geological map of the Paraná Basin (location is shown in the inset). Most of the glacial Itararé Group is covered by Cretaceous lava flows of the Serra Geral Formation and terrestrial sandstones of the Bauru Formation (França & Potter, 1991). Only uppermost Itararé Group rocks are exposed in outcrop belts along the south-east and north-west basin margins (modified from Franca & Potter, 1991). The study area is shown with a red star.

The Paraná Basin was developed on continental crust of the former Gondwana supercontinent. Precambrian basement that underlies the sedimentary and volcanic infill of the basin is complexly structured. It consists of several cratonic nuclei bounded by orogenic mobile belts which are composed of thrust sedimentary rocks intruded by granites (Eyles et al., 1993). The uplift and subsidence of these belts, and eustatic cycles, controlled the sedimentary infill producing hiatus in the sedimentation.

The stratigraphy of the Paraná Basin has a total thickness of over 6 km and is grouped into three depositional successions: 1. Siluro-Devonian, 2. Late Carboniferous to Jurassic and 3. Cretaceous (Fig. 11). Each record a distinct period of tectonic subsidence and sediment preservation within the basin (Eyles et al., 1993).

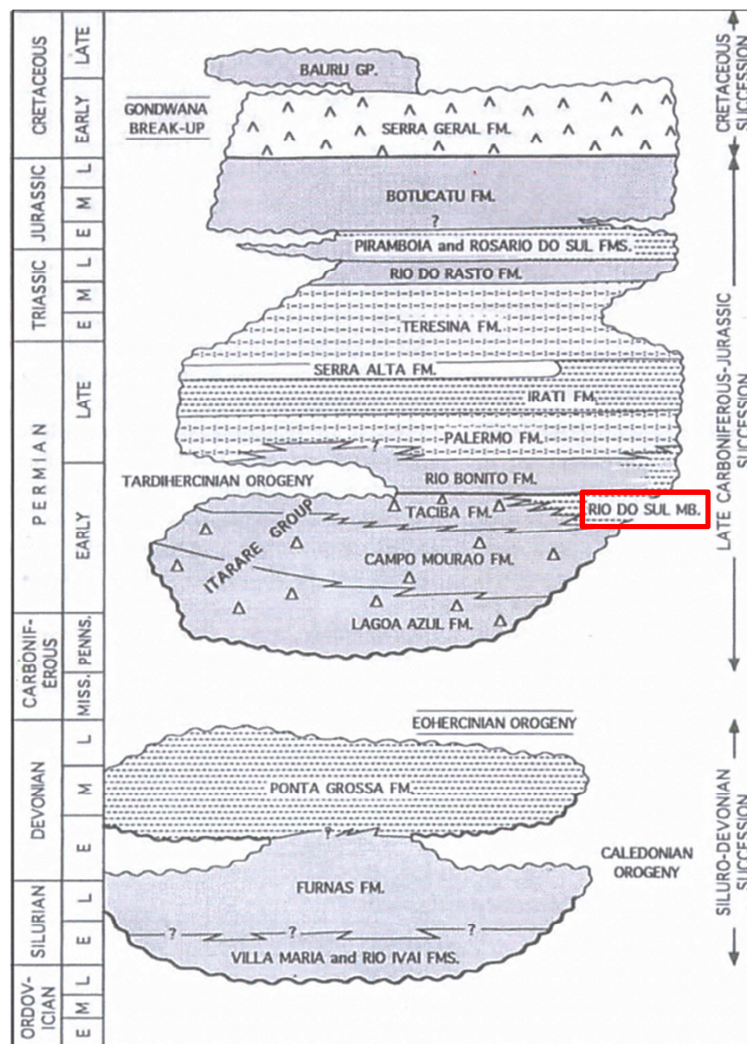


Fig. 11: Stratigraphic column for the infill of Paraná Basin showing three principal stratigraphic successions (Modified from França, 1987). The red rectangle indicate the Rio do Sul Formation (sensu Schneider et al., 1974), object of this study.

The Itararé Group, object of this study, corresponds to the Permo-Carboniferous part of the Late Carboniferous to Jurassic succession (Fig. 11). The term Itararé was used for the first time by Oliveira (1927) who designated all the sediment with glacial influence as Itararé Series. Twenty years later, Gordon (1947) proposed the term of Group instead of series, and Schneider et al. (1974), based on outcrop observations, divided the Itararé Group into four formations (Table 1):

- *Campo do Tenente Fm.*: corresponding to glaciomarine siltstones and shales, glaciofluvial diamictite, sandstones and conglomerates that occur at the base of the Itararé Group. Striated pavements and striated and faceted clasts are common. The formation unconformably overlies rocks of Paraná Group or basement.

- *Aquidauana Fm.*: characterized by fluvial fine-to coarse-grained sandstones and glaciomarine diamictite. This formation is the only one that occurs just in the North and West flank of the basin. Both the upper and lower contacts are unconformities (Castro et al., 1994).

- *Mafra Fm.*: composed chiefly of deposits that was originated during deglaciation. The lower interval consists of a glacio-deltaic succession that is replaced upwards by a tide-influenced shallow-marine succession, consisting of medium- to large-scale, trough cross-stratified sandstone representing tidal bars. The middle interval consists of very thinly bedded silty-muddy rhythmites filling incised valleys. Dropstones are abundant, ranging from granules to boulders. The upper interval of the formation consist of thinly interbedded, fine-to very fine grained sandstones and siltstones, and fine- to medium-grained sandstone with trough cross-stratification, herringbone cross-stratification and possibly hummocky cross-stratification. Matrix-supported diamictite with faceted clast occurs throughout the whole succession (Buatois et al., 2010).

- *Rio do Sul Fm.*: consists essentially of fine-grained heterolithic deposits with subordinate diamictites and fine-grained sandstones. In Santa Catarina State the widespread shales and siltstones with varve-like aspect at the base are known as "Lontras Shale" and record a maximum flooding surface.

On the other hand, França & Potter (1988), using well data, divided the Itararé Group into (Table 1):

- *Lagoa Azul Fm.*: contains two members, a lowermost, sand-rich member (Cuiaba Paulista) and an upper, diamictite-rich member (Tarabai; Fig. 5). The Cuiaba Paulista Member consists dominantly of massive and poorly graded sandstones with minor conglomerates (turbidites). The Tarabai Member forms the upper (diamictite rich) member of the Lagoa Azul Formation and is characterized by stratified diamictites, formed predominantly by debris flows. An isopach map suggests that the deposition of the formation was controlled by tectonism restricting the sedimentation to the central portions of the basin.

- *Campo Mourão Fm.*: is characterized by complexes of stratified diamictites and graded, massive and deformed sandstones and conglomerate facies, all indicative of rapid sedimentation by gravity flows. This supports the notion that the basement lineaments were active faults at that time, and defined a series of grabens. At the top the formation is composed by marine shales that pass laterally into diamictites; these deposits correspond to the Lontras Member. Isopach maps identify a far more extensive distribution than for the Lagoa Azul Formation. This increased areal distribution of units is consistent with basin subsidence and expansion.

- *Taciba Fm.*: this formation can be subdivided into a lower sandy member (Rio Segredo), a diamictite-rich member (Chapeu do Sol) and a shale-rich member (Rio do Sul, object of this study). Taciba Formation sediments cover the entire Paraná Basin and are the only units of the Itararé Group exposed in outcrops around the whole basin. Sandstones of the Rio Segredo Member are characterized by massive and graded facies, interpreted as turbidites. Some shallow water indicators, such as wave ripples, were also recorded in cores from the northern part of the basin. The Chapéu do Sol Member consists of massive to crudely stratified diamictites interpreted as mudstones with ice-rafted clasts (rain-out facies), locally modified by downslope resedimentation. In the South part of the basin the diamictites interfinger with marine shales with dropstones of Rio do Sul member. Overall, the Taciba Formation appears to represent deposition in relatively

quiescent tectonic conditions. The chaotic, resedimented deposits characteristic of the Lagoa Azul and Campo Mourao formations are succeeded in the Taciba Formation by regionally extensive units, such as massive diamictites, which indicate more 'passive' depositional conditions suggestive of thermal subsidence. Resedimentation processes at this time were probably most effective in 'filling in' a substrate relief created during earlier episodes of tectonic activity and faulting (Eyles et al., 1993).

		Schneider et al. (1974)	França & Potter (1988)	
Itararé Group	Rio do Sul Fm	Fine grained heterolithic deposits	Taciba Fm.	Rio do Sul Mb.: shales
		"Lontras Shale"		Chapeu do Sol Mb.: diamictites
				Rio do Segredo Mb.: sandstones
	Mafra Fm.	Upper: sandstones, siltstones, diamictites	Campo Mourao Fm.	"Lontras Shales"
		Middle: silty-muddy rhythmites		diamictites, sandstones
		Lower: sandstones		
Campo do Tenente Fm.	Shales, diamictites, sandstones and conglomerates	Lagoa Azul Fm.	Tarabai Mb: diamictites	
			Cuiaba Paulista Mb.: sandstones	

Table 1: Stratigraphy of the Itararé group, according to definitions of Scheneider et al. (1974) and França & Potter (1988). Modified from Weinschütz & Castro (2004).

5. RESULTS

In this chapter are presented the data obtained in the both areas of study, Cerro Bola (Argentina) and Vidal Ramos (Brazil), after 175 field days distributed into 130 days in Paganzo Basin and 45 days in Paraná Basin. The difference of field time is related to the degree of outcrop exposure.

5.1 Cerro Bola

The Cerro Bola presents the same stratigraphic sequences described by Valdez (2011), in Sierra de Maz located approximately 7 km to northwest (Fig.1 and 6), with the exception that the basement is not exposed in Cerro Bola.

Structurally the area corresponds to a large, west-vergent, doubly plunging, north-south oriented, hanging wall anticline to a thrust that dips SE at about 24°, related to Late Tertiary to Quaternary Pampean Range orogenic deformation, beginning at about 4.5 Ma and continuing today (Zapata and Allmendinger 1996, Jordan et al., 2001).

Stratigraphically the Cerro Bola anticline exposes a Carboniferous to Triassic record. The approximately 1,100 m of Carboniferous deposits correspond to Paganzo Group, and represents five glacial-deglacial cycles (Valdez et al., 2013), each consisting of mass-transport deposits (MTD) interpreted as remobilized aquatills; turbidite intervals; and fluvio-deltaic sediments (Fig. 12).

Cycle 1 comprised the Fluviodeltaic 1, composed of medium to coarse-grained sandstones with granules and pebbles with traction sedimentary structures; and the overlying MTD 1. The contact between both units corresponds to a zone with deformation and incorporation of fluviodeltaic blocks. The MTD 1 presents a silt-sand matrix, with clasts ranging from granule to cobble in size and compositionally corresponding mostly to granites and metamorphic rocks indicating basement origin (Valdez, 2013).

Cycle 2 corresponds to the sand-rich Fluviodeltaic 2 that upwards presents channelized conglomerates and MTD 2. This unit presents a silty-sandy matrix with sand blocks, up to 30-40 m above the basal contact, from the underlying unit. Towards the top folding is common at variable range of scales, with many slide surfaces (Dykstra et al., 2011).

The ice rafted debris of **Cycle 3** is overlying the MTD 2 and corresponds to a 5 mm mud-silt intercalation with dropstones, overlaid by sandy deposits of the Pondered Turbidite unit. The thickness of this unit is directly related to the topographic relief left by the MTD 2 (Fairweather, 2013).

The Black Shales, as its name indicates, are dark fine-grained sediments that correspond to a maximum flooding surface. This deposit represents the first major transgression into Paganzo Basin during the Pennsylvanian, and is well documented in the Guandacol, Lagares, Malazán and Jejenes Formations (Limarino et al., 2002; Net et al., 2002; Pazos, 2002; Kneller et al., 2004; Dykstra et al., 2006).

Cycle 3 culminates with the Upper Turbidites unit, which is divided into five Stages, ordered from I (bottom) to V (top) (Fallgatter et al., 2013). It consists of sheet turbidites that present, in general, a thickening pattern; Stage IV and V are analysed in this dissertation.

Cycle 4 corresponds to the Fluviodeltaic 3 (aim of this study, see below for description) and the overlying Green Unit, that correspond to poorly laminated silty-muddy turbidites that present locally deformation and metamorphic dropstones at the lower part. The unit finish with lenticular sandy beds.

Medium to coarse-grained sandstones, with well-developed clinoforms, of the Fluviodeltaic 4 (**Cycle 5**) overlies the Green Unit, and finish the Carboniferous sedimentation. The stratigraphy culminates with Permian red-beds (Fig 12) (Milana et al., 2011).

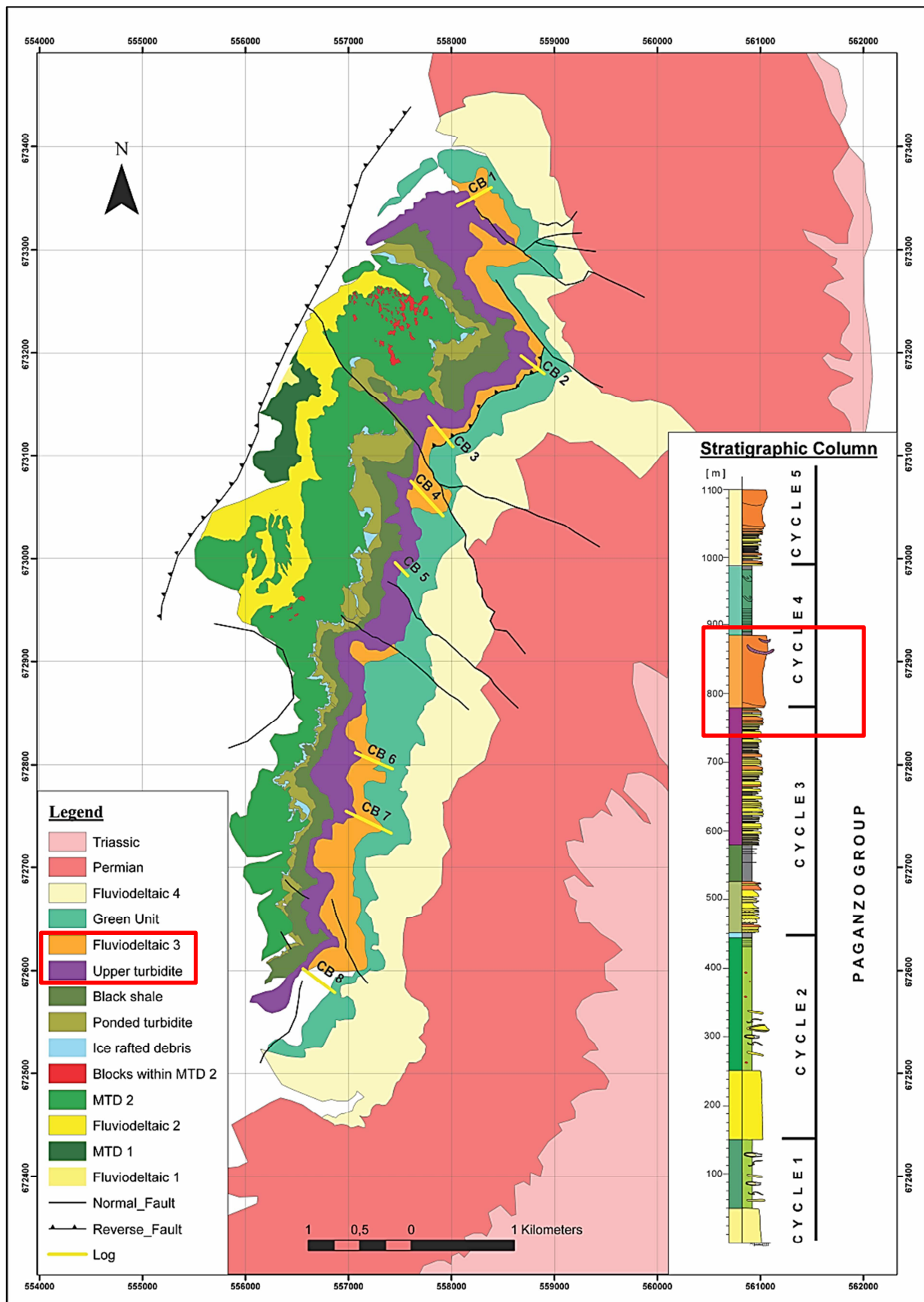


Fig. 12: Geological map of Cerro Bola (modified from Milana et al., 2011), at the right is shown the stratigraphic column of the Paganzo Group with the five cycles defined by Valdez (2013). This work studied the relationship between the upper part of **Upper turbidite** (purple) and **Fluviodeltaic 3** (orange), that belong to the Cycle 3 and 4 respectively (red rectangle). See text for explanation. The yellow lines in the map indicate the locations of the logs.

5.1.1 LOGS DESCRIPTION

For the purpose of this research eight sedimentary logs, named CB 1 to CB 8, were made along the outcrop including the upper part of the Upper Turbidite (Stage IV and V) to the first metres of the Green Unit (Fig. 12). Each log is described below from North (CB 1) to South (CB 8) (Attach 1).

Log CBI

Located at the northern part of Cerro Bola (Fig 12), this log recorded 64 m of the Upper Turbidites and 167m of the Fluviodeltaic 3. (Attach 1)

Upper Turbidites:

- Stage IV: is characterised by thick turbidites (~ 1 to 4 m), mostly amalgamated sand beds (Fig. 13). The grain size varies from medium to fine sand, grading to very fine sands or in few cases to mudstones. Massive sandstones, load casts and horizontal laminations are the common features, but also present are mudclasts and climbing ripples (Fig 14). The palaeocurrent analysis indicates northwest as the main flow direction. The total thickness of this stage is 24 m.
- Stage V: corresponded to thin-bedded turbidites, each bed 5-50 cm thick, of fine to very fine-grained sandstones grading to mudstones (Fig. 15). Compared with the previous stage, the proportion of mud is higher and sedimentary structures such as parallel lamination, climbing ripples, sole structures and dewatering are common. Some layers show internal deformation with abundant mudclasts (Fig. 15 C). The grain size and the thickness of the beds increases towards the top, finishing with a coarse-grained, 2 m thick bed followed by two beds of 20 cm thick turbidites. The palaeocurrent analysis based on current ripples indicates a flow direction toward northwest.



Fig. 13: Upper Turbidites Stages. Note the differences in bed thickness between the Stage IV and V. Person for scale (yellow circle).

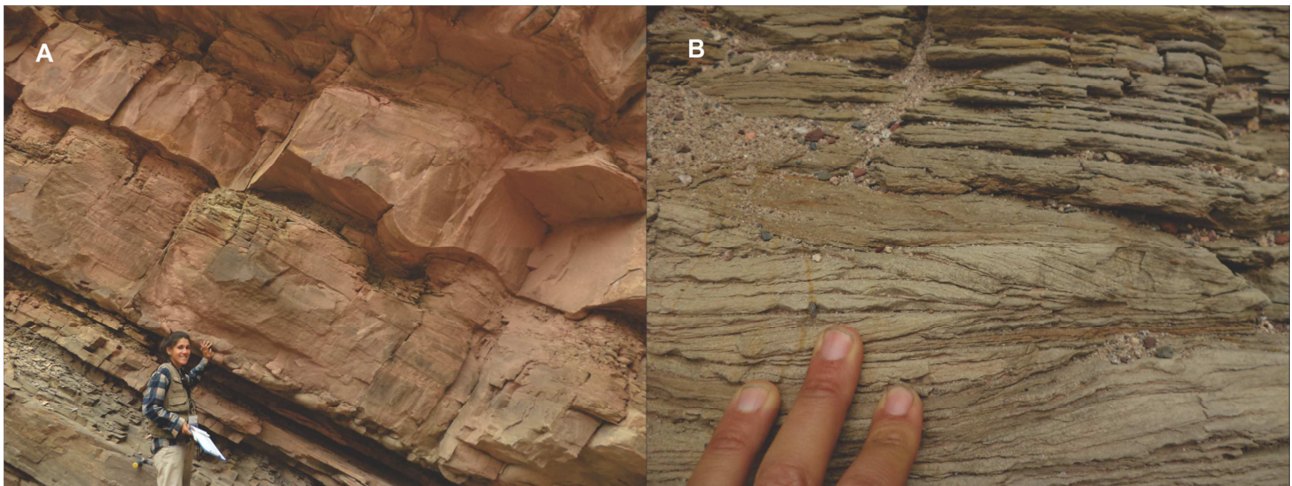


Fig. 14: Common features of Stage IV. (A) Load cast structures followed by parallel lamination. (B) Ripple cross-lamination and parallel lamination.

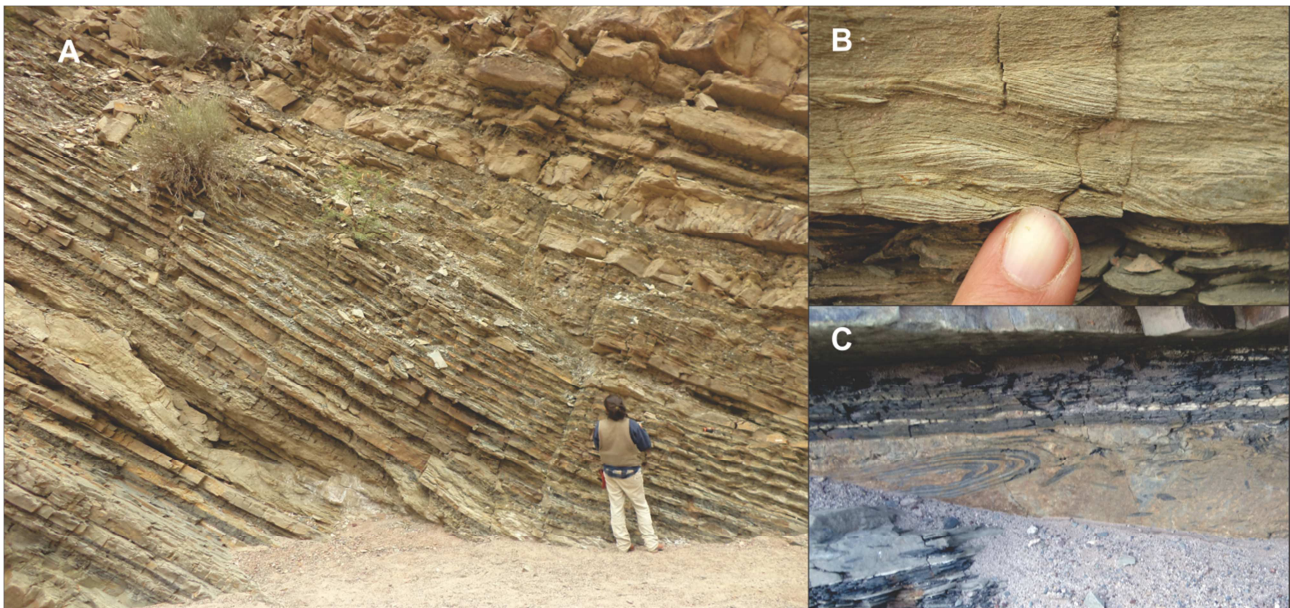


Fig. 15: Upper Turbidites, Stage V. (A) General aspect of this Stage, the thickness of the beds varies from 5- 50 cm. (B) Climbing ripples in fine-grained sandstones This sedimentary structure is very common. (C) Deformed bed, note the abundance of mudclasts.

Fluviodeltaic 3

In sharp contact with the underlying Upper Turbidites (Fig. 16) the fluviodeltaic sequences can be divided into four Units based in their sedimentary characteristics (Fig. 17).



Fig. 16: Sharp contact between the Upper Turbidites and Fluviodeltaic 3. Note the massive aspect of the 13 m thick bed. Person for scale (black circle)

- Unit 1: is characterized by massive, thick (0.5-13 m) medium-grained sandstones, starting with a 13m thick bed (Fig. 16) that become thinner and structured to the top of the unit, with parallel lamination and climbing ripples at the top of the bed (Fig 17). The composition of the sand grains is quartz, K feldspar and a lot of muscovite. The grains are sub-rounded and show poor sorting. The massive aspect of the sandstones characterizes this unit. The total thickness is 36 m.

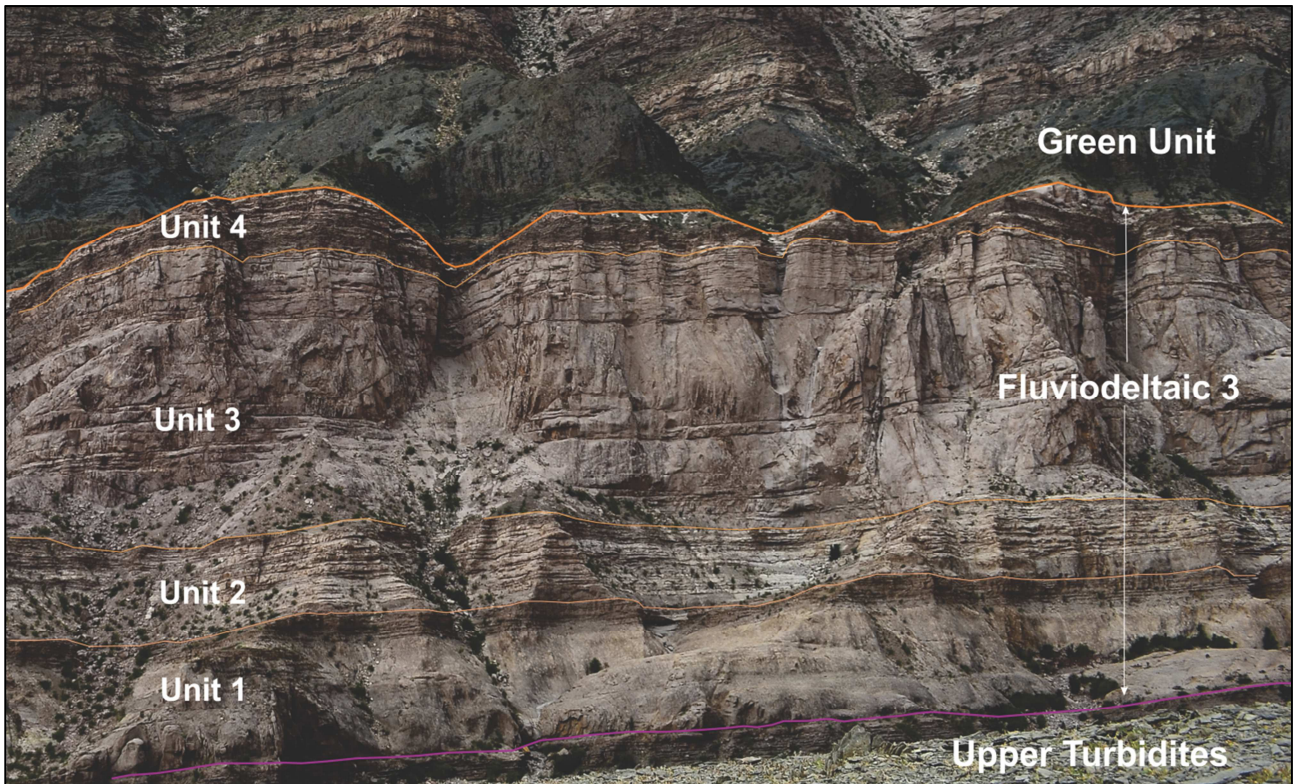


Fig. 17: Units of the Fluiodeltaic 3. The contact with the underlying Upper Turbidites sequence is shown by the purple line and with the upper Green Unit (orange line). See text for thickness of each unit.

- Unit 2: this unit is characterized by thinner beds (0.6 -2 m) of cross-stratified sandstones (Fig. 17 and 18 A). It consists of coarse to medium-grained sandstones composed mostly of quartz grains (80%) and shows poor sorting. At the bottom the unit shows conglomeratic sandstones and lenses of conglomerates which becomes sandier towards the top (Fig. 18). The palaeocurrents of ripples and cross-stratifications indicated a main flow direction towards NW-NE (Attach 1). Total thickness is 29 metres.

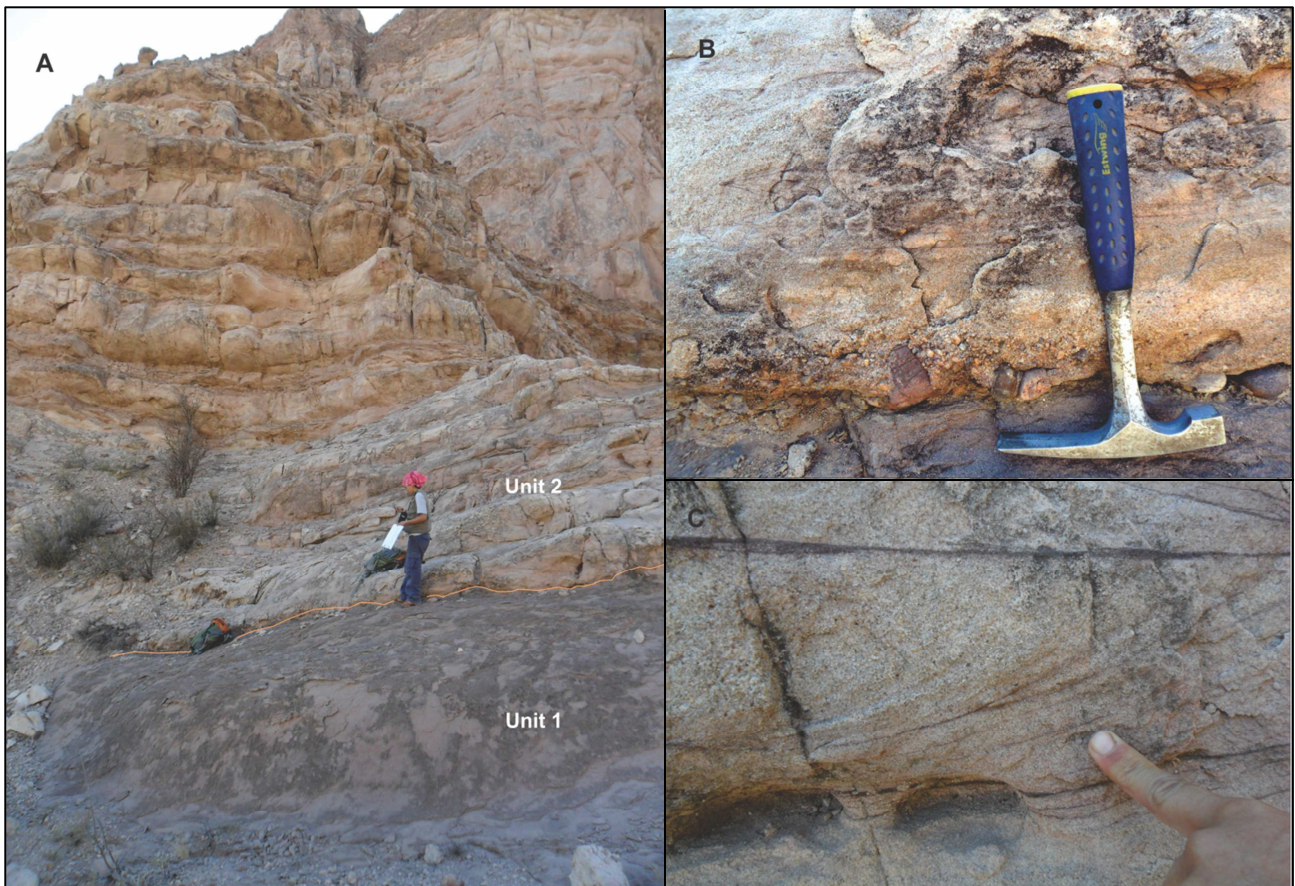


Fig. 18: Characteristics of Unit 2. (A) General aspect of the unit, the oranges line indicates the contact with the Unit 1. (B) Matrix-supported conglomerates at the base of the bed grading to medium-grained sandstone to the top. Geological hammer for scale. (C) Cross-stratification at the base of the bed.

- Unit 3: present thick lenticular sandy beds (10-1m) that amalgamate laterally. At the base the unit shows thick beds (4 to 7 m), becoming thinner towards the top (Fig 17). The composition of the sand is quartz, K-feldspar and mica, of medium sand grain size, poorly sorted. Mostly of the packages are massive but in the bottom of the cycle sometimes it is possible to observe parallel lamination and cross-stratification at the top of some beds. The palaeocurrents indicate a northerly direction. Also present are lenses of conglomerates sand and intraclasts of very fine-grained sandstones of purple colour (Fig. 19). The thickness of this cycle is 71 m.



Fig. 19: Principal characteristics of Unit 3. (A) General view of the outcrop, note the discontinuities of the bedding planes due to amalgamation. Note person for scale. (B) Medium-grained sandstone with sparse granules. (C) Tabular intraclasts of very fine-grained sandstones parallel to the bed plane.

- Unit 4: This unit corresponds to conglomerates organized in channels with erosional bases. Both type, matrix and clast-supported, are found. In general the matrix corresponds to coarse sand and presents normal grading. The clasts compositions vary from schist, sandstones, granite and quartz, they are well-rounded and poorly sorted (clast size vary from 40 cm to granule) (Fig. 20). In this package also appear beds of coarse and very coarse-grained sandstones with cross-stratification and lens of conglomerates. The palaeocurrents analysis indicates NW-NE flow direction. Total thickness is 31 m.

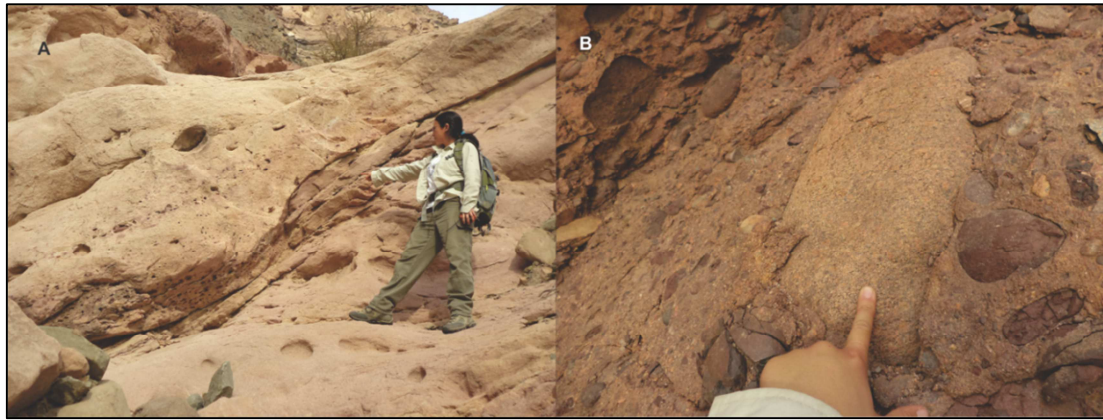


Fig. 20: (A) Erosional conglomeratic channel. Note the concentration of clasts at the base. (B) Detail of matrix-supported conglomerate. The biggest clast corresponds to granite. In general all clasts are well rounded

Green Unit

This Unit overlies Fluviodeltaic 3 (Fig 21 A). The contact between the two units in some places shows polished surfaces of the sandstones (Fig 21 B). This Unit consist of green, very fine grained sandstones grading to silt that become mainly/wholly resedimented towards the top. Also dropstones were observed in the upper parts (Fig. 21 C). In the North the Unit has 70 m of thickness.

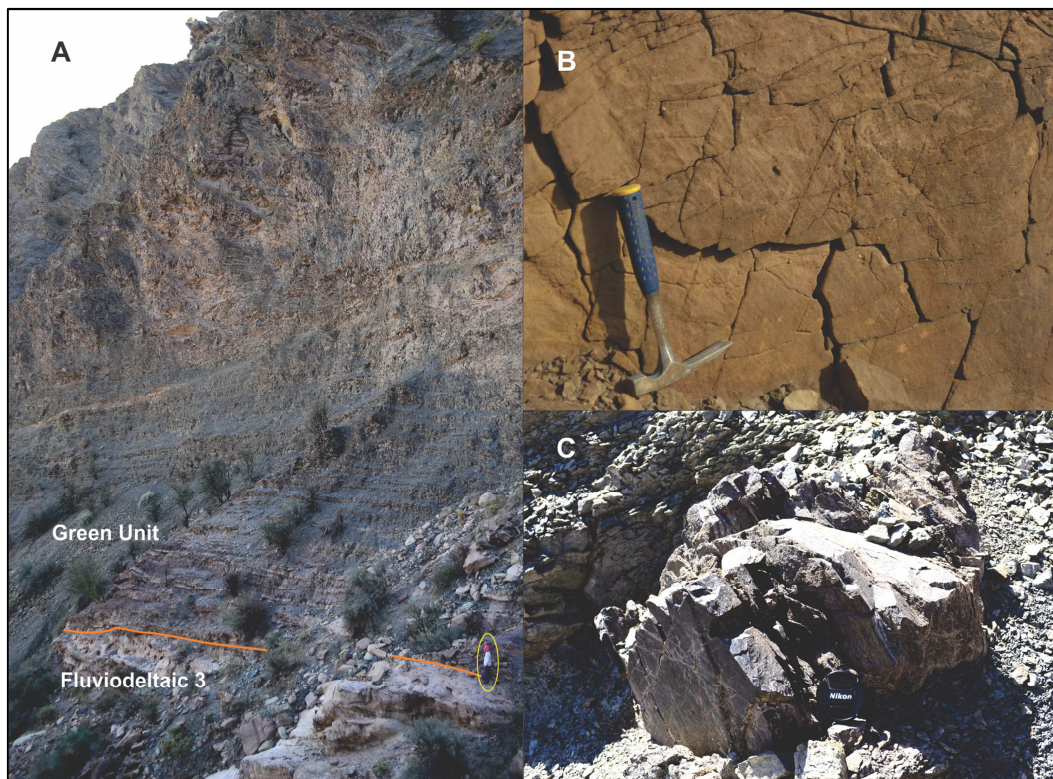


Fig. 21: Main characteristics of the Green Unit. (A) Erosive contact with the Fluviodeltaic 3. (B) Polished and striated surface of the Fluviodeltaic sandstones at the contact with the overlying Green Unit. (C) Metamorphic clast (gneiss) within a silty matrix located in the upper part of the unit, interpreted as a dropstone.

Log CB 2

Located 1.26 km to SE (Fig. 12), this log recorded 57 m of the Upper turbidites (Stage IV and V) and 148 m of the Fluviodeltaic 3 (Fig. 22) (Attach 1).

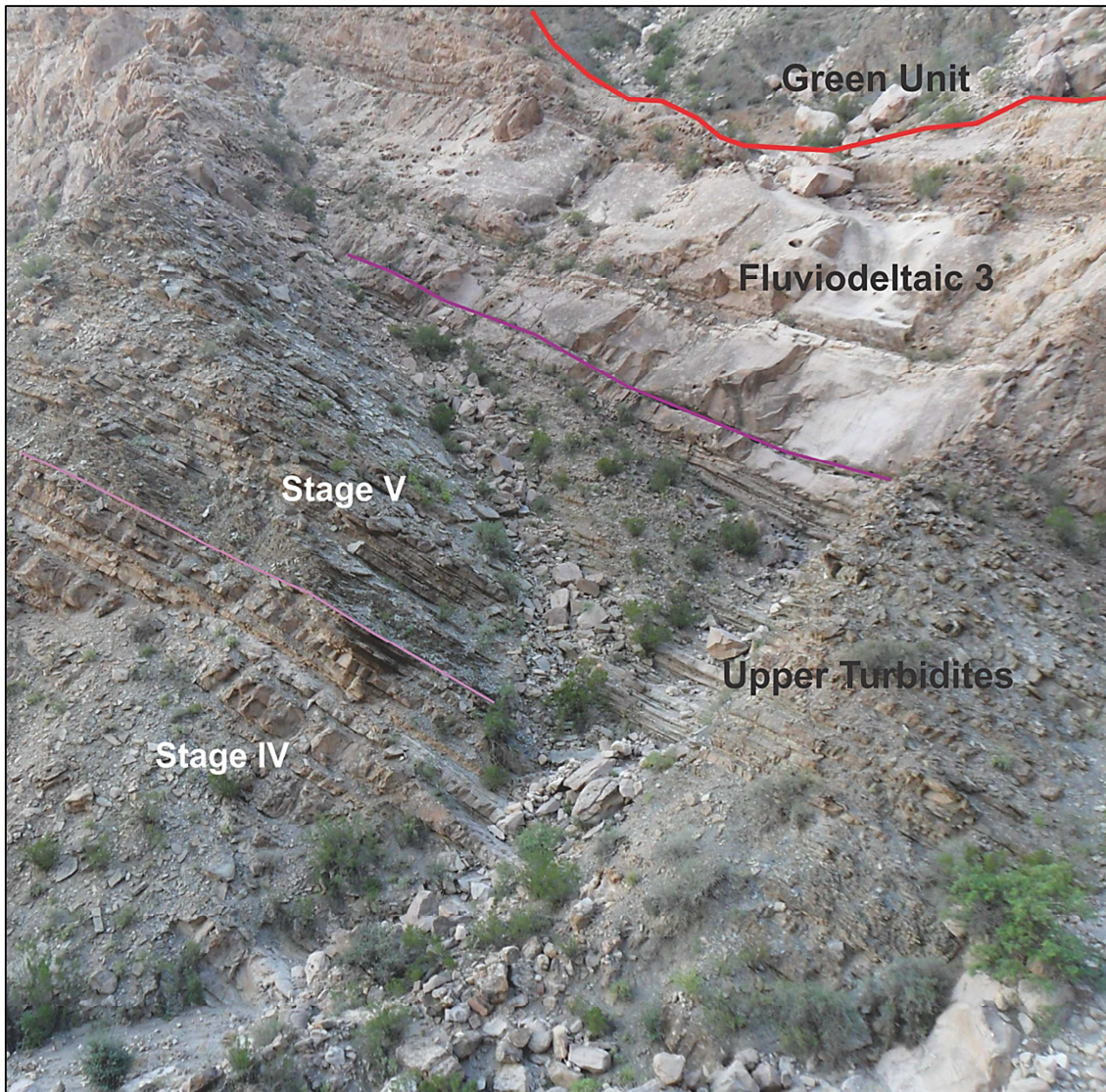


Fig. 22: Outcrop view of the log CB 2. The thicker purple line indicate the contact between the Fluviodeltaic 3 and the Upper Turbidites which its respective stages (IV and V, light purple line). The red line corresponded to a fault inside the page.

Upper Turbidites

- Stage IV: As in the previous log (CB 1) the stage is characterize by thick turbidites, ranging from 0.5-4 m thick, consisting mostly of medium to fine-grained sandstones grading to very fine sands, or mudstones in rare cases. Sole structures are common as well as parallel lamination and climbing ripples. Beside the bed thickness this stage is characterized by bed amalgamation (Fig. 23). Total thickness 22 m.

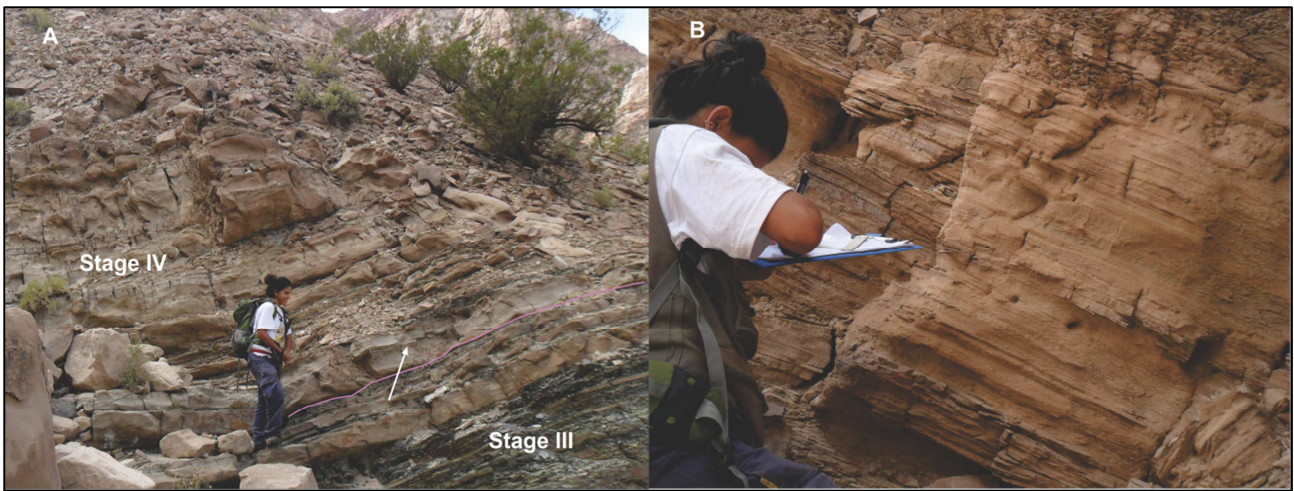


Fig. 23: (A) Upper Turbidite, contact between the Stage III and IV (purple line). Note the amalgamation of the beds (white arrows). (B) Detail of medium-grained sandstones with parallel lamination.

- Stage V: In contrast with the previous stage, this is characterized by the presence of thinner turbidites (0.5-0.7 m thick) of fine to medium-grained sandstones grading to mudstones (Fig. 22). Sedimentary structures such as climbing ripples, parallel lamination, flute and groove casts, flame structures and dewatering are abundant. Sediment deformation and mudclasts were also observed in some beds (Fig. 24). The stage ends with a 3 m thick medium sand bed with normal grading, followed by two 20 cm thick turbidites (Fig 22). The total thickness of the stage is 35 m.

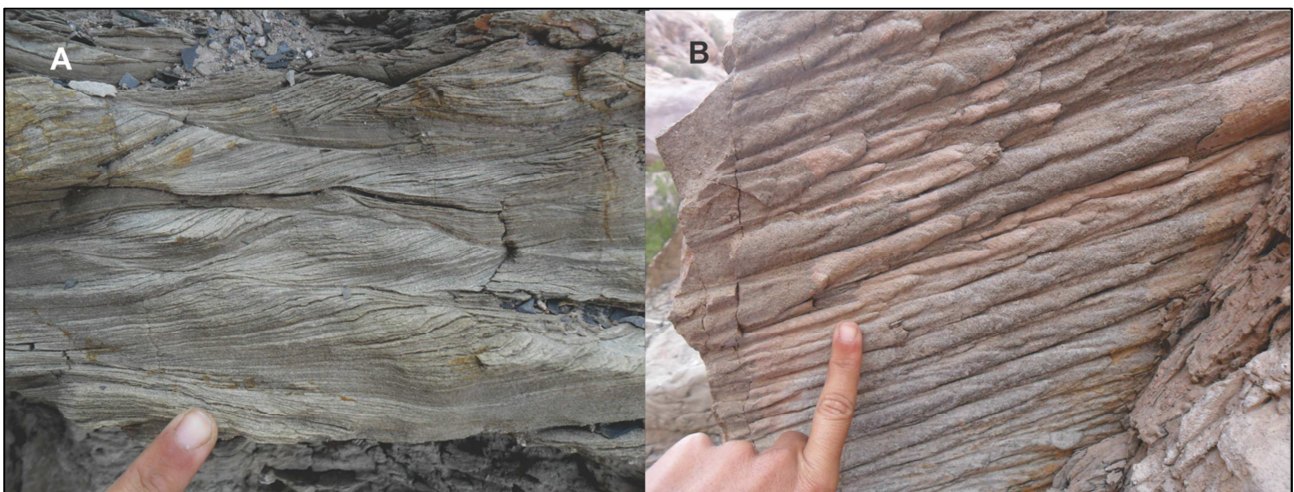


Fig. 24: Common sedimentary structures in the Upper Turbidite Stage V. (A) Climbing ripples indicating NW flow direction. (B) Sole marks indicating NW direction.

Fluviodeltaic 3

In this section the Fluviodeltaic 3 consists of 148 m of sediment, overlying in sharp contact the Upper Turbidites. The contact with the overlying Green Unit is a fault (Fig. 25).



Fig. 25: The four Units of Fluviodeltaic 3 overlying the Upper Turbidites (purple line). The contact with the Green Unit is by fault (red line).

- Unit 1: correspond mostly to massive medium-grained sandstones organized in thick packages (0.5-13 m thick) (Fig 22 and 25), finishing with a 1 m thick package of purple very fine-grained sandstone with thin layers (5 cm) of fine grained sands. The sorting of the unit is poor, and quartz and K-Feldspar are the most abundant components. Some beds show lens of coarse-grained sandstones and intraclasts of very fine sand at the top of the bed (Fig.26). The total thickness is 27 m.

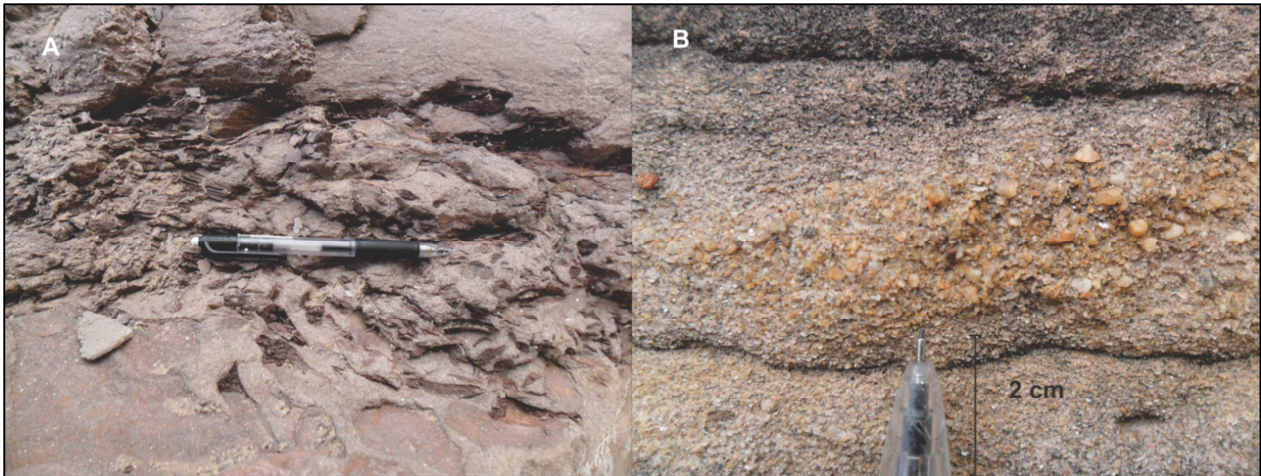


Fig. 26: Fluviodeltaic 3, Unit 1. (A) Very fine sand with intraclast at the top of the unit. (B) Lens of coarse grained sand within a medium sandstone bed.

- Unit 2: Compared with previous unit, this is organized into thinner sandstone beds (0.5-1 m thick) that sometimes appear amalgamated to form 3 m thick layers (Fig. 25). The principal characteristic is the abundant presence of sedimentary structures such as climbing ripples, cross-stratification and parallel lamination (Fig. 27). The palaeocurrent analysis indicates a NW flow direction. Thickness: 31 m.



Fig. 27: Unit 2: Medium-grained sandstones with parallel lamination at the base, followed by cross-stratification and parallel lamination to the top.

- Unit 3: consists of medium-grained sandstones organized in amalgamated beds. In the lower part are frequent intraclasts at the base of the beds. Upward the Unit become more structured, showing parallel lamination and ripples that indicate NW trending currents. Some few beds present soft sediment deformation (Fig. 28). Total thickness: 117m.



Fig. 28: Principal characteristics of the Unit 3. (A) Bed amalgamation. (B) Climbing ripples followed by parallel lamination. (C) Parallel lamination at the top of the bed. (D) Soft sediment deformation.

- Unit 4: poor sorted matrix-supported conglomerates with erosive bases. The composition of the clasts includes mostly granites, fine grained sandstones and quartz. Normal grading is present (Fig. 29). This unit present a total thickness of only 7 m due the presences of the fault (Fig. 25).

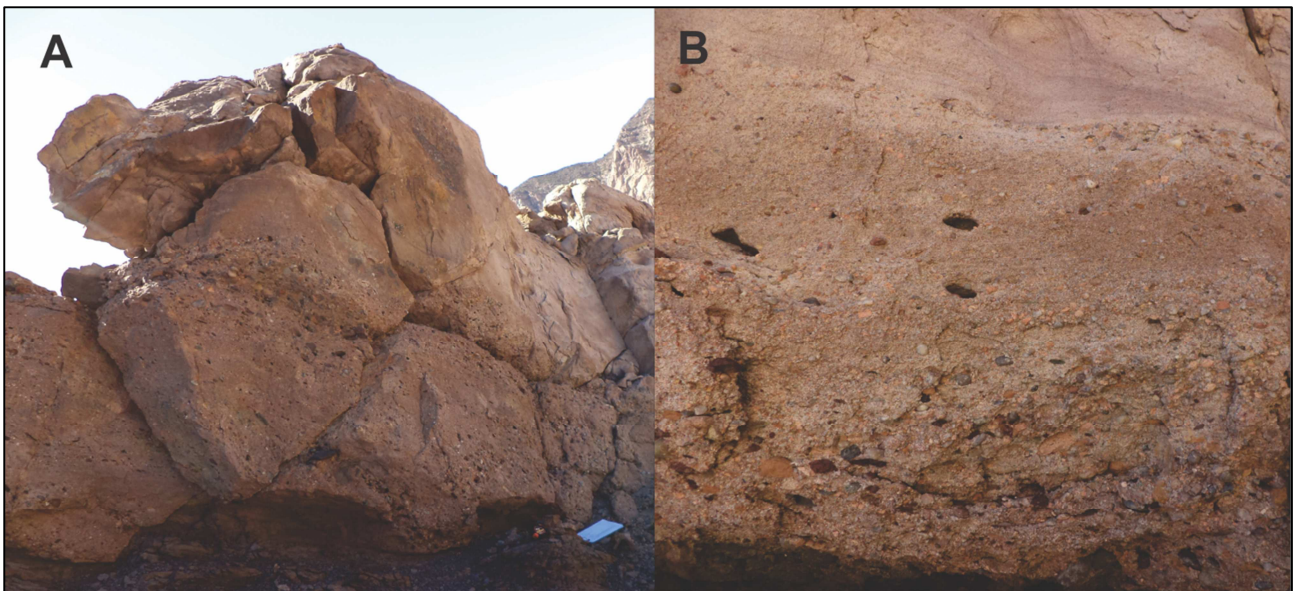


Fig. 29: Conglomerates of the Unit 4. (A) Erosive conglomeratic channel. (B) Tractive structures and normal grading. The clast size varies from granules to pebbles.

Green Unit

In this part of the Cerro Bola the contact with the Fluviodeltaic 3 is by a fault. It consists of silty-sandy matrix, sometimes slumped, containing subrounded clast from basement, (Fig. 30).

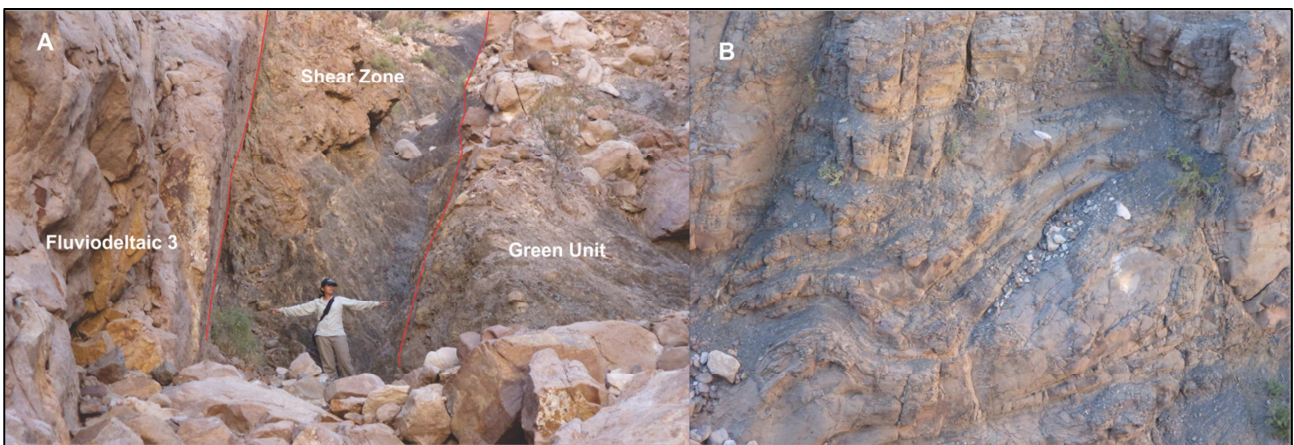


Fig. 30: Green Unit. (A) Detail of the fault (160°/65 SW) that put the Fluviodeltaic 3 in contact with the Green Unit. The shear zone is about ~3 m. (B) Slumped sediments.

Log CB 3

Located at 1,6 km to SW of CB 2 (Fig. 12) this log records 46 m of the Upper Turbidites and 136 m of the Fluviodeltaic 3 (Fig 31) (Attach 1).

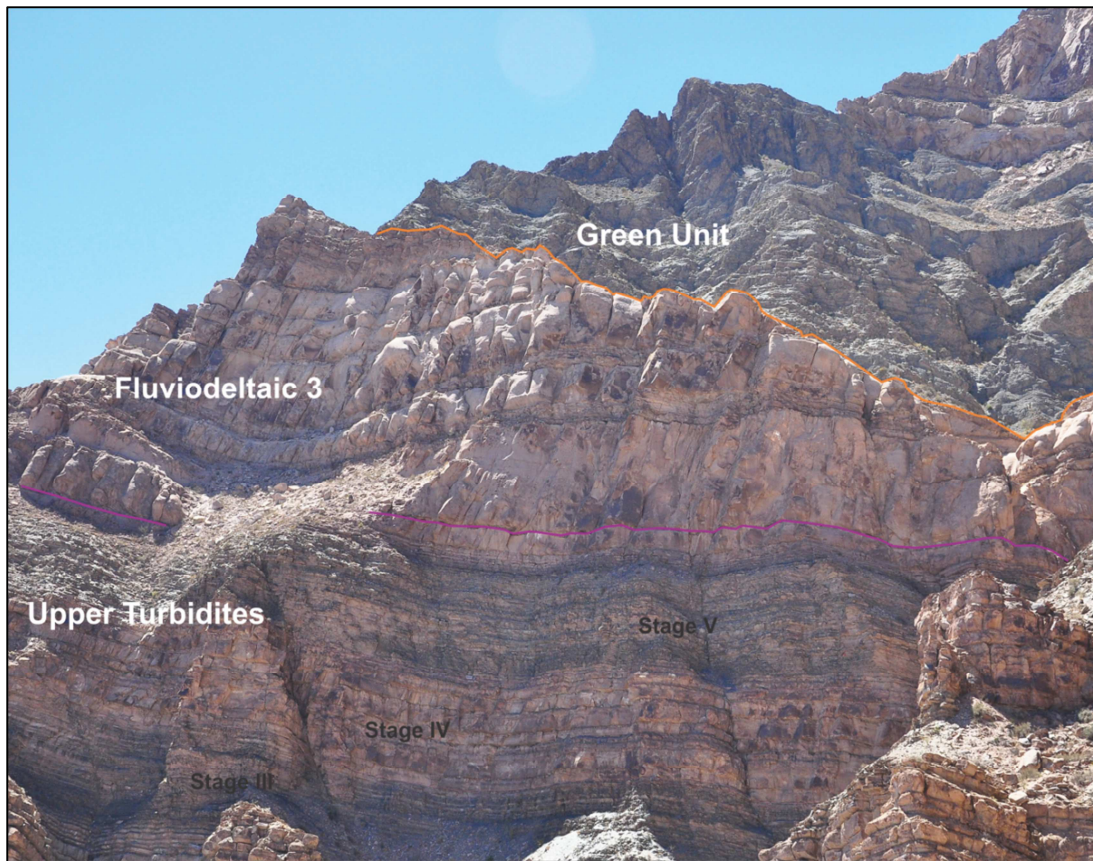


Fig. 31: General view of outcrop of log CB 3. The purple line indicates the top of Upper Turbidites, and the orange line the contact between the Fluviodeltaic 3 and the Green Unit. See text for details and thickness of each unit.

Upper turbidites

- Stage IV: the base of the stage is covered in the valley recording only 14 m of thickness, but 20 m of thickness was measured with laser in the valley wall (Fig. 31). It consists mostly of thick turbidites (3-1 m) that become thinner to the top. The grain size varies from medium to fine sand grading to mudstones. The sedimentary structures are parallel lamination, climbing ripples and loading (Fig. 32). Palaeocurrents analysis indicates NW flow direction.
- Stage V: comprised turbidites organized in thin layers (30- 5cm) that become thicker to the top, finishing with a ~3m thick sand body (Fig. 31), which in some places is amalgamated with the Fluviodeltaic 3 and deforms the underlying bed (Fig. 33 A and B). The turbidites usually show climbing ripples, parallel lamination, loading, mudclasts and fluidisation (Fig. 33 C and D). Flow direction is toward NW. Total thickness 32 m.

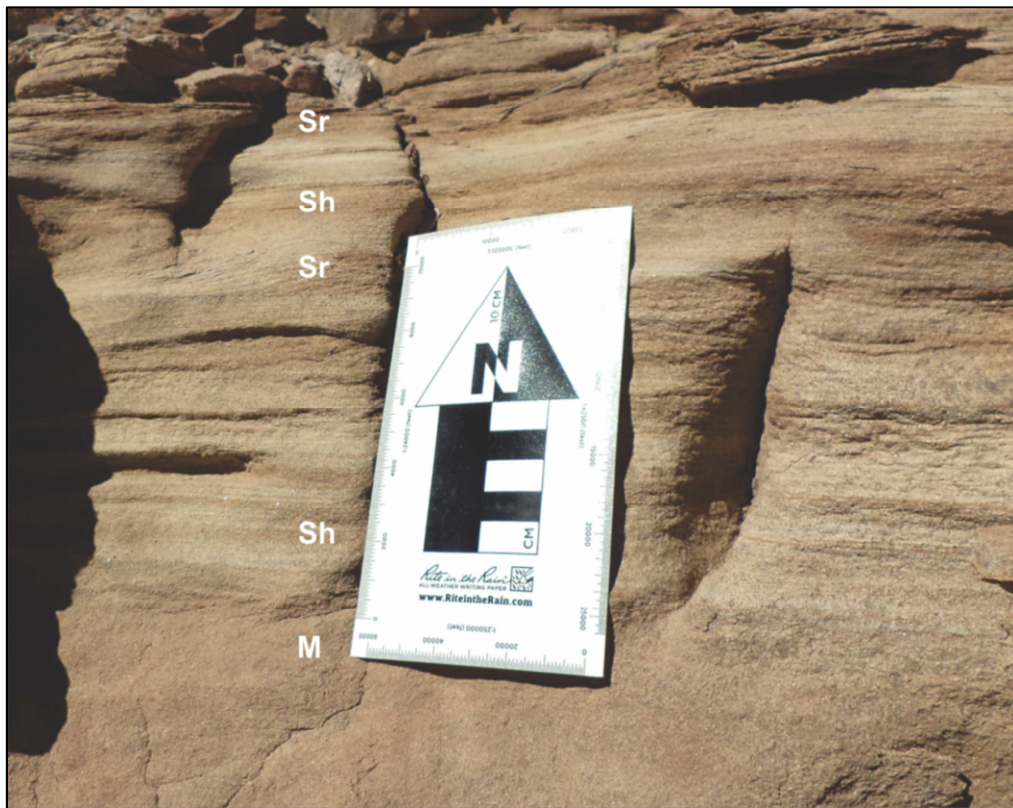


Fig. 32: Sedimentary structures present in a fine sand turbidites of the Stage IV. From bottom to top: massive (M); parallel lamination (Sh); climbing ripples (Sr); parallel lamination (Sh) and climbing ripples at the top (Sr).

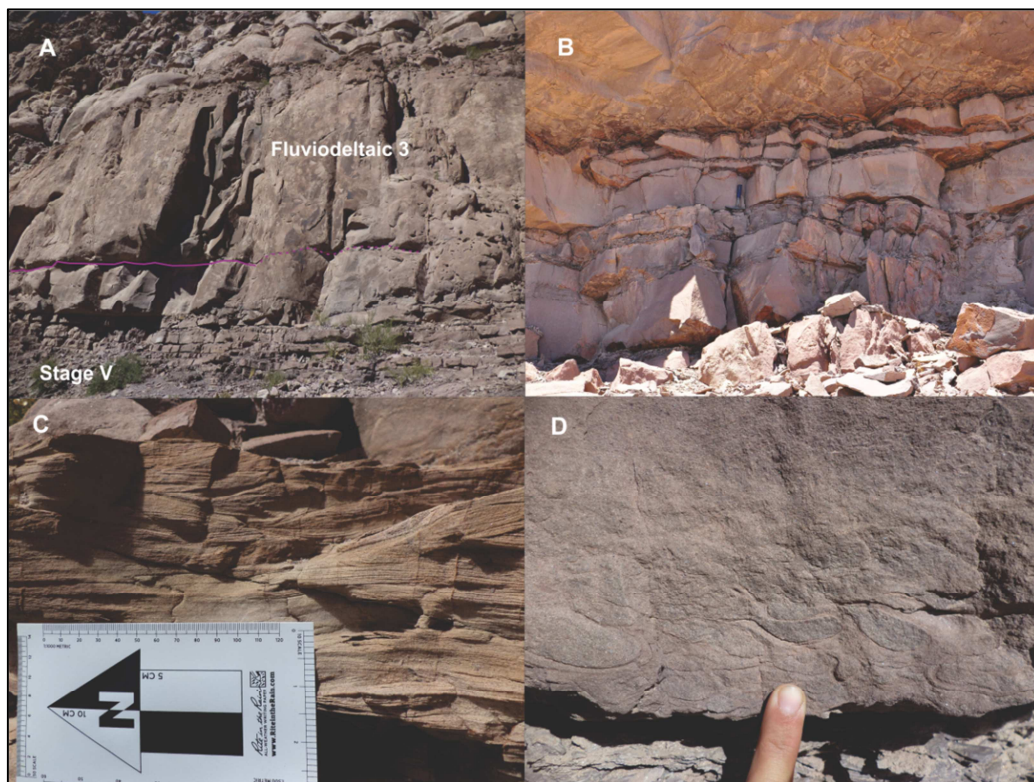


Fig. 33: (A) Contact between Upper Turbidites and Fluviodeltaic 3. Note the 3 m thick sandy bed amalgamated with turbidites to the right. (B) Detail of the deformation of the bed situated under the 3 m thick bed of (A), hammer for scale. (C) Climbing ripples in fine-grained sand. (D) Fluidisation at the bottom of the bed.

Fluviodeltaic 3

- Unit 1: starts with a 9 m thick massive sandy body (Fig. 31) which corresponds to the amalgamation of at least 2 beds that present fluidisation near the contact. The sand present bad sorting and is common the occurrences of disperse granules along the bed. The upper part of the unit is organized in thinner beds (0.5-1 m thick) with parallel lamination and ripples which indicates a main flow direction toward NW (Fig. 34). Total thickness of this unit is 12 m.

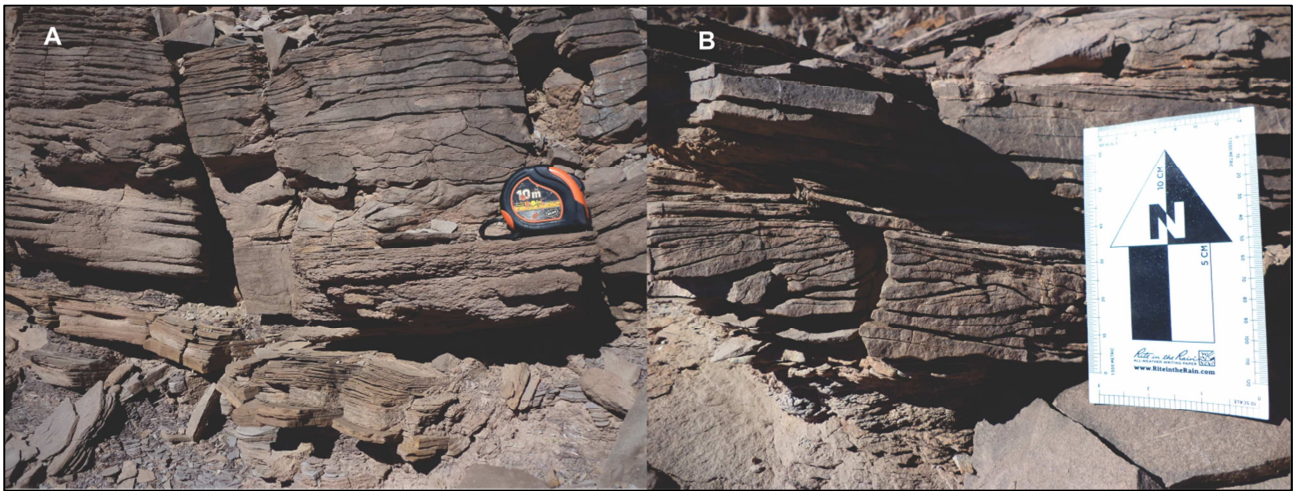


Fig. 34: (A) Amalgamated beds with parallel lamination. Note the fluidisation in the beds contact. (B) Climbing ripple.

- Unit 2: this unit can be subdivided into a lower part organized in layers 1.5 to 0.2 m thick with climbing ripples, cross-stratification and parallel lamination, sometimes deformed; and an upper part corresponding to coarse-grained sandstones with lens of very coarse sand and thick beds (6 to 12 m) of medium-grained sandstones mostly massive, but sometimes presenting lamination to the top. The thicknesses of the beds decrease upward and become more structured. The Unit finish with 0.8 m of sand grading to mudstones with levels of very fine sand with climbing ripples indicating NW-NE flow direction (Fig. 35). Total thickness: 26 m.



Fig. 35: (A) Thick sandstone layer massive with parallel lamination to the top characteristic of the first metres of upper part of the unit. (B) Parallel lamination followed by climbing ripples. (C) Top of the Unit, reddish mudstones with fine layers of sand with ripples.

- Unit 3: As the previous unit, this can be subdivided in two parts (Fig. 36 A): the lower part consists of white medium sandstones organize in two thick massive beds (13 and 7m), intercalated by 1-2 m sands bed with parallel lamination, ripples and cross-stratification indicate NW-NE flow direction. This part finish with 1 m thick of purplish mudstones with 3cm levels of cross laminated very fine sand (Fig. 36 B). The upper part began with a 6 m thick massive sandstone bed and followed by thinner and structured layers. The principal sedimentary structures are parallel lamination, climbing ripples and cross-stratification that indicate NE direction (Fig. 36 C). Total thickness: 31 m.
- Unit 4: consists of 18 m of channelized massive matrix supported conglomerates, sometimes it observed normal grading. The clasts are composed of reddish sandstones, granites and metamorphic rocks, rounded to subangular in shape. The grain size of the matrix varies from coarse sand to granules (Fig. 37).

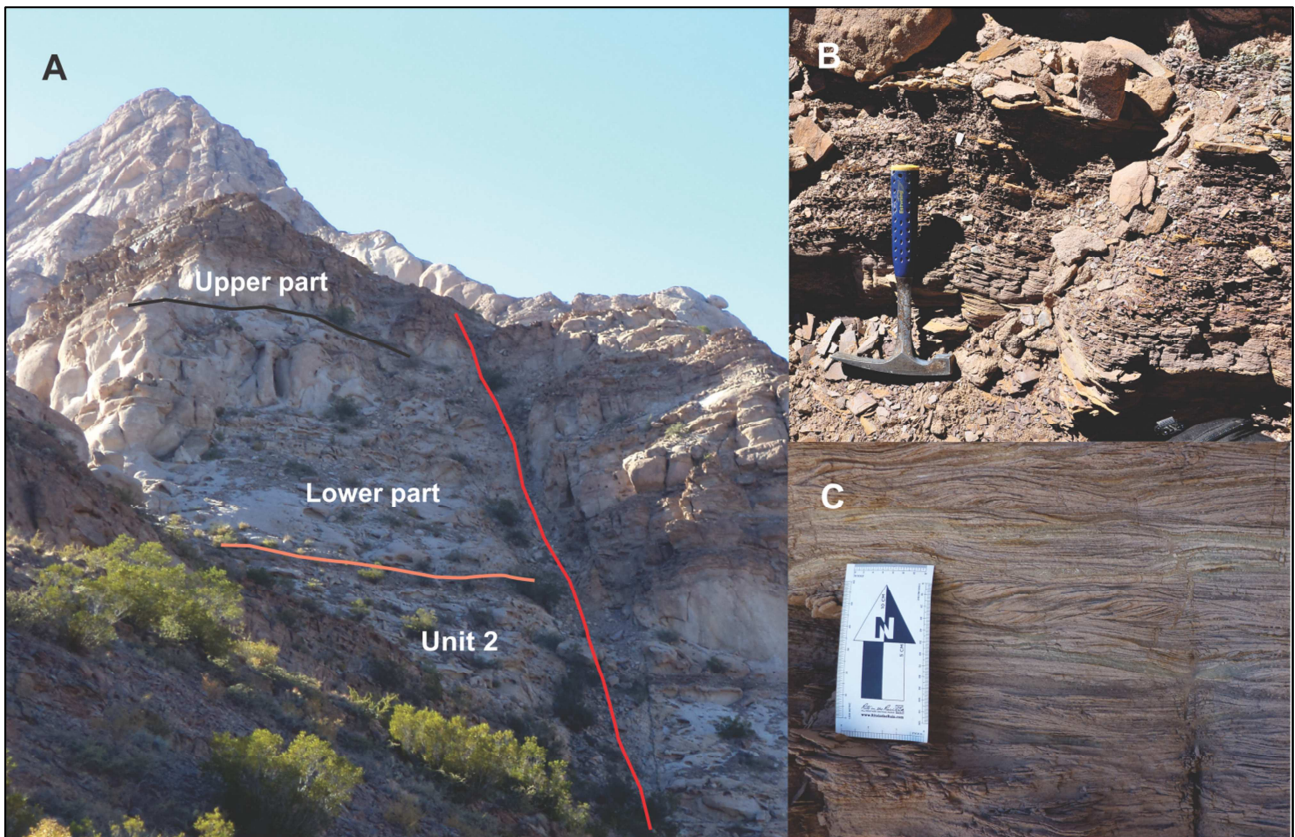


Fig. 36: Unit 3 of the Fluviodeltaic 3. (A) Outcrop view of the Unit 3, the orange line indicates the contact with Unit 2 and the black line subdivided the unit in a lower and upper part. See text for details and thickness of each unit. (B) Mudstones with millimetre sandstones layers at the top of the lower part. (C) Sandstones layer of the Upper part climbing and parallel lamination.



Fig. 37: Conglomerates of the Unit 4. (A) Lenticular matrix supported conglomerate grading to coarse-grained sandstone. The clasts are composed by fine-grained sandstones, granites and schist. The clast size varies from 70 cm to 2 cm. (B) Channel conglomerate erosive on medium-grained sandstones bed. Hammer for scale.

Green Unit

In this section the Green Unit overlays Fluviodeltaic 3 in sharp contact and it was observed polish sand surfaces. The Green Unit corresponds to thin layers of very fine sand grading to silt that are deformed and altered in the first metres (Fig. 38).

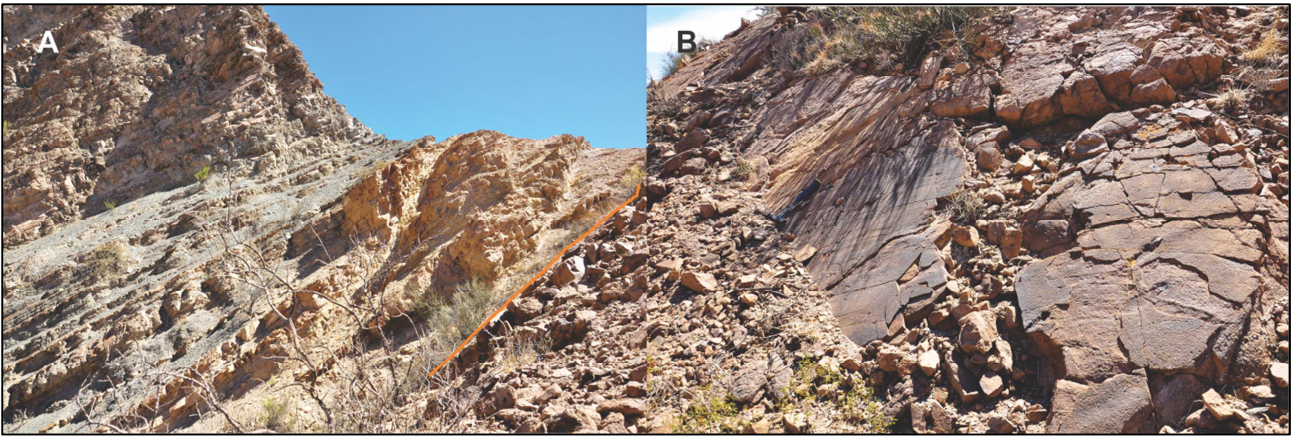


Fig. 38: (A) Contact between the Fluviodeltaic 3 (Unit 3) and the Green Unit (Orange line). (B) Detail of the polished surface (230°/49° SE) on the Fluviodeltaic 3 sandstones at the contact with the Green unit.

Log CB 4

Located at 870 m to the South from log CB 3 (Fig. 12), this section record 55 m of the Upper Turbidites and only 41 m of Fluviodeltaic 3, the Unit 3 and 4 are absent. (Attach 1)

Upper Turbidites

- Stage IV: characterized by thick turbidites (3 to 1 m thick) very distinct in outcrop, sometimes amalgamated. The grain size varies from coarse, medium and fine grained sandstones grading to mudstones with climbing ripples, parallel lamination, dewatering and loading (Fig. 39). Total thickness: 25 m.
- Stage V: thin layered turbidites consisting in fine sand grading to mudstones that show increasing grain size and bed thickness to the top. The Stage finishes with ~1 m thick bed of coarse sand grading to very fine sand followed by a 0.7 cm of fine sand (see Fig. 39 A). The abundances of climbing ripples, parallel lamination, dewatering, loading structures and groove marks and the higher mudstones proportion characterize this Stage (Fig. 40). The analysis of palaeocurrents based in ripples indicates a NW flow direction. Total Thickness: 30 m.

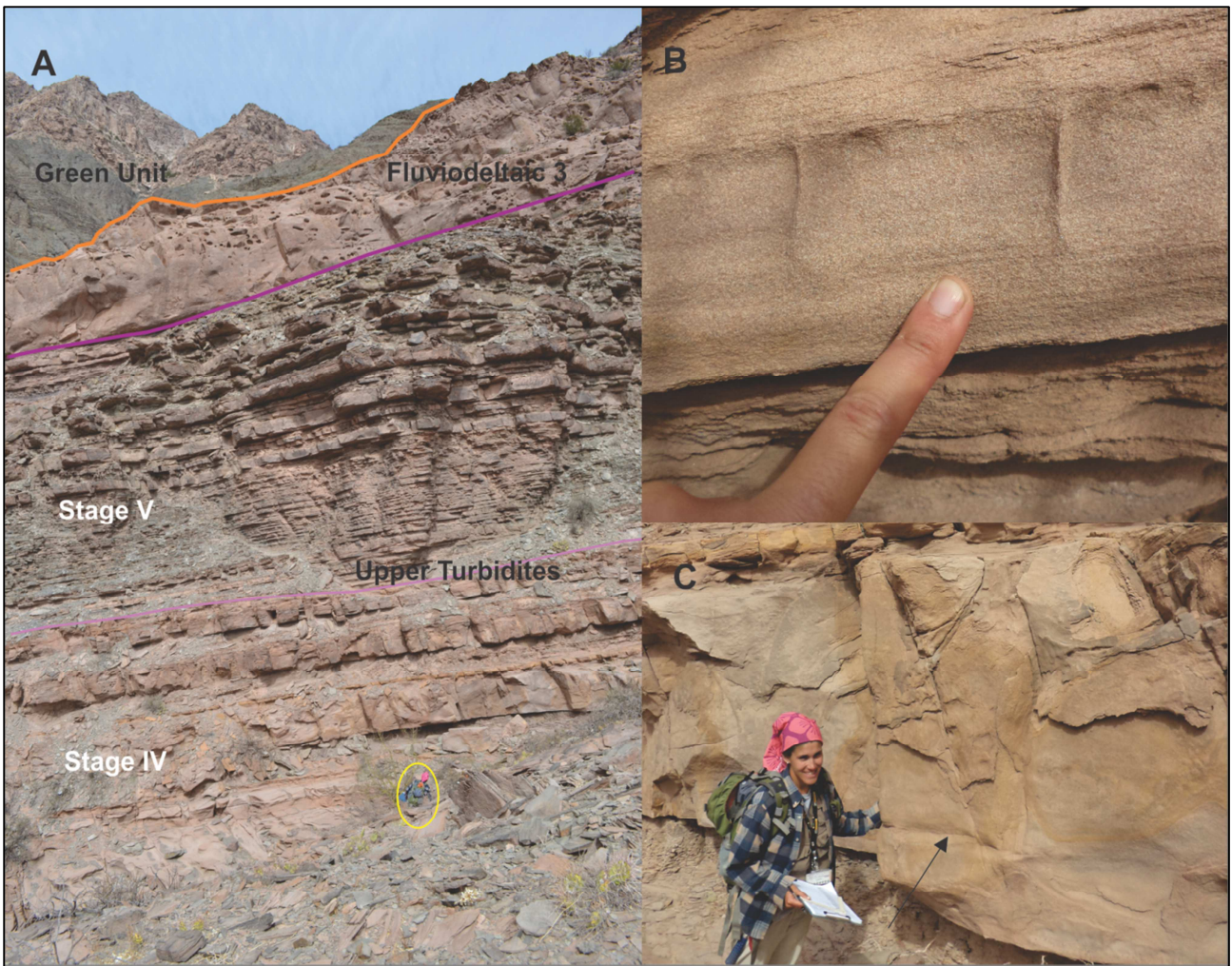


Fig. 39: Upper Turbidites general characteristics of the Stage IV. (A) Outcrop view of the log CB 4 indicating the Stage IV and V of the Upper Turbidites (light purple line), and the contact with the overlying Fluviodeltaic 3 (purple line). The upper contact with the Green Unit is indicated by the orange line. Note the differences in bed thickness between both stages (person for scale, yellow circle). (B) Parallel lamination followed by dewatering structures. (C) Bed amalgamation (black arrow).

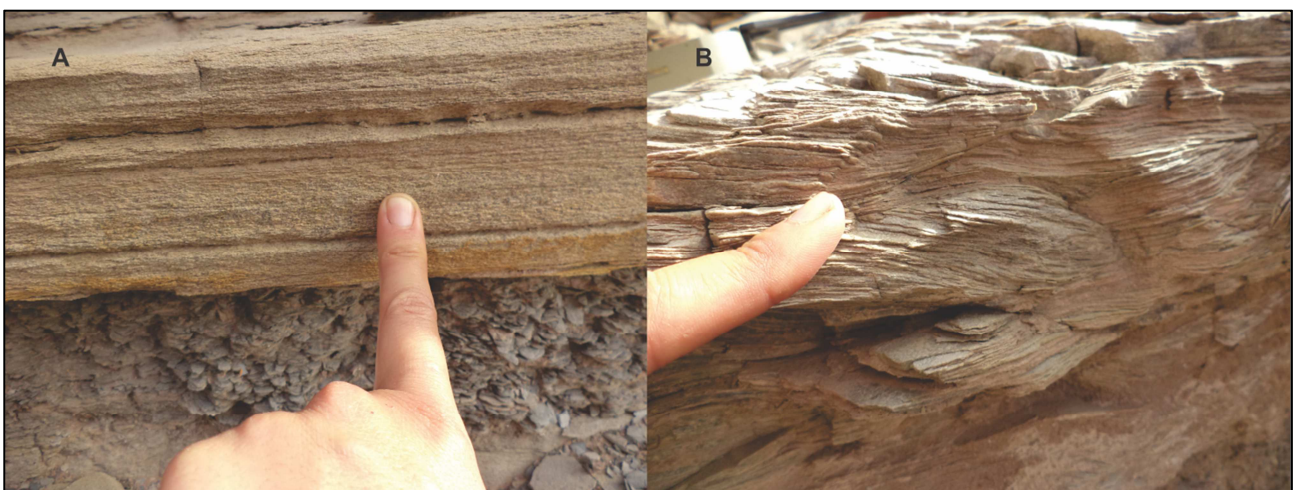


Fig. 40: Upper Turbidites main structures of the Stage V. (A) Fine-grained sandstones with parallel lamination. (B) Climbing ripples lamination.

Fluviodeltaic 3

The contact with the underlying Upper Turbidites is sharp, like in previous logs (Fig 41).

Fig. 41: Sharp contact between the Fluviodeltaic 3 and the upper Turbidites.

- Unit 1: it is characterized by lateral amalgamation of massive sandstones beds forming big layers (9 m thick). In general, the composition of the sand is quartz as principal component and mica and K-feldspar in less proportion. The grains are subrounded and bad sorted. Thickness of beds decreases to the top (0.9 to 1 m) and present parallel lamination, climbing ripples and cross stratifications, indicating palaeocurrents to NE (Fig. 42). Total Thickness: 17 m.
- Unit 2: it consists of massive thick medium-grained sandstones (~4 m thick) (Fig. 42 A) with 4 m of lenticular, matrix and clast supported conglomerates in the upper part. Normal grading is common. The granules and pebbles are concentrated at the base of the beds and consist of reddish very fine-grained sandstones, quartz and igneous rocks. The unit finishes with sandstones organized in thin layers (0.5 to 1 m thick) (Fig. 43). Total thickness: 24 m.

The Units 3 and 4 of the Fluviodeltaic 3 are absent in this area and the Unit 2 is in direct contact with the Green Unit.



Fig. 42: (A) Outcrop view of the Fluviodeltaic 3. Light orange line divided the Unit 1 and 2, and the orange line represents the contact with the Green Unit. (B) Fine-grained sandstones with climbing ripples. (C) Cross stratification at the top of a 1 m thick bed of medium-grained sandstones.



Fig. 43: Matrix supported conglomerate. The clast composition varies between fine-grained sandstones, granites and quartz.

Green Unit

This unit overlay the Unit 2 of the Fluviodeltaic 3. The deposit consists in deformed fine grained sandstones and silt that become more stratified to the top (Fig. 44).



Fig. 44: (A) contact between the Fluviodeltaic 3 and the Green Unit (orange line). (B) Deformed beds at the bottom of the Green Unit (black narrow).

Log CB 5

Located at 870 m to the South from Log CB 4 (Fig. 12) this log recorded 46 m of the Upper Turbidites and 53 m of Fluviodeltaic 3 (Attach 1).

Upper Turbidites

- Stage IV: consist in 21 m of turbidites organized in thick layers (1 to 3 m thick) of fine-grained sandstones grading to very fine sand or mudstones, sometimes amalgamated. The bed thickness decreases to the top finishing with a 20 cm thick turbidite. The sedimentary features recognized in this stage are: parallel lamination, climbing ripples, dewatering, loading structures and mudclasts. In general the thicker beds are massive (Fig. 45).
- Stage V: correspond to thin bedded turbidites (60 – 5 cm) of fine-grained sandstones grading to mudstones (see Fig. 45) it was recognized features as climbing ripples, parallel lamination, loading, groove mark and dewatering (Fig. 46). The analysis of palaeocurrents of ripples indicates north flow direction. The Stage finish with 1.5 m thick medium sand grading to very fine sand, followed by 3 amalgamated fine-grained sandstone beds. Total Thickness: 24 m.

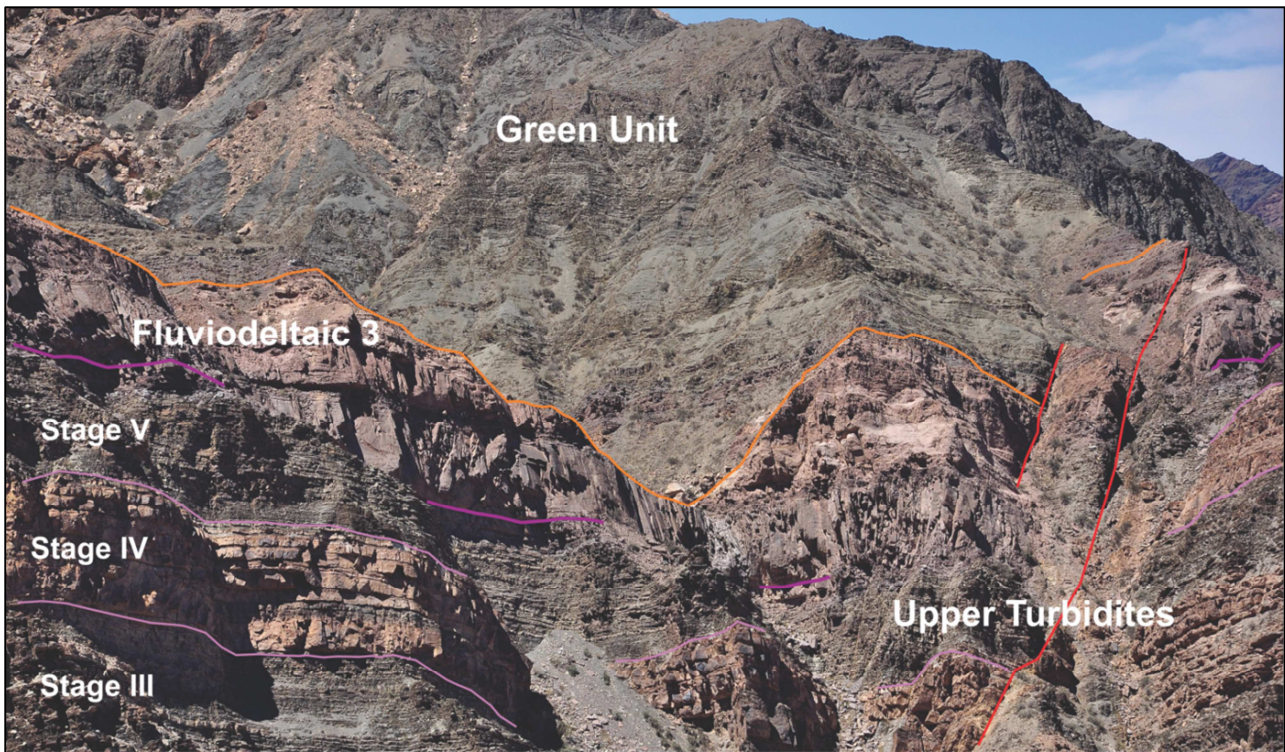


Fig. 45: General view of the section, the different Stages of Upper Turbidites is shown by the purple lines. The erosional contact between the Fluviodeltaic 3 and Green Unit is indicated by the orange line. Note the differences in thickness between Stages. Faults are indicated by red lines.



Fig. 46: Sedimentary features of the Upper Turbidites Stage V. (A) Parallel lamination at the base of the bed and fluidisation at the top. (B) Groove cast indicating direction through 330°/150°.

Fluviodeltaic 3

The contact with the underlying Upper Turbidites is sharp (Fig. 47). In this part of the Cerro Bola the Unit 4 was not present, and the Green Unit is in direct contact with the Unit 3 of Fluviodeltaic 3.



Fig. 47: Sharp basal contact of Fluviodeltaic 3 with the Upper Turbidites, indicated by the orange line.

- Unit 1: initiated with a 9 m thick poorly sorted massive medium sandstone bed. The bed thickness decrease to the top of the unit finishing with 1 m medium sand grading to mudstones with levels of fine sand with climbing ripples indicated NW-NE palaeocurrents directions. Total thickness 12 m (Fig. 48).

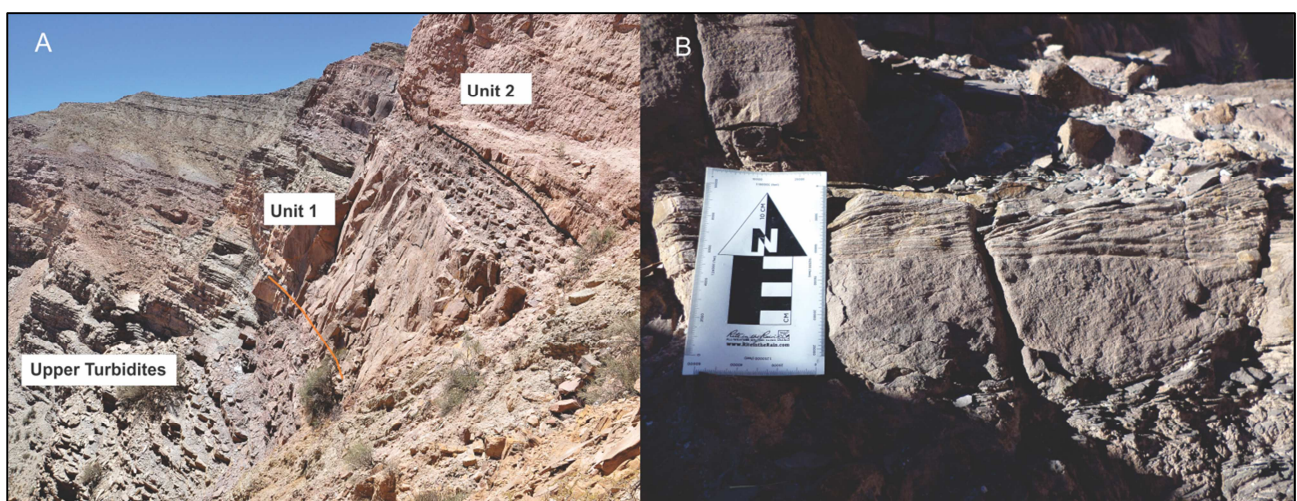


Fig. 48: Outcrop view of Fluviodeltaic 3-Unit 1 in sharp contact with the Upper Turbidites (Orange line). (A) Note the massive aspect of the 9 m thick bed that initiated the unit. (B) Fine grained sandstones in the upper part of Unit 1 showing parallel lamination following by cross-lamination at the top of the bed.

- Unit 2: characterized by presence of conglomeratic sandstone with small pebbles at the bottom, matrix to clast-supported conglomerates grading to medium-grained sandstones. The sandstones packages present parallel lamination, ripples and cross-stratification indicating a NE-SE direction. It is also common to see medium/coarse-grained sandstones associated to lens of conglomerates. The Unit 2 finished with 1m thick bed of medium-grained sandstones with parallel lamination grading to mudstones. Total thickness 35 m (Fig.49).

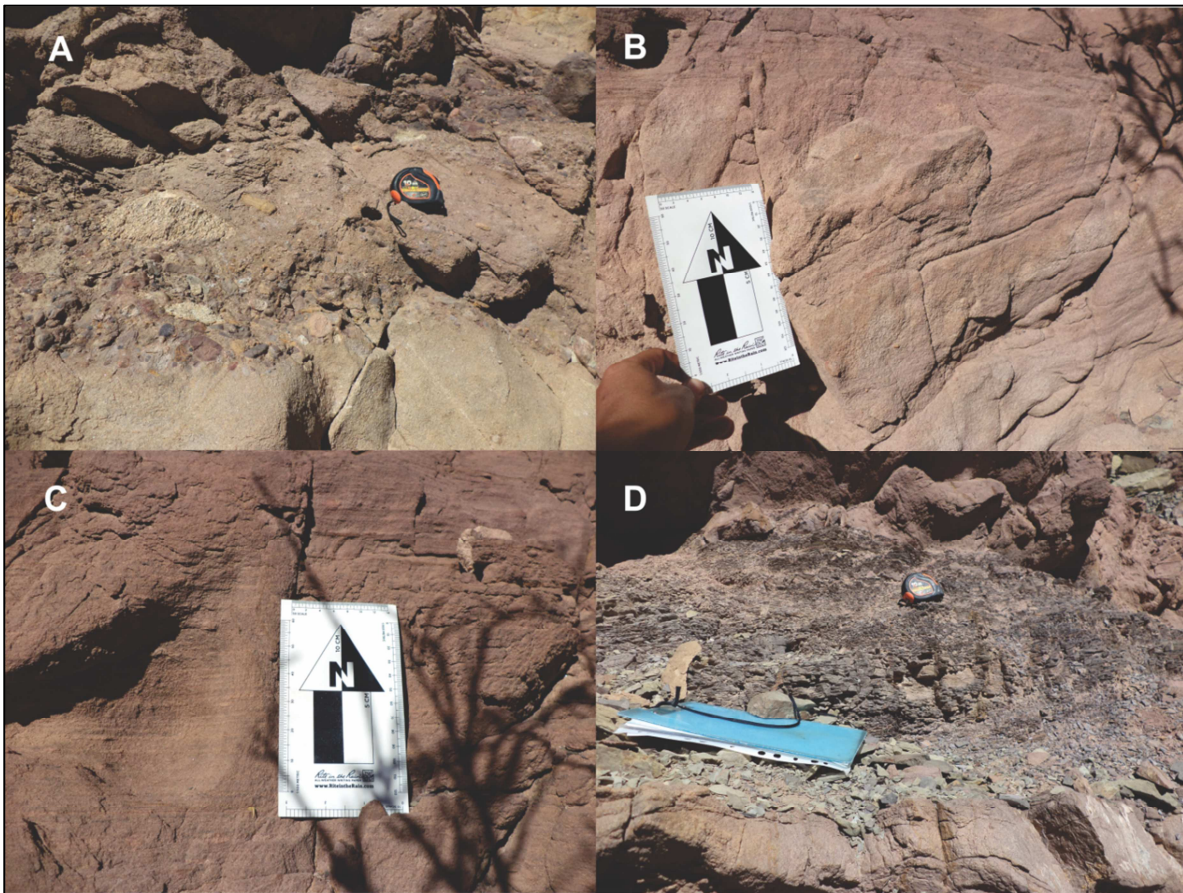


Fig. 49: Principal characteristic of Fluviodeltaic 3-Unit 2. (A) Lenticular clast support conglomerated at the base, grading to coarse sand. The clasts are subrounded and poor sorted (30 to 2 cm). The composition varies from granites, sandstones and metaphoric rocks. (B) Cross-stratification in a medium-grained sandstones bed indicating NE flow direction. (C) Parallel lamination at the top of a sand body. (D) Medium sand grading to purple mudstone at the top of the Unit.

- Unit 3: Present a total thickness of only 6 m of massive medium-grained sands beds sometimes amalgamated. The bed thickness varies from 0.5 to 2.5 m (Fig. 50).

Green Unit

The Green Unit overlays in irregular contact the Fluviodeltaic 3 (Fig 50). It corresponds to very fine-grained sandy-silty facies deformed at the first metres and showing incipient lamination. In the middle part of the deposit it was founded a metamorphic block (gneiss) surrounded by silty matrix and also lenticular layer of medium-grained sandstones with mostly granules of quartz. (Fig 51)

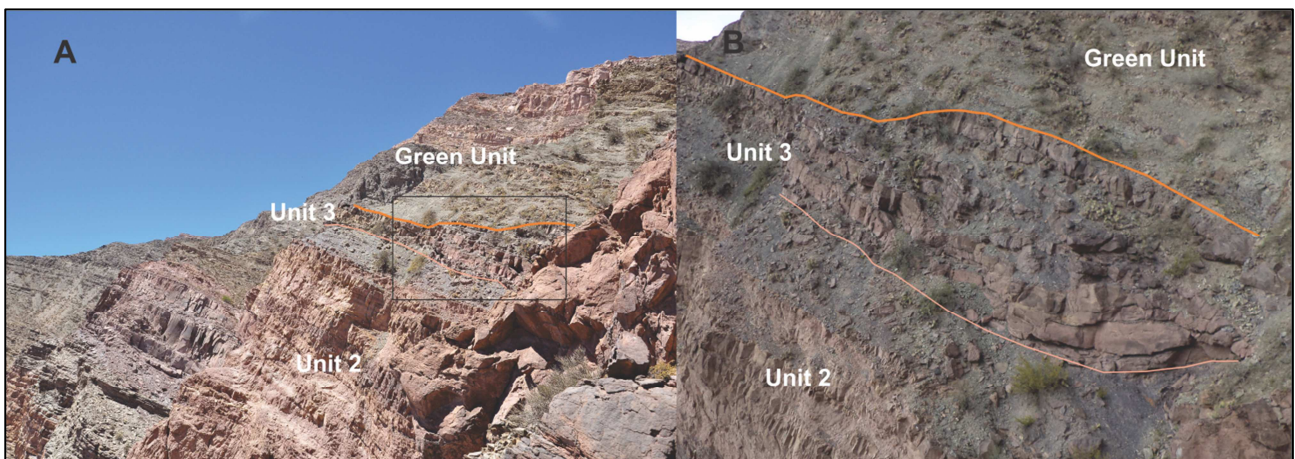


Fig. 50: Fluviodeltaic 3 _Unit 3. (A) The thicker orange line indicates the upper contact with the Green Unit. Note thinning of the Unit 3 to the left. The light orange line shows the contact between Unit 2 and 3. (B) Detail of the sand beds. lack square in A) note the deformation inside the package.

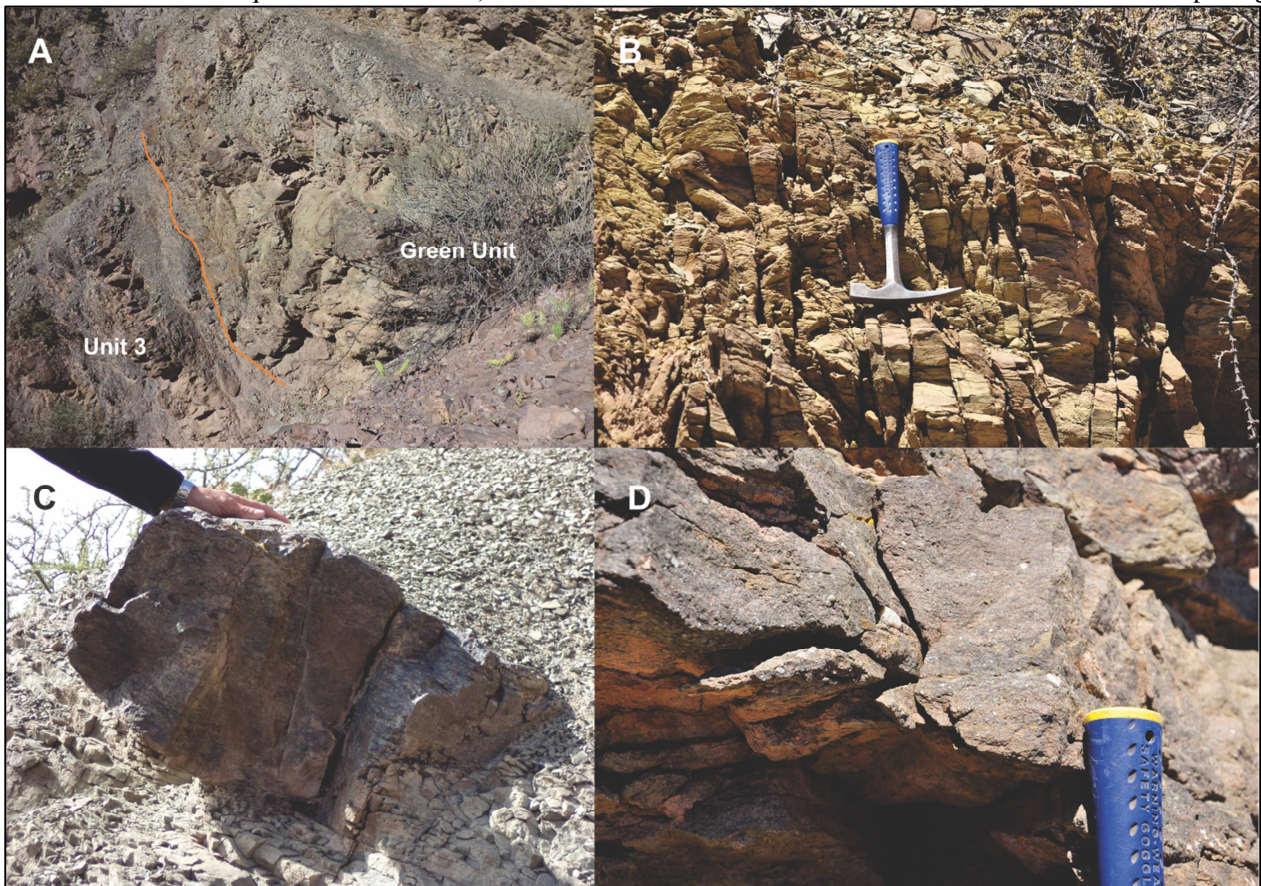


Fig. 51: Green Unit. (A) Contact between the Fluviodeltaic 3 and the Green Unit. Note the deformation of the sediment. (B) Very fine-grained sandstones and siltstones with incipient lamination. (C) Gneiss blocks immerse in a silty-sandy matrix. (D) Lenticular beds of medium-grained sandstones containing disperses granules.

Log CB 6

Located at 1.82 km to the South from log CB 5 (see Fig. 12), this log recorded ~50 m of Upper Turbidites (Stage III, IV and V) and ~142 m of the Fluviodeltaic 3 (Fig. 52). In the next step it will be described only the Stage IV and V.

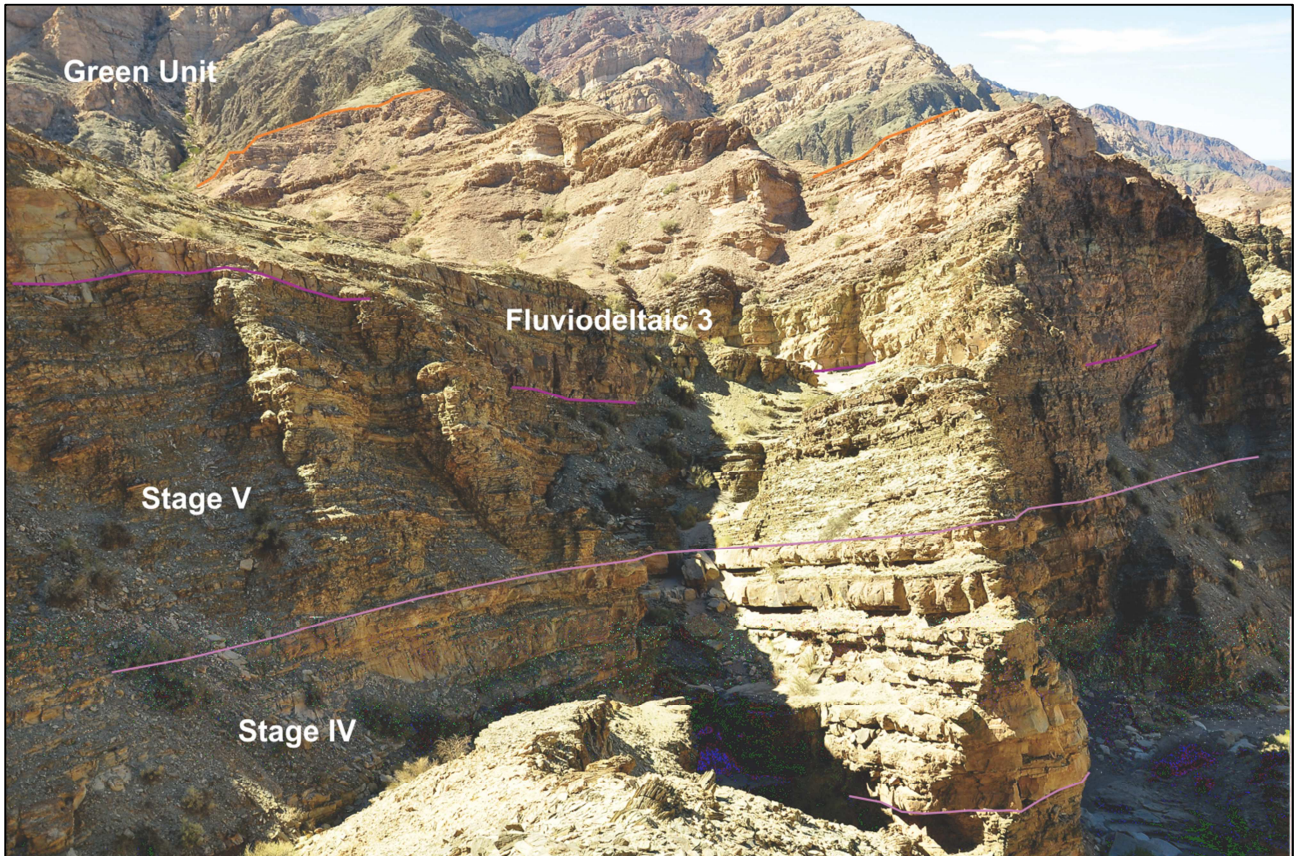


Fig. 52: Outcrop view of Log CB 6. The purple line indicates the contact between Fluviodeltaic 3 and Upper Turbidites, the light purple line the different Stages and the orange line the bottom of the Green Unit.

Upper Turbidites

- Stage IV: it consist mostly in thick sandstones turbidites (2.5 to 1 m thick), most of them product of amalgamation, intercalated with 20 cm beds (see Fig. 52). The sedimentary features recognized in this stage are climbing ripples, parallel lamination, loading, groove mark, flame structures and dewatering (Fig. 53). The palaeocurrents indicates a flow direction toward N-NW. Total thickness: 21 m.
- Stage V: it consists of fine-grained sandstones grading to mudstones organized in thin layers (50 to 5 cm) were the mud proportion is higher than sand. Climbing ripples, parallel lamination are the common sedimentary structures (Fig. 54). The bed thickness increase to

the top finishing with 1 m thick medium-grained sandstones that amalgamated with the Fluviodeltaic 3 (Fig. 55) Total thickness: 24 m.

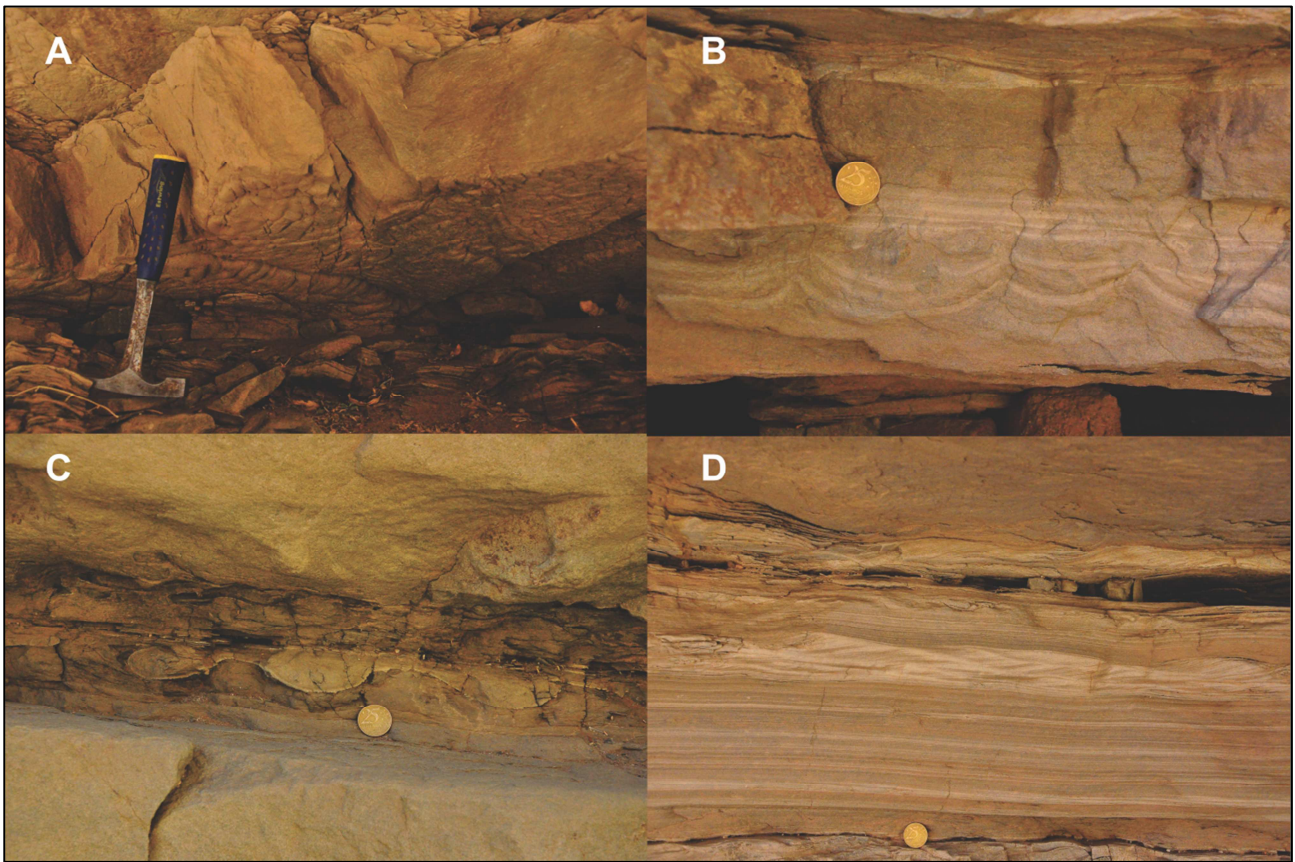


Fig. 53: Sedimentary features of the Upper turbidites-Stages IV. (A) Loading at the base of fine-grained sandstones grading to mudstones. (B) Fluid scape breaking the parallel lamination. (C) Loading and a flame structure. (D) Fine-grained sandstones bed presenting from bottom to top: parallel lamination, climbing ripples and parallel lamination.

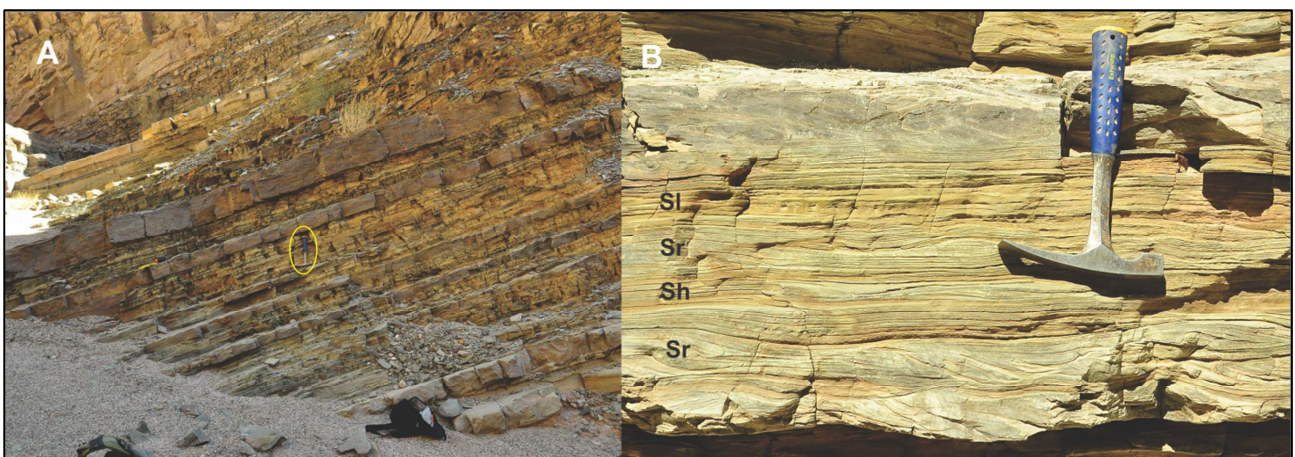


Fig. 54: (A) Bedding style of Upper Turbidites-Stage V. Note the increases of thickness to the top. (B) Sedimentary structures present in a fine-grained sandy turbidites of the Stage V. From bottom to top: climbing ripples (Sr); parallel lamination (Sh) and climbing ripples at the top (Sr). Modified from Miall (1977).

Fluviodeltaic 3

In this section it was recognized the four units of the Fluviodeltaic 3. The contact with the underlying Upper Turbidites is by amalgamation as was described above (Fig. 55).

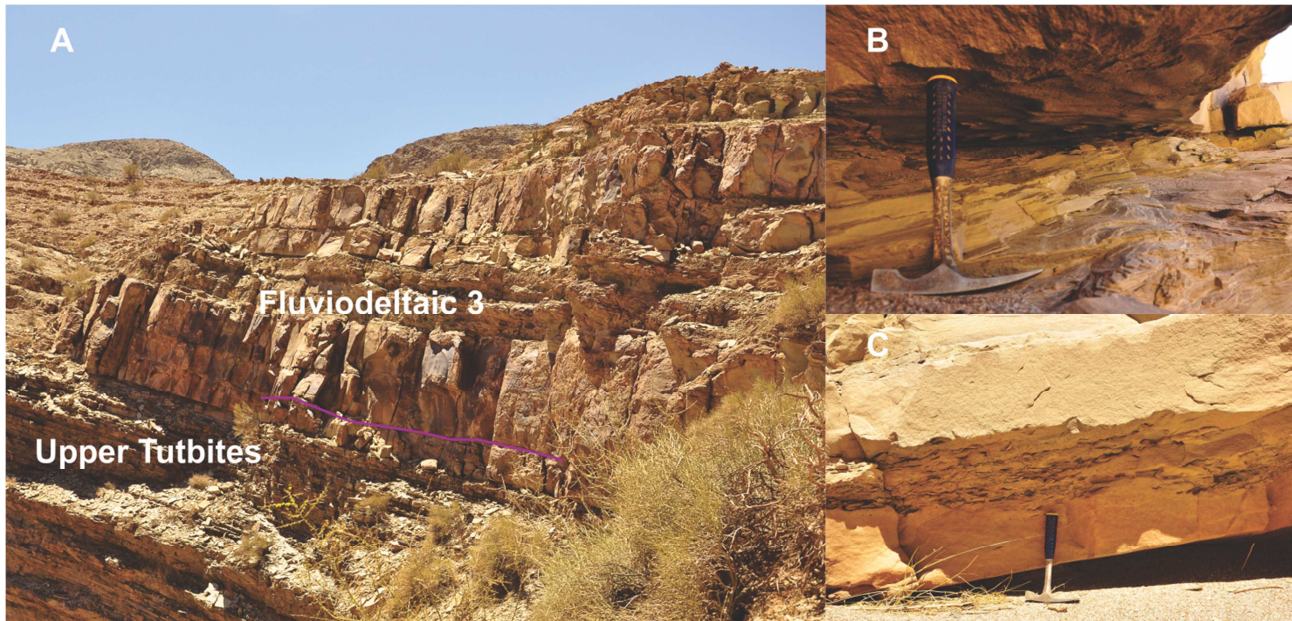


Fig. 55: Contact between the Upper Turbidites and the Fluviodeltaic 3. (A) General view of the contact (purple line). Note the beds amalgamation to the left. (B) Flute marks at the base of the last bed of Stage V (palaeocurrent to NW). (C) Mudclast product of amalgamation.

- Unit 1: Corresponds to medium-grained sandstones organized in bed ranging from 0.5 to 2 m thick, sometimes presenting loading and massive aspect at the bottom and parallel lamination and climbing ripples at the top of the bed. The thickness decreases upward finishing with 0.2 m thick beds of reddish fine-grained sandstones. These beds grade to very fine-grained sandstones with parallel lamination and climbing ripples, followed by 1 m thick deformed layer of very fine-grained sandstones and siltstones with blocks of fine-grained sandstones (Fig. 56). Total Thickness: 23 m.

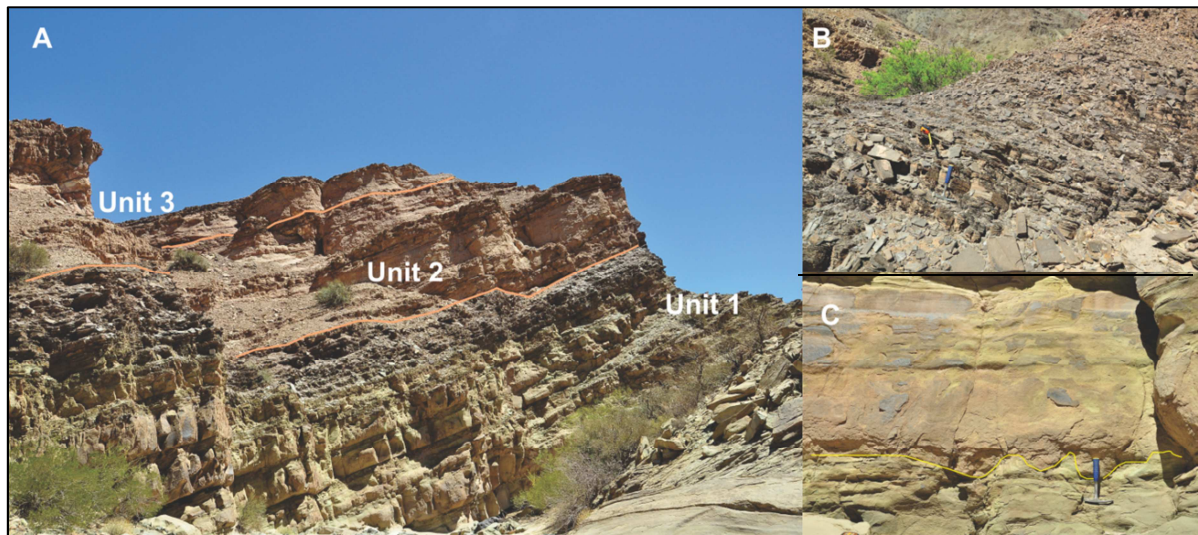


Fig. 56: (A) General aspect of Fluviodeltaic3-Unit 1, 2 and part of Unit 3. Note the decreasing bed thickness to the top of Unit 1. See text for details and thickness of each unit. (B) Detail of the upper part of the Unit 1, thin bedded fine-grained sandstones grading to very fine sand. (C) Loading structures at the base and parallel lamination at the top of Unit 1.

- Unit 2: Begin with 1.5 m thick coarse sand bed and is characterized by lenticular beds of medium-grained sandstones with parallel lamination and ripples at the top of the beds indicating NW-NE flow direction. Also, it was observed lens of very coarse sand and small to medium pebbles at the base of the bed. The bed thickness decreases upward finishing with 20-50 cm thick layers (Fig. 57). Total thickness: 21 m.

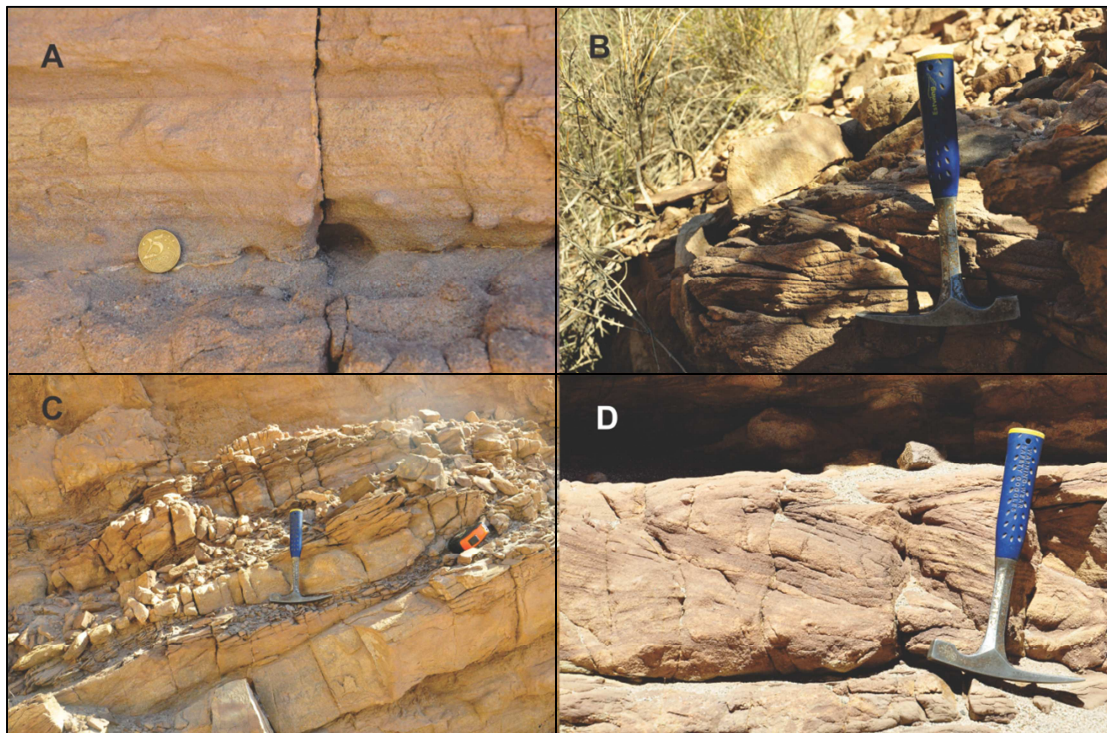


Fig. 57: Main characteristics of Unit 2. (A) Parallel lamination at the top of the bed. (B) Climbing ripples. (C and D) Lenticular cross-bedded sandstones.

- Unit 3: This unit is initiated with a 4 m thick layer, product of amalgamation of at least 3 beds, with a lens of very coarse-grained sandstones with some disperse small pebbles. This two aspects, amalgamation and lens of conglomeratic sands, characterize this Unit. Cross stratification, ripples, parallel lamination and intraclasts of very fine sand were observed in some layers. The palaeocurrents indicates a NW-NE flow direction (Fig. 58). Total thickness: 76 m.

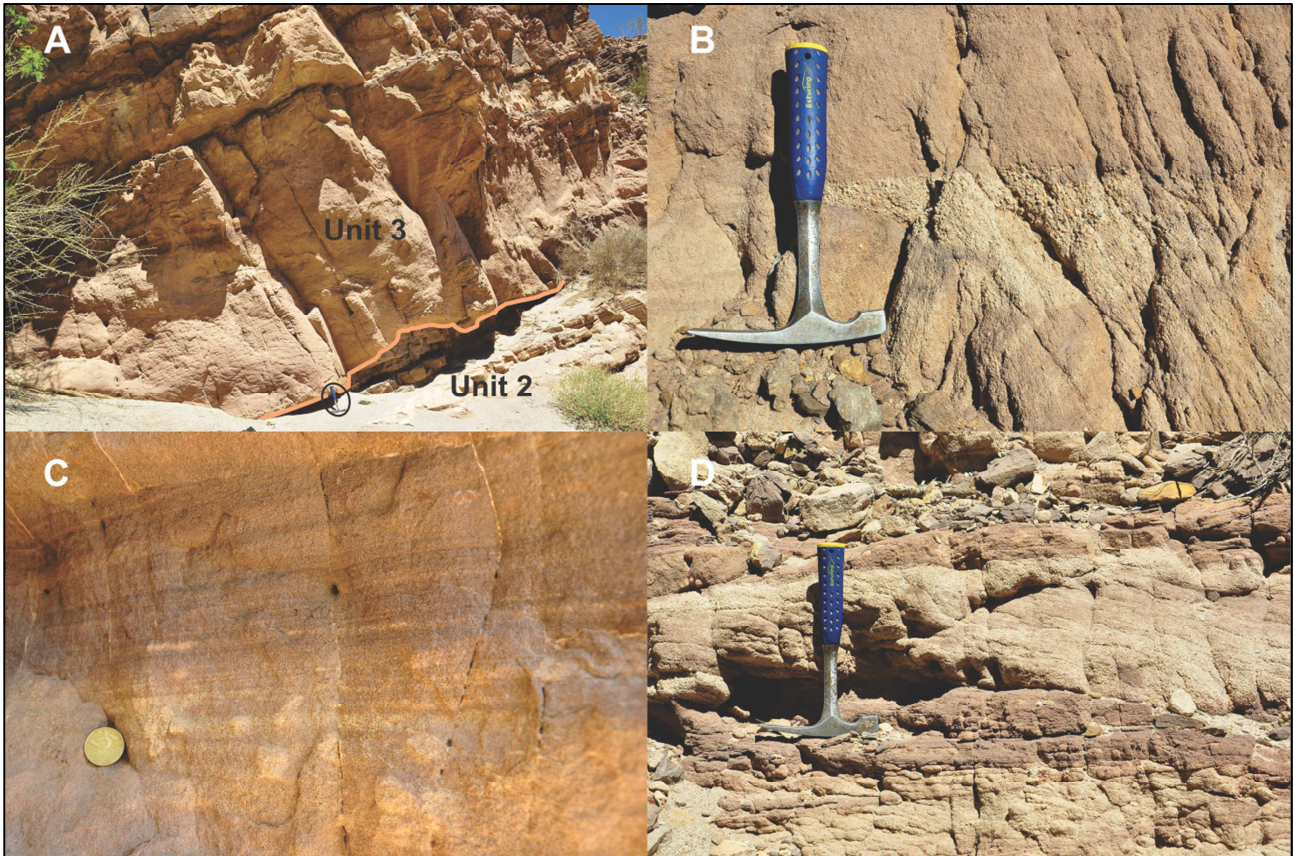


Fig. 58: Characteristics of Unit 3. (A) Erosive contact with Unit 2, note the differences in bed thickness. (Hammer for scale, black circle). (B) Lens of very coarse-grained sandstones, characteristic of this unit. (C) Parallel lamination at the top of a medium sandy bed. (D) Sandstones with through cross-stratification.

- Unit 4: Correspond to lenticular matrix supported conglomerates with no gradation that become normally graded in the upper part of the unit. Only one bed presented inverse grading followed by normal grading. In all cases 80 % of the clasts correspond to very fine-grained sandstones dark red in colour (intraclast). The unit finishes with a 6 m thick deformed bed followed by sandstones with parallel lamination (Fig. 59). Total Thickness: 21.5 m.

Green Unit

The contact with the Fluviodeltaic 3 is irregular. Corresponds to very fine sandy-silty matrix without organization with a few clast (~3 cm) (Fig. 60)

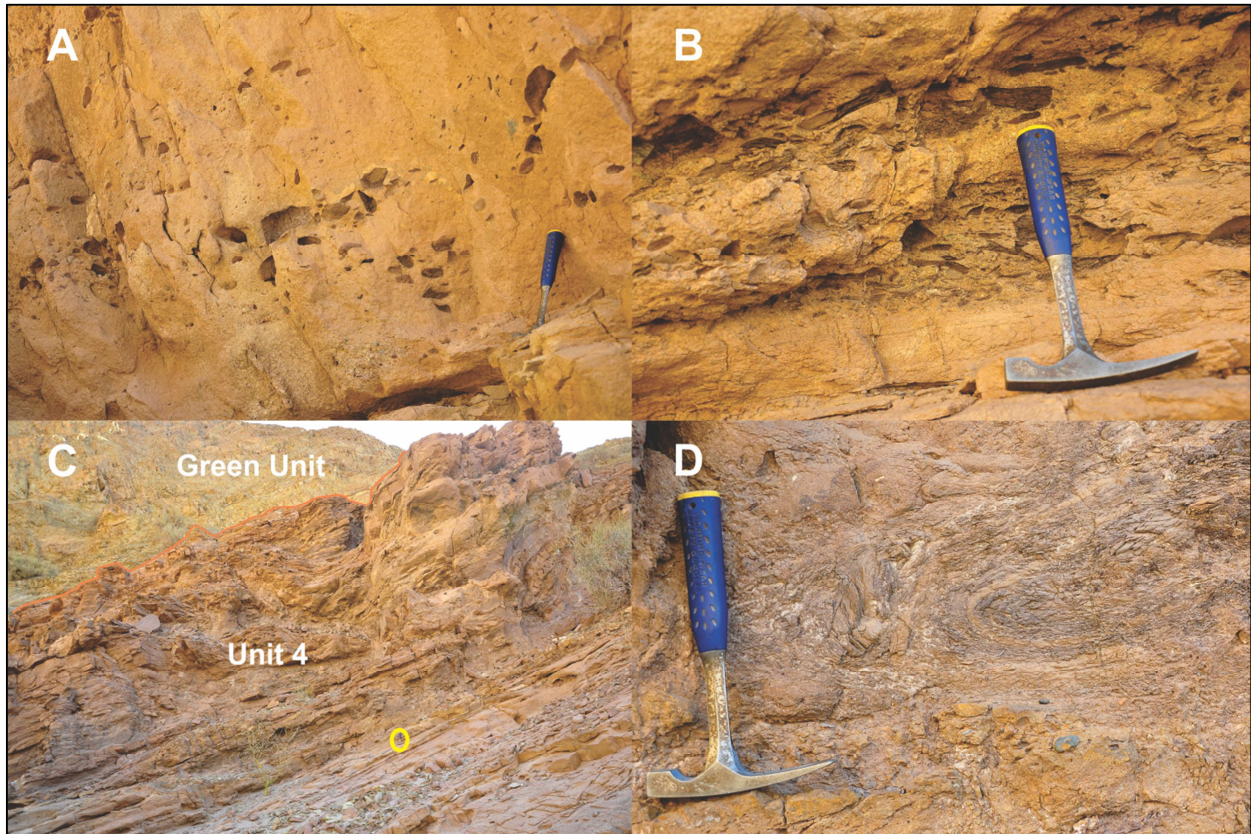


Fig. 59: General aspect of Unit 4. (A) Inverse to normal graded conglomerate. (B) Matrix supported conglomerate without organization. Note that almost all the clasts consist of dark reddish very fine-grained sandstones. (C) Deformed beds at the top of the unit near to the contact with the Green Unit. The yellow circle indicates the position of a geological hammer (30 cm). (D) Detail of the deformation depicted in C



Fig. 60: Clast of a volcanic rock immersed in a sandy- silty matrix at the first metres of the Green Unit. Hammer for scale.

Log CB 7

Located at 740 m to the South of Log CB 6 (Fig. 12), this log recorded 46 m of Upper Turbidites (Stages III, IV and V) and 157 m of Fluviodeltaic 3. (Attach 1)

Upper Turbidites

For the aim of this research only Stages IV and V are described.

- Stages IV: Characterized by fine and medium-grained sandstones turbidites, mostly organized in thick bed (4 to 0.7 m thick). Most of the packages present parallel lamination and climbing ripples, amalgamation is also common (Fig. 61). Total thickness: 19 m.

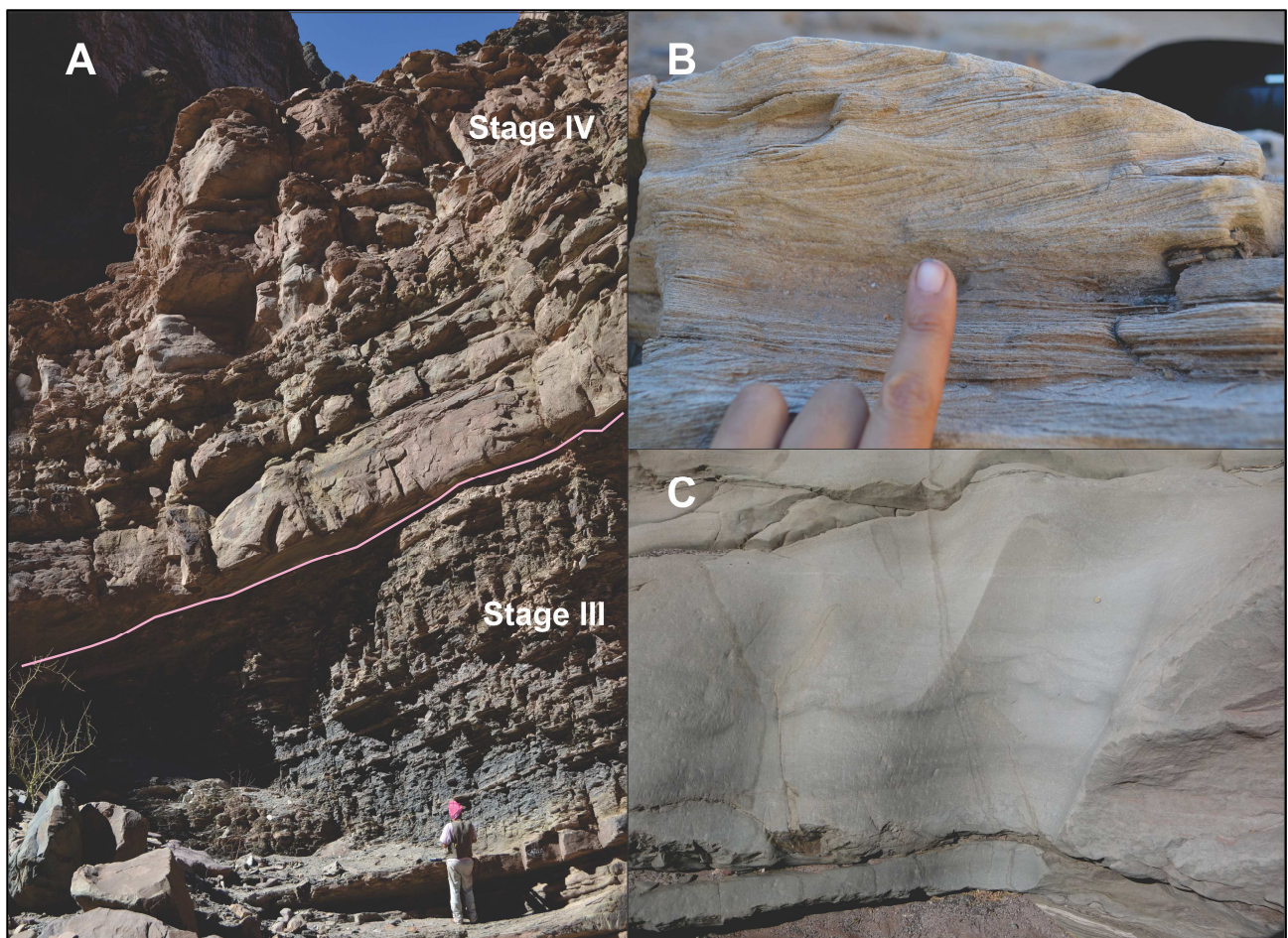


Fig. 61: Principal aspect of Upper Turbidites-Stages IV. (A) Contact with the underlying Stages III, note the differences in bed thickness. (B) Parallel lamination followed by climbing ripples in fine-grained sandstone. (C) Amalgamated beds.

- Stages V: Corresponds to thin bedded turbidites (50-5 cm thick) in which the proportion of mud is higher than sand. The most abundant sedimentary structures are climbing ripples and parallel lamination. Palaeocurrents measures indicate NW main flow direction. The bed

thickness increases upward finishing with 2 m thick fine-grained sandstones grading to mud (Fig. 62). Total thickness: ~23 m.

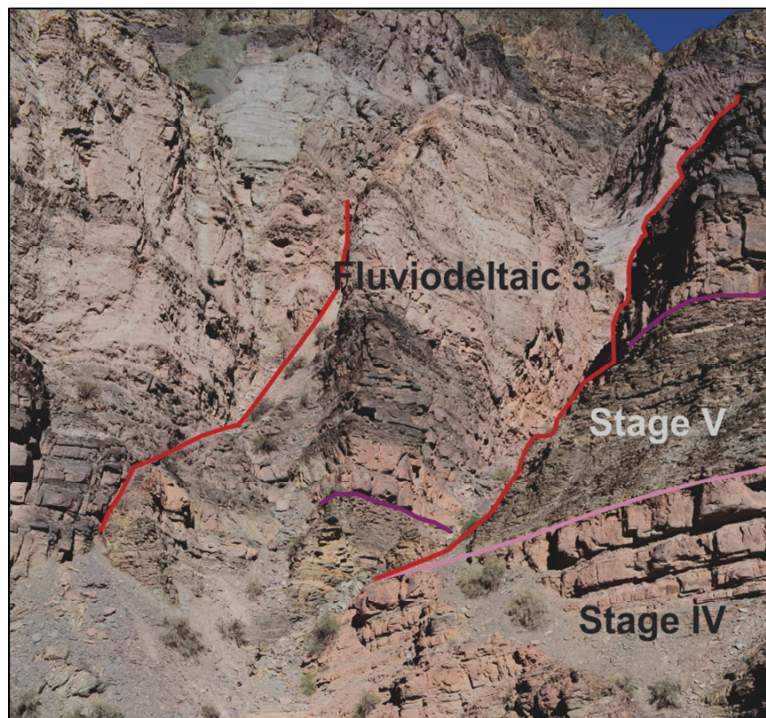


Fig. 62: Outcrop view of the Upper Turbidites Stages IV and V. Note the differences in bed thickness with Stages IV and V (pink line). Faults are indicated with red lines and the contact with Fluviodeltaic 3 with purple line.

Fluviodeltaic 3

The contact with the underlying unit is sharp (Fig. 63). In this part of Cerro Bola the four units were recognized.

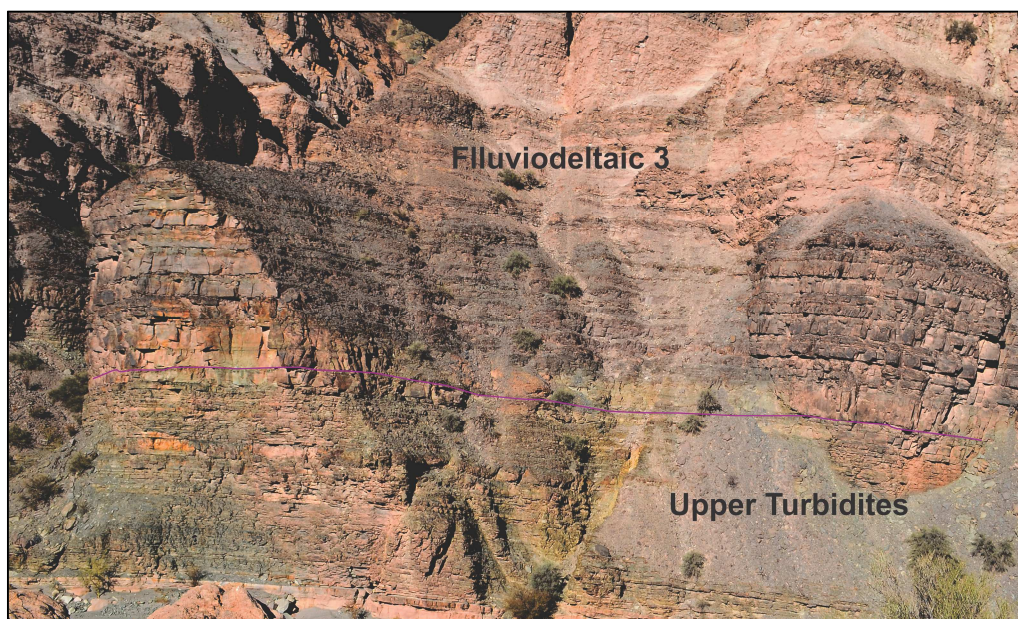


Fig. 63: Contact between the Upper Turbidites and Fluviodeltaic 3 (purple line).

- Unit 1: Consists in 1 to 6 m thick beds of massive medium-grained sandstones with parallel lamination at the top. The thickness and grain size decreases upward and the unit culminates with ~50 cm fine-grained sandstones grading to mudstones (Fig. 64). Total thickness: 25 m.



Fig. 64: General view of Unit 1, note the decreasing bed thickness to the top.

- Unit 2: At the bottom the unit composed by coarse-grained sandstones with dispersed clasts, mostly small to medium pebble, with the exception of one 60 cm rounded clast of igneous rock. The principal characteristic of this unit is the presence of cross-lamination and cross-

stratification; the measures of palaeocurrents indicate SE-NE flow direction. The grain size decreases to the top finishing with fine-grained sandstones (Fig. 65). Total thickness 33 m.

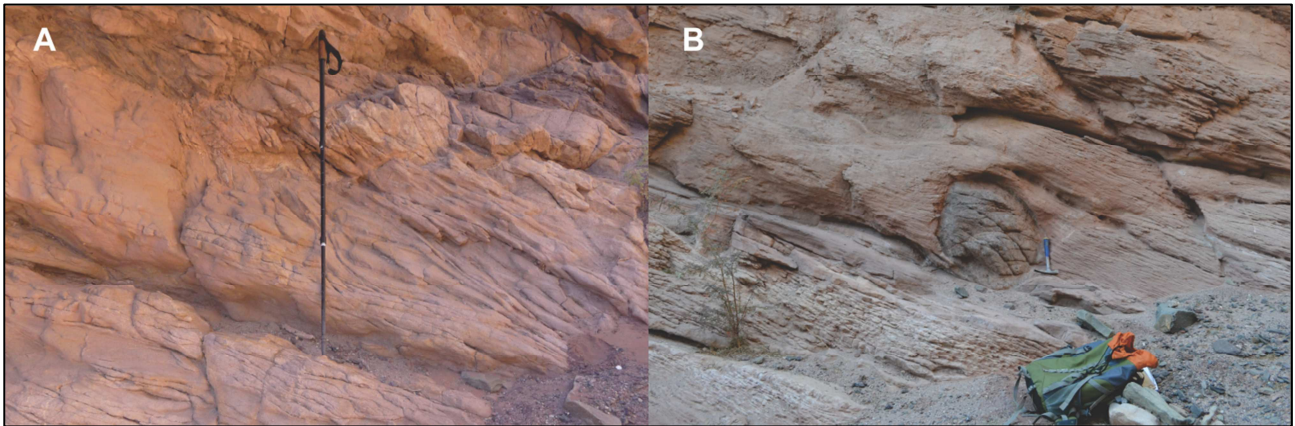


Fig. 65: (A) Medium-grained sandstones with cross-stratification. (B) Exotic rounded clast, granitoid in composition, immersed in coarse sand.

- Unit 3: characterized by medium-grained sandstone, mostly massive, that sometimes presents parallel lamination and ripples at the top. The bed thickness varies from 3 to 1 m. The presence of coarse and very coarse-grained sandstones lens is common. The cycle finishes with a ~ 7 m thick bed of medium sand with dispersed granules (Fig. 66). Total thickness: 79 m.

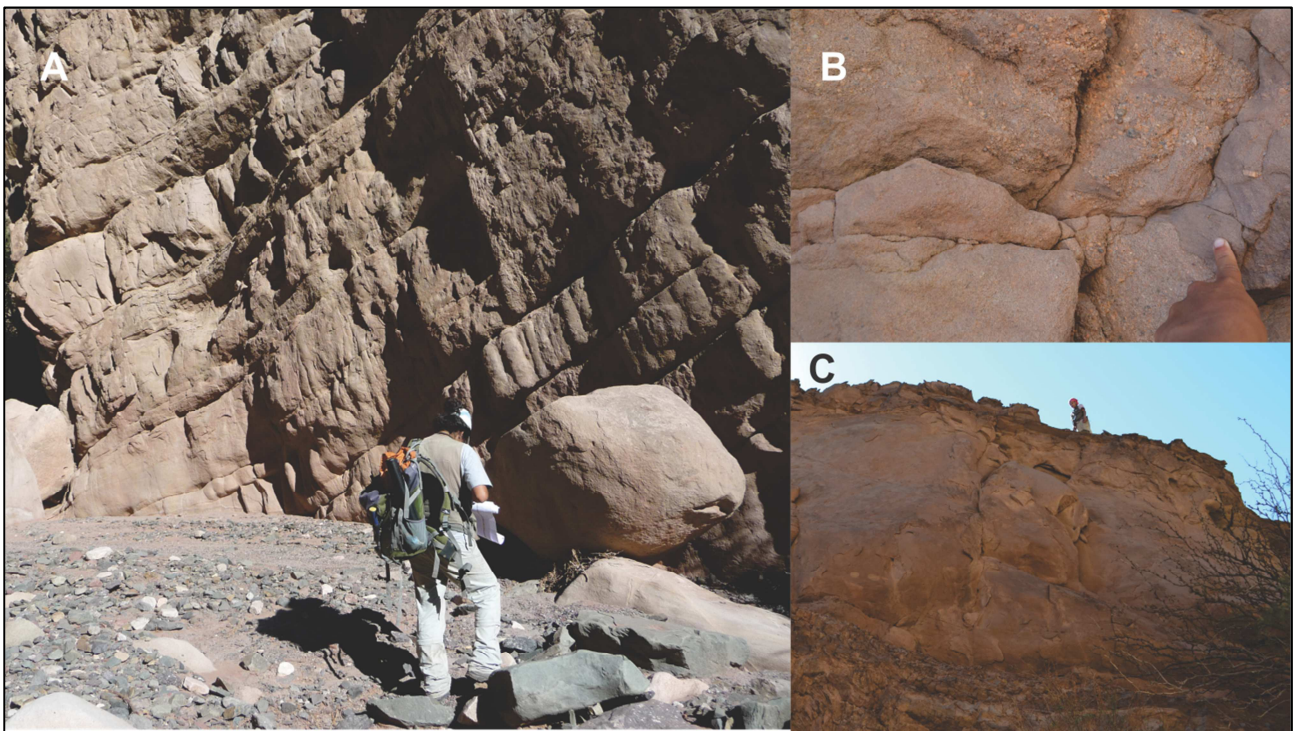


Fig. 66: Principal characteristics of Unit 3. (A) Massive medium sand organized in thin beds (3 -1 m thick). (B) Lens of very coarse-grained sandstones in a medium-grained sandstones bed. (C) 7 m thick bed at the top of the unit.

- Unit 4: consists of erosive matrix and clast-supported channelized conglomerates. The clasts are subrounded to subangular in shape with bad sorting (clast sizes varies from 2 to 30 cm). The composition varies from granites, very fine-grained sandstone (intraclasts) and metaphoric rocks at the bottom. Pa The percentage of intraclasts with tabular shape increases to the top (Fig. 67). Total thickness: 20 m.



Fig. 67: (A) Erosional contact between Unit 4 and 3. (B) Details of a matrix-supported conglomerate, the clasts composition is mostly granite, metamorphic and volcanic rocks. (C) Conglomerate in the upper part of the unit Note the increasing amount of intraclasts to the right.

Green Unit

The unit in this section began with an intercalation of silt and mud layers with dropstones, followed by a sandy-silty matrix with clast of metamorphic rocks and quartz. It was observed striation at the top of the Fluviodeltaic 3 (320°/ 140°) (Fig. 68).



Fig. 68: (A) Striation at the top of the Fluviodeltaic 3, yellow arrow. (B) Fine laminated silt and mudstones with dropstones. (C) Block in a silty-sandy matrix. (D) Granit block.

Log CB 8

This log is located at the southern part of Cerro Bola, at 1.1 km to the South of CB 7 (see Fig. 12). Comprises the Upper Turbidites, with a total thickness of 39 m including Stage III to V. The Fluviodeltaic 3, part was logged and part measure with laser.

Upper Turbidites

- Stage IV: Corresponds to medium to fine-grained turbidites organized in thick layers (3 to 0.3 m thick). The thicker beds are massive and present ripples and parallel lamination just in the upper part. The palaeocurrents measures indicated a main flow direction towards NW (Fig. 69). Total thickness: 20 m.
- Stage V: Thin bedded turbidites with high proportion of mud. The sandy beds thickness varies from 40 to 5 cm, and become thicker upward finishing with 1 m thick fine-grained sandstone. The principal features are parallel lamination and ripples (Fig. 70). Total thickness: 14 m

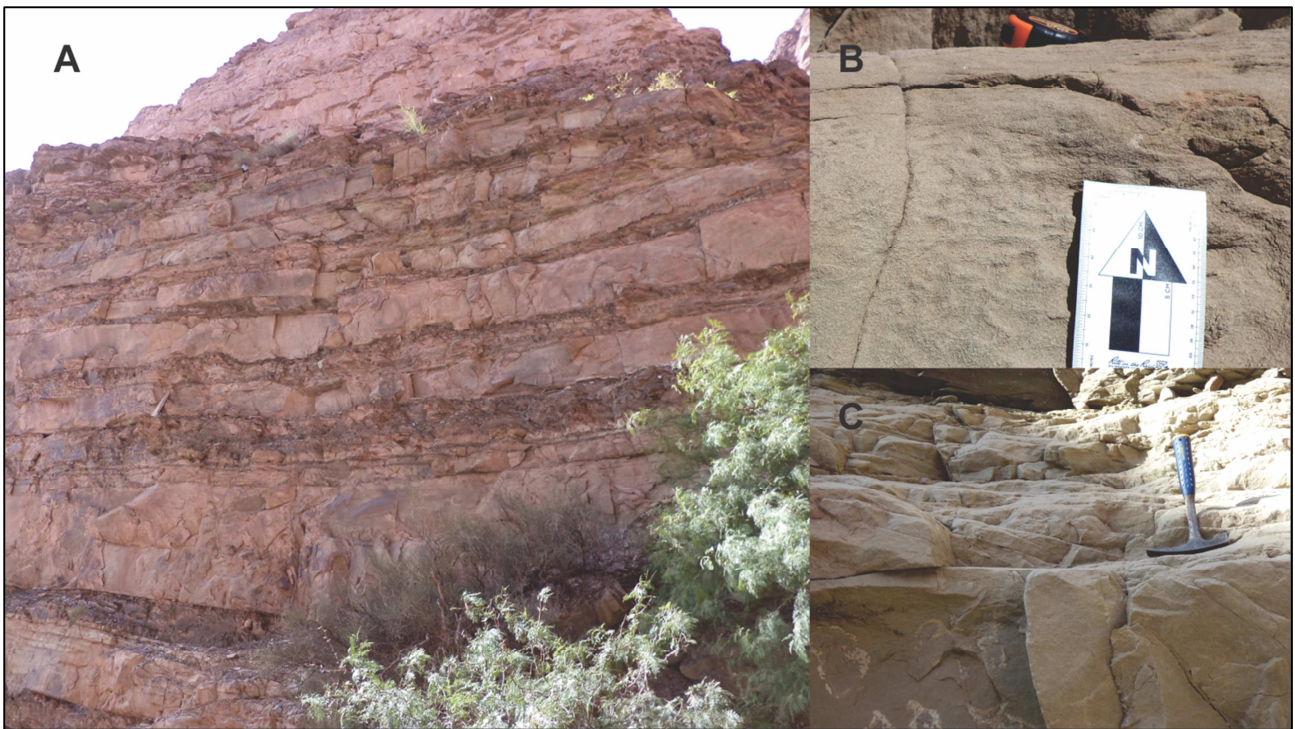


Fig. 69: (A) Thick turbidites of the Stages IV. (B) Fine-grained sandstones presenting fluidisation and parallel lamination at the top. (C) Cross-stratification in sandstones.

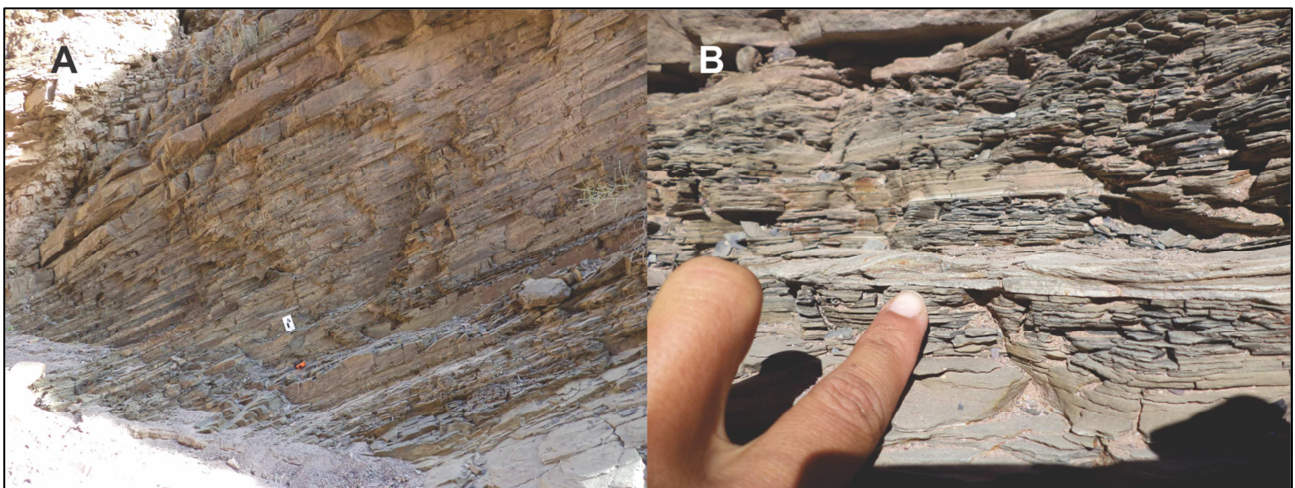


Fig. 70: Principal aspects of Stages V. (A) Outcrop view. Note the bed thickness. (B) Climbing ripple in a 5 cm thick turbidite.

Fluviodeltaic 3

In this section the Fluviodeltaic 3 are eroding the Upper Turbidites. Only Unit 1 and part of Unit 2 were logged. The rest of the sequences was measure with laser and described the principal lithological aspect.

- Unit 1: This unit is eroding the Upper Turbidites Stages V, corresponding to lenticular matrix-supported conglomerates grading to cross-laminated sandstones. Clast size varies

from granules to large pebbles, presenting bad sorting. The clasts composition is quartz, igneous and metamorphic rocks. The unit passes upward to medium-grained sandstones organized in thick layers, finishing with a 1 m thick medium-grained sandstone bed (Fig. 71). Total thickness: 39 m.

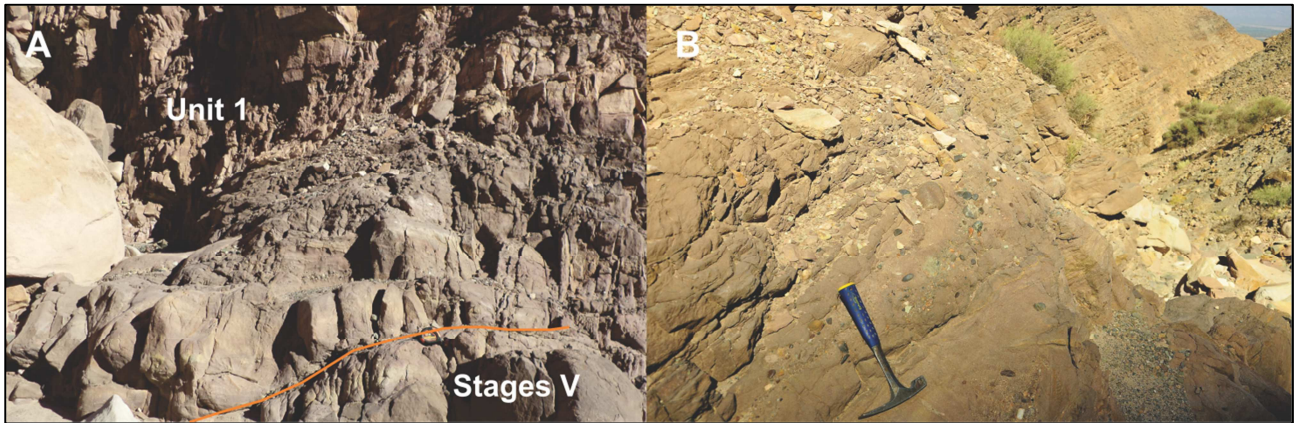


Fig. 71: (A) Unit 1 of the Fluviodeltaic 3 eroding the Upper Turbidites. The contact is indicated by the orange line. (B) Matrix-supported conglomerate with clasts sizes ranging from 5 cm to granules.

- Unit 2: Consists of thick beds of medium-grained sandstones (~ 4m thick) sometimes amalgamated (Fig. 72).
- Unit 3: Corresponded to amalgamated beds of medium-grained sandstones with dispersed granules, organized in thin layers (~1 m thick), with the exception of a thick massive bed of medium-grained sandstone (~8 m).
- Unit 4: Characterized by matrix-supported conglomerates. The composition of the clast is quartz, K-feldspar and very fine-grained sandstones intraclasts, purple in colour. The proportion of intraclasts increases to the top of the unit (Fig. 73).



Fig. 72: Fluviodeltaic 3-Unit 2. Amalgamated massive sandstones beds of Unit 2.



Fig. 73: Fluviodeltaic 3-Unit 4. Matrix-supported conglomerate, almost 85% of clast corresponds to very fine-grained reddish sandstones.

Green Unit

Consist in a silty matrix with incipient lamination at the lower part, becoming massive with concretions upward (Fig. 74).

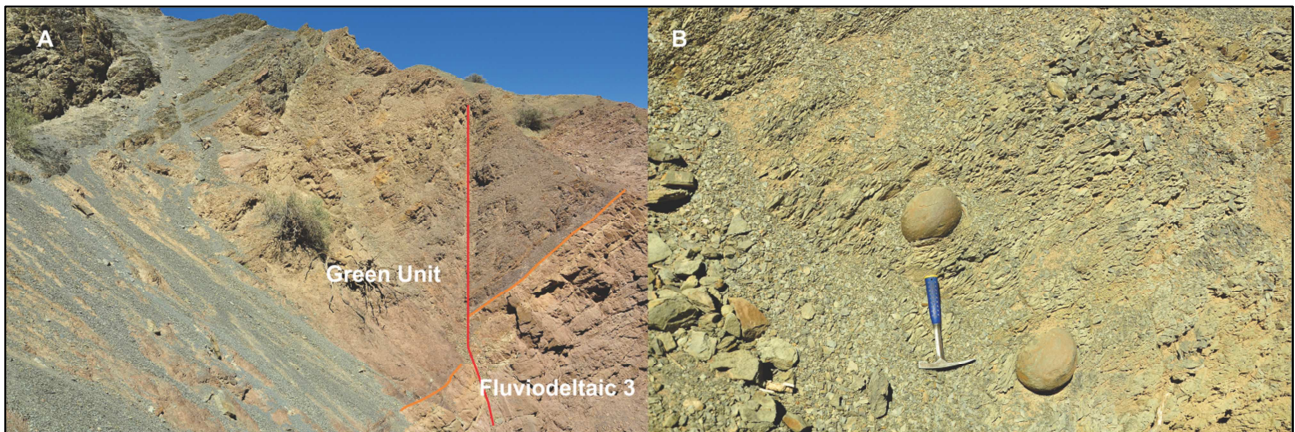


Fig. 74: (A) Sharp contact between the Fluviodeltaic 3 and the Green Unit (orange line). The red line represents a fault. (B) Concretions in a silty matrix of the Green Unit.

5.1.2 *PROVENANCE ANALYSIS*

In order to understand the relationship between the Upper Turbidites and Fluviodeltaic 3, in parallel with the palaeocurrents analysis (see attach 1), provenance analyses were made. Sampling intervals were selected to represent the main units of each sequence at the North (Log CB 1) and South (Log CB 7) of Cerro Bola. A total of 9 samples, 4 from Upper Turbidites (Stages III, IV and V) and 5 from Fluviodeltaic 3 (Unit 1, 2 and 3) were analysed (Fig. 75).

Sandstones sample were thin sectioned, using blue tint to see porosity, and point counting (50 point per sample) (Table 2). The date was plotted into QFL and QmFLt diagrams. Provenance discriminations are based on schemes by Dickinson et al. (1983) and consider the hierarchy of different depositional environments for provenance interpretation, as defined by Ingersoll et al. (1993) (Fig. 76).

The data indicates that both Upper Turbidites and Fluviodeltaic 3 correspond to feldspatharenites and indicate provenance from continental block of the plutonic-metamorphic basement of Sierras Pampeanas and Famatina Systems, both of Pre-Cambrian in ages.

This results are in agreement with the data published by Net & Limarino (2006) for Cerro Guandacol, also known as Sierra de Maz (see Fig 1), located ~7 km to north of Cerro Bola.

They analysed 19 samples of the interval DI-3, correlative with the Upper Turbidites and Fluviodeltaic 3 in the area of Cerro Bola, and point counting 300-500 grains per sample. The results proposed a progradation of the basement petrosome from the eastern-sourced, plutonic-metamorphic Sierras Pampeanas and Sierra de Famatina systems at the time of the deposition (Net & Limarino, 2006) (Fig. 77).

The provenance analysis is consistent with the palaeocurrents founded in Cerro Bola which show a main flow direction toward NW.

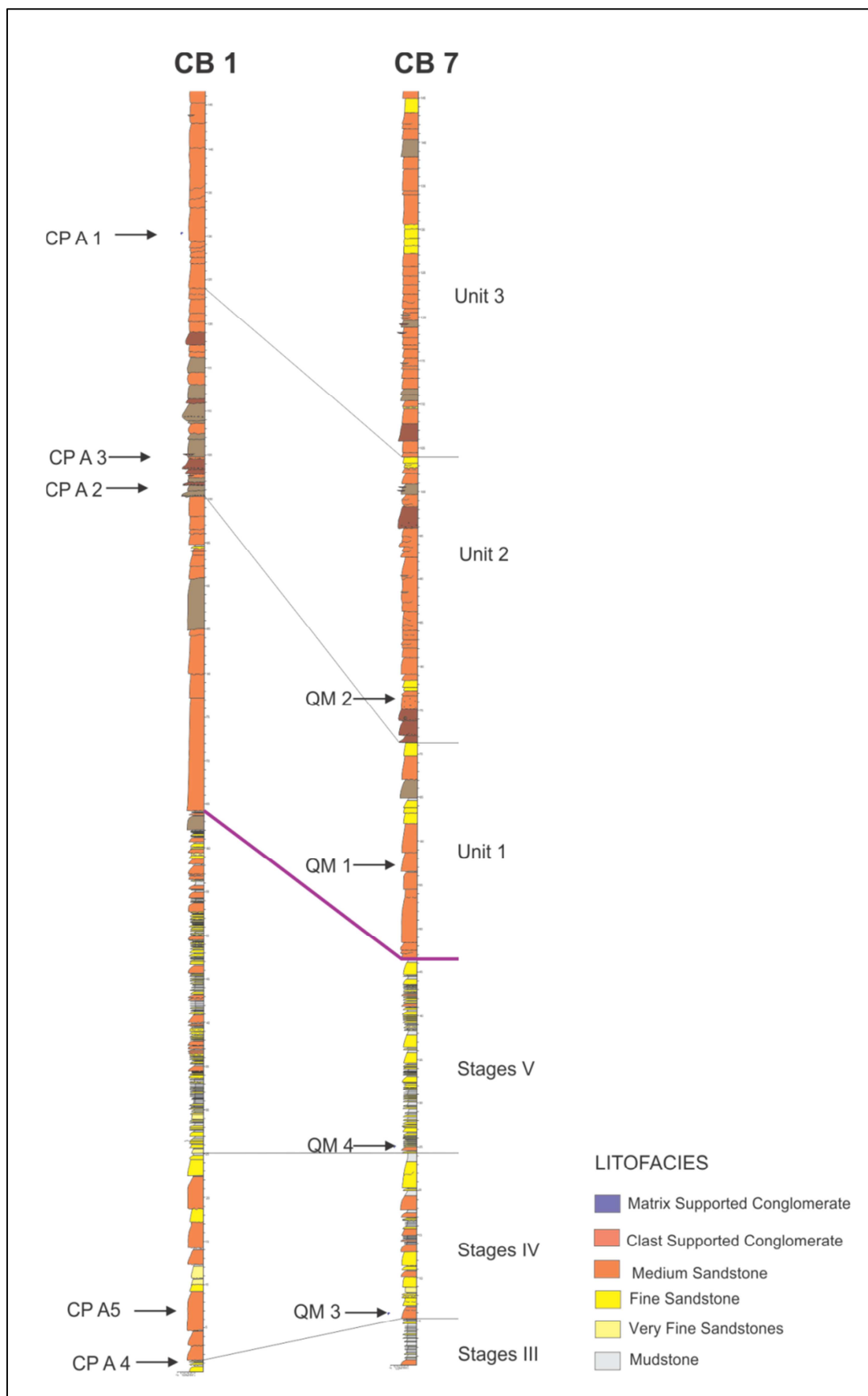


Fig. 75: Part of log CB 1, located at the North and CB 7 located at the South of Cerro Bola, indicating the sampled intervals.

Unit	Sample	Qm	Qp	Plg	FK	L	Q	F	Lt	Location		
Upper Turbidite	CP A4	27	4	13	1	2	31	17	6	NORTH		
	%	54	8	26	2	4	62	34	12			
	CP A5	21	3	6	6	2	24	24	5			
	%	42	6	12	12	4	48	48	10			
Fluvio-deltaic 3	CP A3	24	2	4	4	4	26	20	6			
	%	48	4	8	8	8	52	40	12			
	CP A1	28	5	4	0	1	33	16	6			
	%	56	10	8	0	2	66	32	12			
Fluvio-deltaic 3	CP A2	26	3	7	1	0	29	21	3			
	%	52	6	14	2	0	58	42	6			
	Upper Turbidite	QM 3	25	1	10	9	0	26	24		1	SOUTH
		%	50	2	20	18	0	52	48		2	
QM 4		23	2	5	10	1	25	24	3			
%		46	4	10	20	2	50	48	6			
Fluvio-deltaic 3	QM 1	20	2	12	9	1	22	27	3			
	%	40	4	24	18	2	44	54	6			
	QM 2	22	2	12	5	2	24	24	4			
	%	44	4	24	10	4	48	48	8			

Table 2: Summary of point-counting data of Upper Turbidites and Fluviodeltaic 3 from log CB 1 and CB 7. Qm=monocrystalline quartz; Qp=polycrystalline quartz; FK=K-feldspar; Plg=plagioclase; L=lithic; Q= Qm+Qp; F= Fk +Plg; Lt= L+Qp.

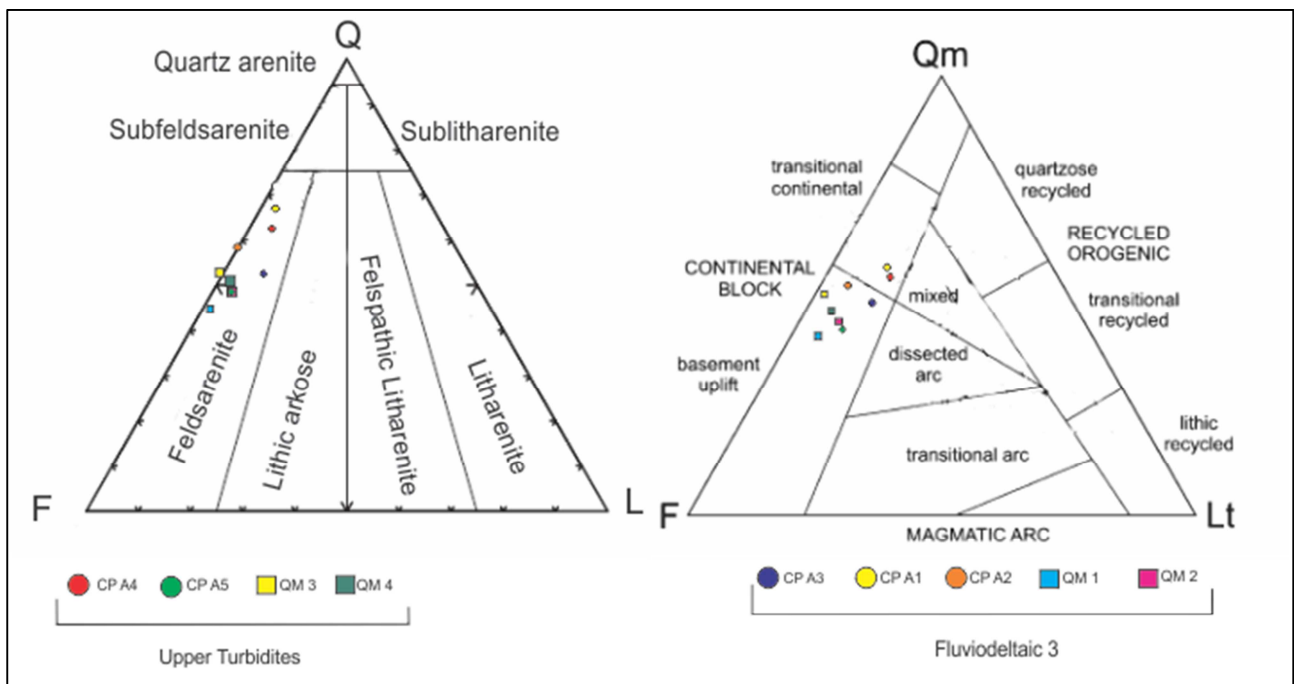


Fig. 76: Plot of the samples analysed in a QFL diagram (Folk et al., 1974) and QmFLt provenance diagram after Dickinson et al. (1983)

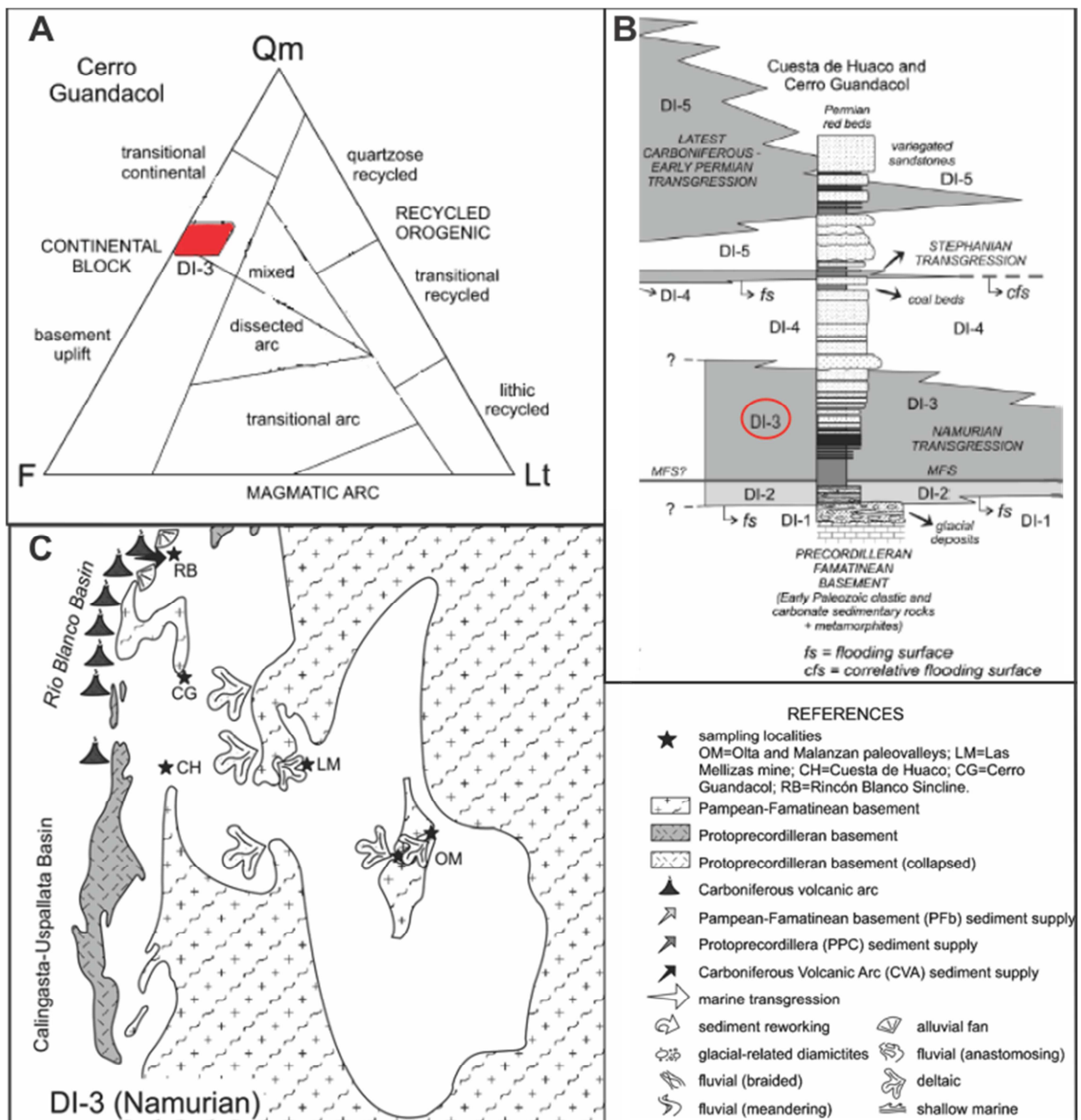


Fig. 77: Data from Net Limarino (2006). (A) QmFLt detrital modes of sandstones of interval DI-3 at Cerro Guandacol indicating a provenance from continental block (n=19). Provenance diagram after Dickinson et al (1983). (B) Integrated profile at Cerro Guandacol showing regionally correlatable chronostratigraphic surfaces that delineate depositional intervals. The deposits studied in this work are correlatable with DI-3 (red circle). (C) Model for the sedimentary infill of Paganzo Basin during the interval DI-3. Paleogeography based on interpreted maximum areal extent of the basin following Salfity & Gorustovich (1983)

The porosity analysis reveals that the Upper Turbidites not constituted good reservoir due the almost inexistent pore space, showing only secondary porosity produce by fractures (Fig. 78). By the other hand the Upper Fluviodeltaic 3 present high porosity in the North (CB 1), with the exception of sample CP-A3 (Unit 2), that presents bad sorting and higher percentage of

matrix than CP-A2 and CP-A3 (Fig. 79). At South the Fluviodeltaic 3 not showed porosity (Fig. 80).

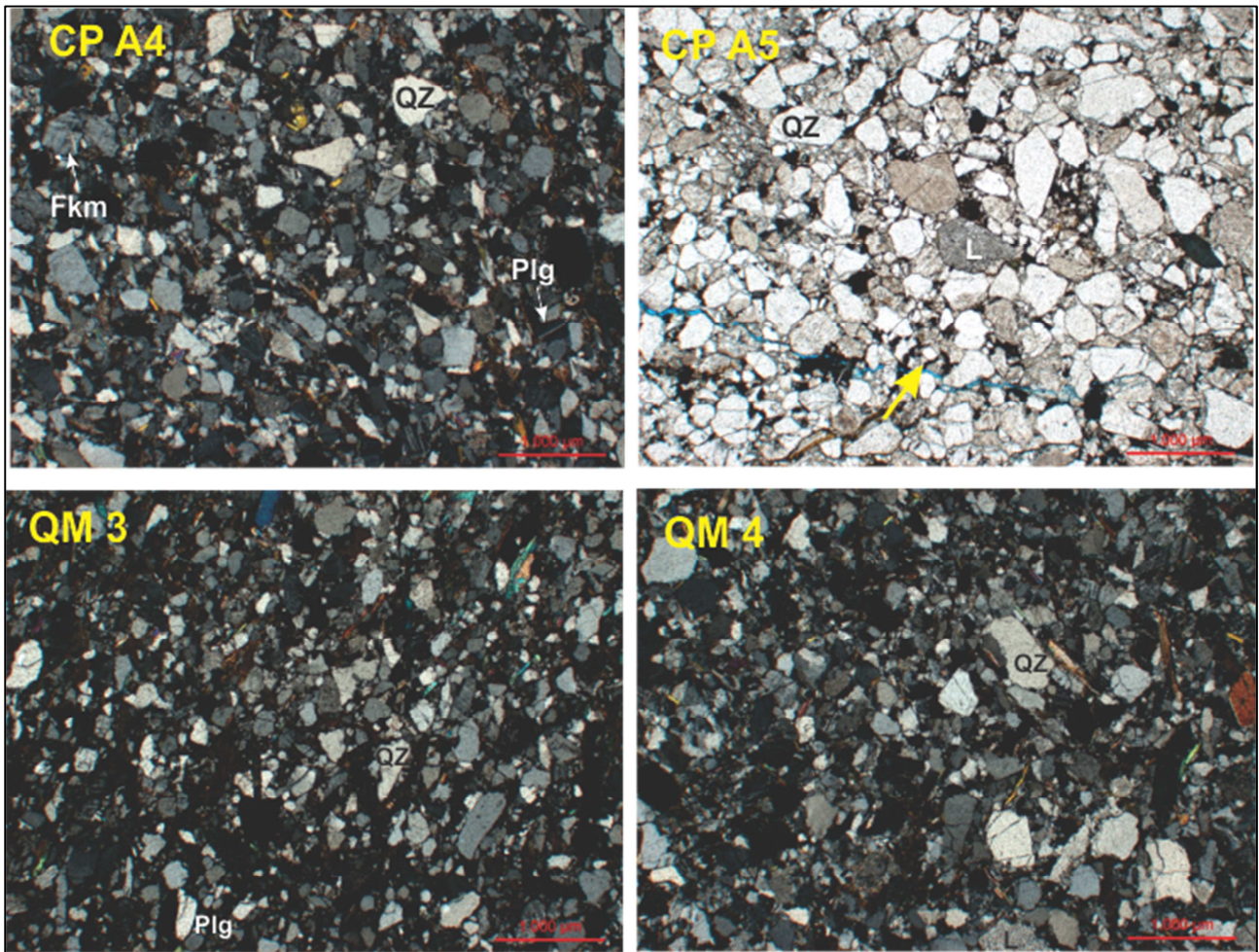


Fig. 78: Thin sections photomicrographs of the samples analysed of Upper Turbidites, CP A 4 and CP A5 correspond to Log CB 1 (North); and Qm 3 and QM 4 to log CB 7 located at South of Cerro Bola (see Fig.75). Note how the primer porosity is none and only show porosity in fractures (CP A5 yellow narrow).

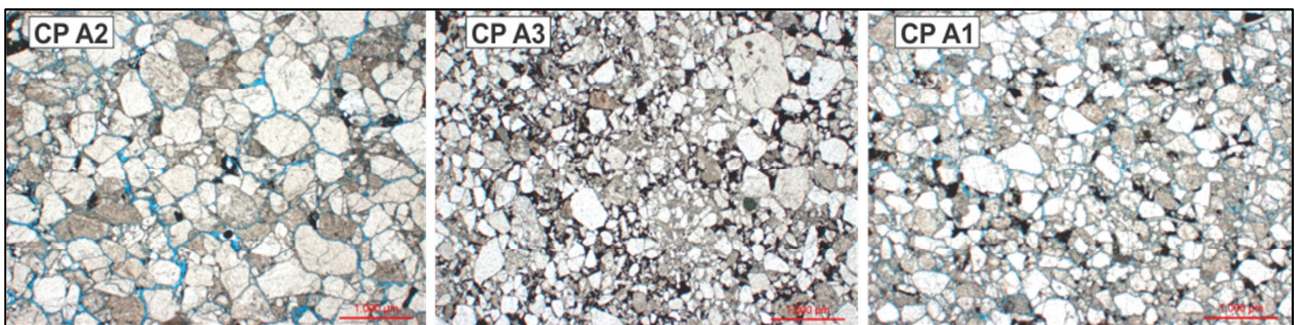


Fig. 79: Microphotography of the sandstones analysed at Log CB 1, note the high porosity (blue tint) of samples CP A2 (Unit 2) and CP A1 (Unit 3) and none porosity CP A3 that shows bad sorting and matrix.

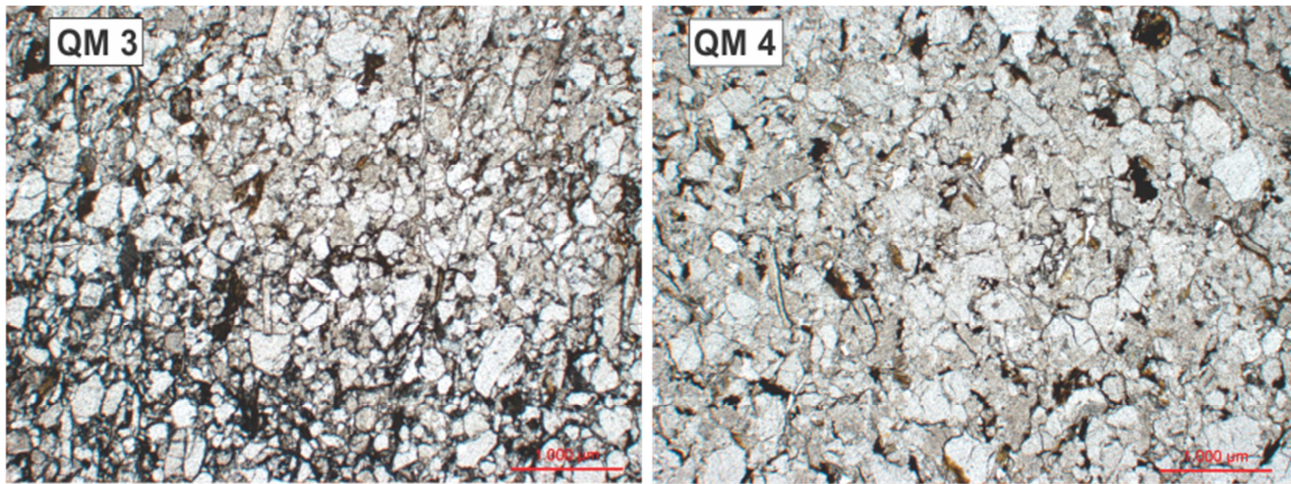


Fig. 80: Microphotography of the sandstones analysed at Log CB 7 located to the South of Cerro Bola. The QM 3 sample correspond to Unit 1 and QM 4 to Unit 2, both not show evidences of porosity, in QM 3 the reason seems to be the bad sorting and QM 4 compaction.

5.1.3 DEPOSITIONAL MODEL: CHARACTERISTICS AND DISCUSSION

In order to facilitated the correlation between logs and appreciate the geometry of the deposits it was necessary the photointerpretation of an aerial photomosaic that cover the entire Cerro Bola (Attach 2). This in addition with the analysis of the sedimentary characteristic presented each log, of the Upper Turbidites and Fluviodeltaic 3 reveals the following sedimentological and depositional evidences:

Upper Turbidites

- Consists of tabular turbidites layers. The thickness of Stage 4 is practically persistent thought the all outcrop. By the other hand the Stages V present at least 5 m of diminutions in bed thickness at the South (Log 8).
- Stages IV is characterized by thick bedded turbidites mostly massive with parallel lamination and ripples at the top of the beds.
- Stages V corresponds to thin bedded turbidites with a big variation of sedimentary structures. The bed thickness increases to the top finishing with a~ 2 m thick medium to coarse-grained sandstone turbidite.
- The contact between the Upper Turbidites and Fluviodeltaic 3 is sharp in most logs, but amalgamation was observed in CB 3 and CB 6; and erosion in CB 7.

Fluviodeltaic 3

- The four Units of this interval are mainly organized in tabular layers, clearly seen in the photomosaic, with the exception of Unit 4 that presents lenticular beds.
- The Unit 3 and 4 are not recorded in the log CB 4 and CB 5, and both log record the coarser grain material of Unit 2.
- The palaeocurrents of Upper Turbidites and Fluviodeltaic 3 present a main flow direction toward NW-NE, this concord with the provenance analysis that indicated as Sierras Pampeanas as source rock that corresponds to granites and metamorphic rocks.
- No evidences of shallow water, like wave ripples, roots, etc. were found.
- No clinofolds were found.

Green Unit

- The contact between the Green Unit and the Fluviodeltaic 3 is by polished surfaces (CB 1, CB 3, CB 7), sharp contacts and also erosional surfaces (CB 4, CB 5 and CB 6). In the Log CB 2 was observed a fault.
- Green Unit corresponds to a silty-sandy matrix with dropstones, mostly of metamorphic rocks and granites, structureless, deformed or with incipient lamination, with dropstones, mostly of metamorphic rocks and granites.

Discussion

The sedimentary features described above for the Fluviodeltaic 3 not correspond to a classical deltaic environment. Instead, are more characteristic of sand-rich submarine fans (Reading, 1996) (Fig. 81) which display a sand content of $\geq 70\%$ (Reading and Richards, 1994). Sand-rich submarine fans are located in tectonically active environments (Mattern, 2005 and references therein) associated with fluvial systems with relative steep gradients and commonly narrow coastal plains (Bouma, 2000a, b). It is well established that sand from littoral drift is intercepted in the heads and gullies of submarine canyons and funneled downslope from the shelves to some sand-rich fans (Howell and Normark, 1982; Nelson, 1983; Reading and Richards, 1994; Schwalbach et al., 1996;

Mattern 2005). Sand-rich fans may also be fed directly by a local river (Nelson, 1983; Nelson et al., 1999).

By the other hand, the Upper Turbidites correspond to mud/sand-rich submarine fans (Reading and Richards, 1994). The differences in bed thickness and sand proportion between stages IV and V is attributed to a diminution of sand supplied into the basin during the deposition of Stages V possibly related to a rise of sealevel.

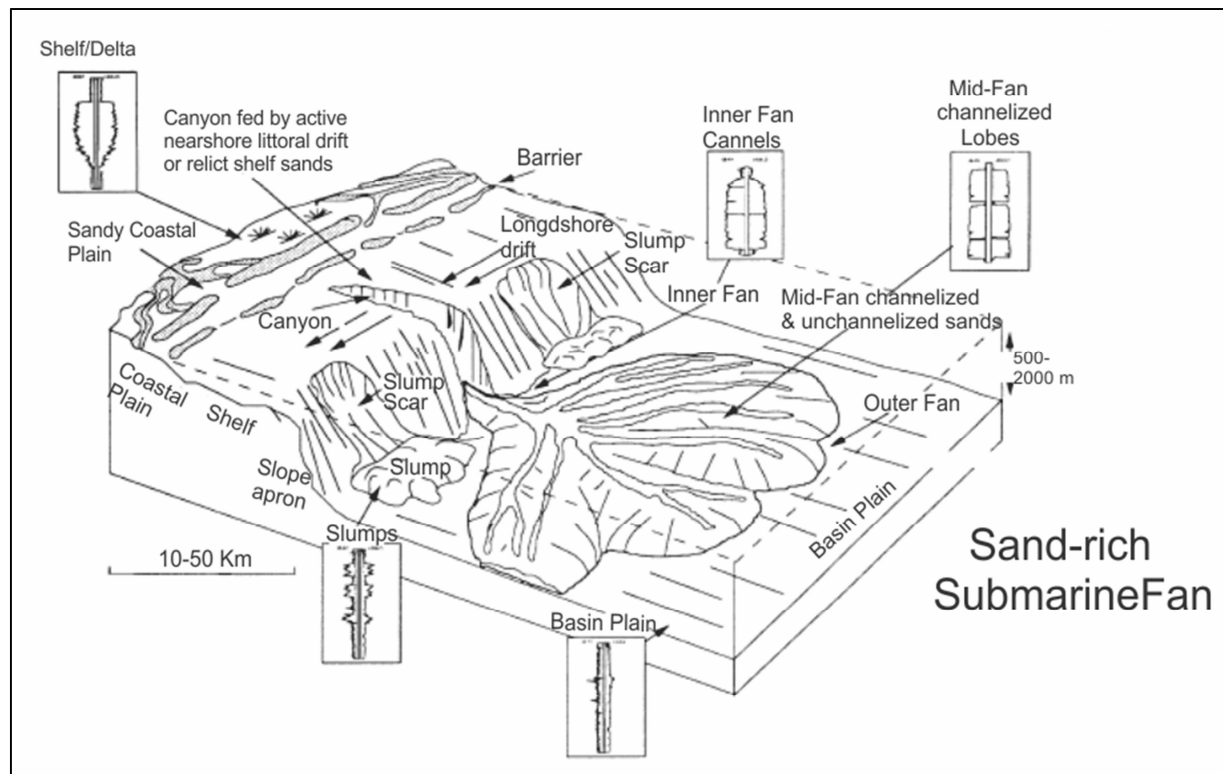


Fig. 81: Block diagrams illustrating the gross depositional facies\ environments and log responses of sand-rich deep-marine clastic systems (modified after Reading and Richards, 1994). The wireline log data provide a general view of the types of log responses expected from gamma ray\ spontaneous potential and resistivity (Richards & Bowman, 1998).

The contact between the Upper Turbidites and Fluviodeltaic 3 indicate changes in the tectonic conditions, from passive during the deposition of Stages IV and V to tectonic active that strongly increased the sand supply basinward during the deposition of the Fluviodeltaic 3. A similar situation was observed in the sand-rich fans of the North Sea formed during the Meso-Cenozoic rifts. (Mattern, 2005 and references therein).

The measured sections made and the correlations of the four units, allow recognise different environments. The Unit 1, characterized by present parallel bedding, good lateral continuity and frequent tabular amalgamation surfaces is interpreted as outer fan deposits. Unit 2 and 3 correspond

to middle fan succession presented a more irregular stratigraphic architecture with a random distribution of channels fills. The channels observed, mostly in Unit 2, corresponded to lenticular matrix supported conglomerates and conglomeratic sandstones with vertical and lateral random distributions are interpreted as distributary channels. The small size and low vertical thickness are common characteristic of ephemeral channels. The lenticular matrix and clast-supported conglomerates of Unit 4 correspond to the coarser sediment found and are interpreted as inner fan deposits.

The log correlations (attach 1) and the aerial photomosaic (attach 2) shown a decrease in thickness of Unit 1 and 2 in the centre of Cerro Bola, from North followed by thickening to South. This variation in thickness indicated the presence of two coalescing sand-rich submarine fans. The interpretation is supported by opposite palaeocurrents direction found between Log 5 and 6 and the difference in clast composition found in Unit 4, in the North (logs 1 to 3) the clasts consist in metamorphic rocks, granites and quartz; in the South (logs 6 to 8) are composed mostly by intraclasts.

As described above main palaeocurrents to NW-NE, this reflects that slope basin was deepening in this direction generating curved submarine fans (fig. 82).

The absence of the Unit 3 and 4 in the logs CB 4 and 5 could be product of an incisive valley created by glacial advance that generate the striation observed at the top of Fluviodeltaic 3 (see Fig. 21 B; 38 B, 68 A) that deposit the proglacial sediments described in the Green Unit. But the possibility of slide scar or fault is not discarded and further studies have to be made to clarify this point.

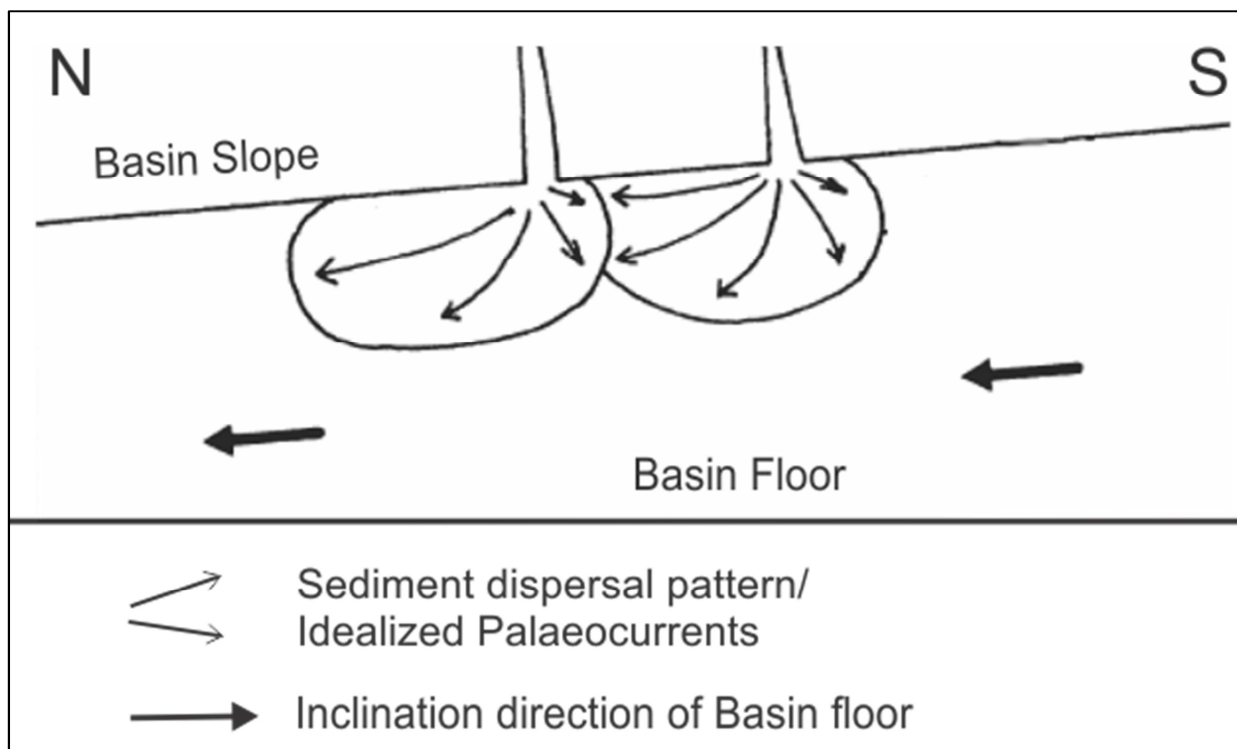


Fig. 82: Alternative model for Cerro Bola Fluviodeltaic3, proposed in this work: plan view of coalescing submarine fans regular curved (modified from Mattern 2005).

5.2 Vidal Ramos

The city of Vidal Ramos is located at 85 km to the west from Florianopolis (see Fig 2). In total the area of study has approximately 336 km². In this part of the Paraná Basin (Fig. 10) the Itararé Group rest in unconformity on the Precambrian basement.

Vidal Ramos is part of the Rio do Sul depression studied by Canuto (1993) and records deposits from Mafra and Rio do Sul Fm. Paim et al. (2004) mapped the zone using a regional scale (1/75,000). For the aim of this research it was necessary to make a detailed geological map of the area (Fig. 83) to identify the deltaic deposits.

The Itararé Group presents in the area a total thickness of 360 m and was identified the following units from bottom to top:

- Mafra Shale: Correspond to hemipelagic dark shales with dropstones resting on the basement unconformity. This deposit is only observed in the paleofjord (Carvalho, 2013).
- Confined Turbidites: Characterized by fine-grained turbidites intercalated with rhythmites with dropstones. This unit is onlapping the basement (Carvalho, 2013).
- Diamictite/MTD: consist in a silty matrix with clast (dropstones), sometimes remobilized with blocks. The unit presents no lateral continuity and in some parts is in contact with the basement.
- Thin-bedded Turbidites/ MTD: this unit is the thicker and presents rhythmites with dropstones just in the lower part, and remobilized diamictites (MTD). Upward the unit are composed by rhythmites with intercalation of ~5 cm sand beds with ripples, except at the East of the study area where 20 m of sandy turbidites was founded. At the top the unit present decreases in the sand proportion, finishing with mudstones.
- Deltaic: this unit is the focus of this research and it will be described in the next step.

The contact with the overlying Rio Bonito Fm. was never found in the area.

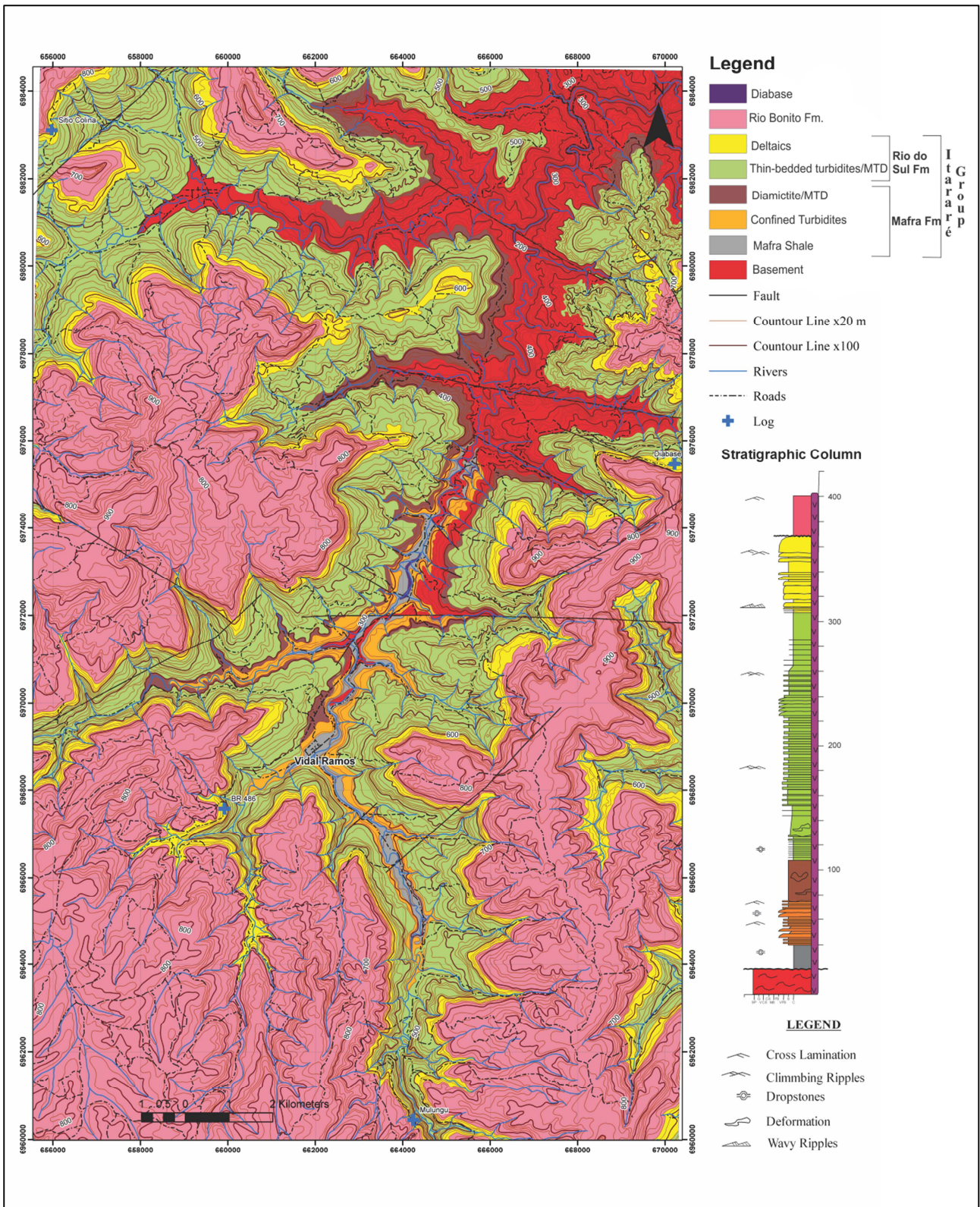


Fig. 83: Geological map (1/60.000) of Vidal Ramos area, the general stratigraphic column is shown at right. The unit analysed in this work correspond to Deltaic (yellow). The detailed sedimentologic logs measured are indicated by a blue cross. (modified from Carvalho et al, 2013).

5.2.1 LOGS DESCRIPTION

Four sedimentologic logs (1:100 scales) were made along the study area where it was found continuously exposed outcrop for at least 15 m. In the next step it will be described the sedimentary facies found in each section from South to North. (See table 3 for facies code description) (Fig. 83).

Code	Lithofacies	Structure
Sm	Very fine to fine-grained sandstones	Massive
Sg	Very fine to fine-grained sandstones	Normally graded
Sr	Very fine to fine-grained sandstones	Current ripples lamination
Srw	Very fine to fine-grained sandstones	Wave ripples lamination
Sl	Very fine to fine-grained sandstones	Horizontally laminated
Sd	Very fine to fine-grained sandstones	Deformed
Fl	Fine-grained (silt to clay)	Horizontally laminated
Fd	Fine-grained (silt to clay)	Deformed

Table 3: Facies code and description of the facies identified in the Deltaic. (Modified from Miall, 1977)

Log VR- 1

This log is located at the South of study area (see fig. 1). In this zone the contacts with the underlying (Thin-bedded Turbidites/MTD) and the overlying (Rio Bonito Fm.) units are covered. This log comprises almost 20 m of the Deltaic Unit continuously exposed. (Fig. 83) and presents, from bottom to top, the following facies:

Deformed sandstones (facies Sd; Fig. 84)

These facies are characterized by disturbed beds of massive, rippled, horizontal laminated deposits and consist of very fine-grained sandstones that occur in bed of 0.5-2 m thick. Deformed sandstones often present a chaotic appearance and slump structures. Mudclasts are common. Such deformed sandstones were probably formed by slump of previously deposited sand facies downslope in a subaqueous environment, caused by seismic shock, high depositional rates on higher slopes, escape of organic gases or by a combination of these processes.

Other type of deformed sandstones facies consist of fine-grained sandstones containing dewatering and loading structures, interpreted as results of rapid escapes of pore water from the sediment in a context of extremely high depositional rates.

Deformed fine grained (facies Fd; Fig. 85 and 86)

This facies consist of siltstones and mudstones with chaotic aspect and slumped features. The thickness of the beds varies from a few centimetres to a 4 m thick bed which presents sandstones block and micro faulting. Slumping may have been triggered by rapid sedimentation, deposition on high relief, oversteepening of depositional slopes, seismic shock or a combination of these factors.

Massive sandstones (facies Sm; Fig.87)

Correspond to fine grained sandstones with no internal sedimentary structures. They occur in beds >0.5 m thick, mudclast are common. This facies probably correspond massive Bouma A turbidites, indicative of subaqueous depositional environment.

Graded sandstones (facies Sg)

Consist of individual normally graded beds from fine or very fine-grained sandstones to siltstones. Sometimes repeated sequences of facies occur, comprising massive, horizontally laminated and rippled sandstones passing upward to laminated siltstones. Graded sandstones facies was deposited by turbidites in subaqueous setting.

Current rippled sandstones (facies Sr; Fig. 88)

This facies occur either as part of a turbidite facies association or as discrete beds. The ripples are asymmetric indicating the action of unidirectional flows and correspond mostly to climbing ripples. The size of the sedimentary structure varies from centimetre to decimetre scale. Fine-grained rippled sandstones represent deposition from a relatively slow velocity traction current with abundant suspended material. The palaeocurrents analysis indicates main flow direction to NW (see fig. 32 B).

Horizontally laminated sandstones (facies S1)

This facies is the less common part of the turbiditic association. It is represented by fine-grained sandstones deposited by currents in upper flow regime.

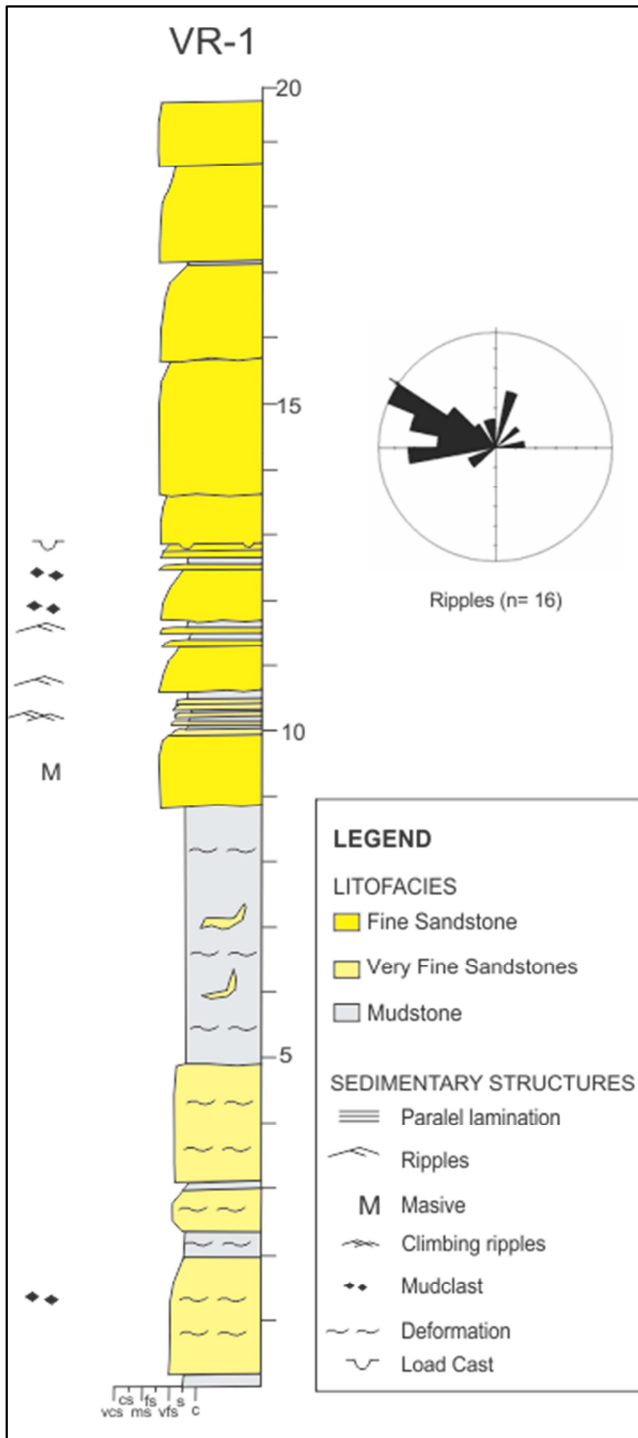


Fig. 83: Sedimentary log of Deltaic deposits located at the South of the study area. Vertical scale in metres. The rose diagram shows 23 measures of palaeocurrents, indicating a NW flow direction.



Fig. 84: Example of the facies Sd, note the slump features of the very fine sandstones.



Fig. 85: Deformed mudstones of the facies Fd, hammer for scale.



Fig. 86: Example of a 4 m thick slump (Fd facies), yellow dot line delineated sandstones block within a mudstone matrix.

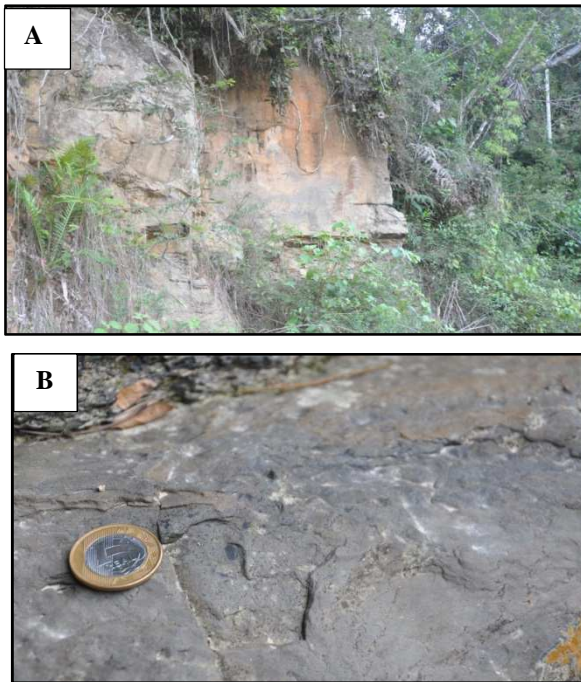


Fig. 87: Examples of the facies Sm: (A) Two metres thick massive fine sandstones bed. (B) Mudclast at the top of a structureless fine grained bed, one Brazilian Real for scale.

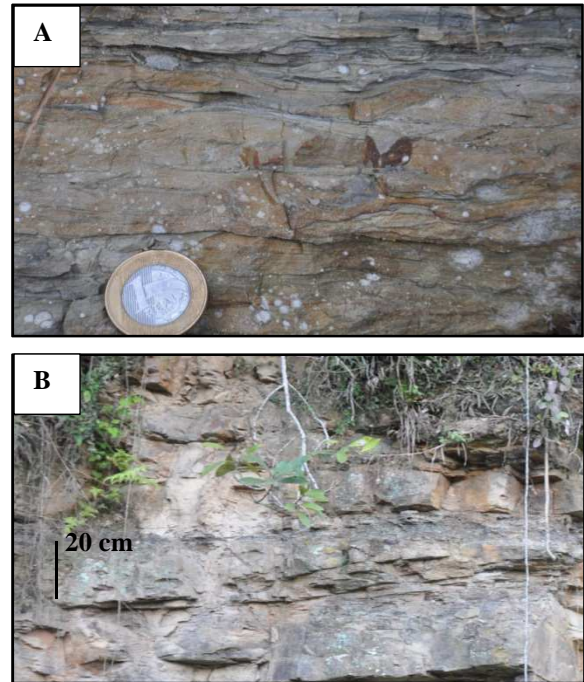


Fig. 88: Examples of facies Sr. (A) Fine grained sandstones with centimetres size climbing ripples; (B) a decimetre size climbing ripple.

Log VR- 2

This log is located along the road BR-486 at approximately 8.3 km to NW from VR-1 Log. In this section it is possible to observe the transitional contact between the Deltaic and Thin-bedded turbidites/MTD Unit, passing from hemipelagic mudstones to intercalation of mudstones and millimetres sand layers that become thicker upward. This contact indicated a normal progradation of the deltaic system. Unfortunately the contact with the overlaying Rio Bonito Fm. is covered.

The VR-2 log recorded 47 m of deltaic sequences corresponding to the most thick measured succession of the unit (Fig. 89). The sedimentary facies recognized in this log are described below:

Laminated fine-grained (Facies Fl; Fig. 90)

This facies consists of laminated graded beds from siltstones to claystones, interbedded very fine rippled sandstones or as individual beds of laminated mudstones. The thicknesses of the beds vary from millimetre scale to a 3 m thick layer (Fig. 90 B). The graded beds are interpreted as

diluted turbidites deposit and the discrete layers as deposited in low energy setting by the settling of suspended fines.

Graded sandstones (facies Sg; Fig. 91)

Graded sandstones are present mostly at first 12 m of the log, corresponded to very fine and fine-grained sandstones grading to mudstones. The repetition of sequences of facies (Sm, Sl, Sr and Fl) indicate deposition from turbid currents.

Massive sandstones (facies Sm; Fig. 92)

Correspond to structureless fine or very fine-grained sandstones present as individual bed or as part of a turbidite successions. It is located mostly at the middle part of the log. Mudclast, dewatering and loading structures are common. The beds thickness varies from a few centimetres to 4 m thick. This facies is interpreted as deposited by gravity flow such dense turbidite currents.

Deformed sandstones (facies Sd; Fig. 93)

Consist in chaotic beds with slumped features, also presenting mudclast, dewatering, and flame structures, probably generated by slump downslope of previously deposited sandy facies.

Horizontally laminated sandstones (facies Sl; Fig 94 A)

The facies Sl is usually found in association with facies Sg, Sr and Sm in very fine to fine-grained sandstones interpreted as deposited by traction currents, in upper flow regime..

Wave ripples sandstones (Facies Srw; Fig. 94 A)

This facies is present at the lower part of the log, occurring associated to the turbidites succession or as discrete beds. Symmetrical wave ripples predominate at the first 13 m of the section, sometimes combined with flaser lamination. This facies is interpreted as deposited by wave action in relatively shallow water depths.

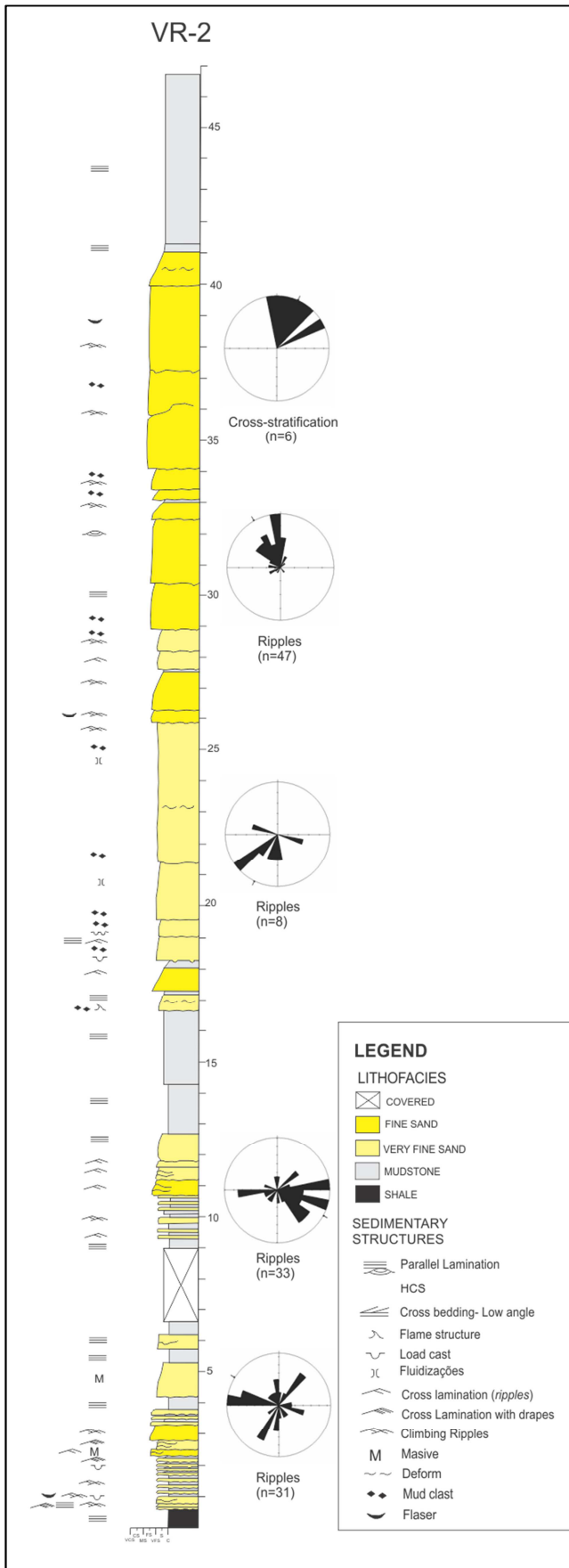


Fig. 89: Sedimentary log of Deltaic Unit. The rose diagram indicates the palaeocurrents direction at different intervals, with the number of measures. Vertical scale in metres.



Fig. 90: Example of facies Fl. (A) Detail of laminated graded beds. (B) Individual bed of laminated mudstones.



Fig. 91: Graded sandstones interpreted as distal turbidites.



Fig. 92: Photo illustrating the Sm facies, note the abundance of mudclast.



Fig. 93: Deformed sandstones (facies Sd), hammer for scale.

Rippled sandstones (facies Sr; Fig. 94)

This facies is characteristic of the upper part. The sandstone beds present climbing ripples across the entire layer indicating unidirectional current flows, suggesting deposition from flows carrying abundant suspended material such as hyperpycnal flows. The palaeocurrent measures are shown in fig. 8.



Fig. 94: Examples of facies Sr; (A) Wavy ripples passing to laminated very fine sandstones (facies SI). (B) Flaser lamination. (C) Cross stratification. (D) Climbing ripples showing NW flow direction.

Log VR- 3

Located at almost 13 km to NE from the previous log (VR- 2), this section record 20 m of the Deltaic Unit, the contact with the under and overlying units are covered (Fig. 95). A sill of diabase intrudes the unit. The facies recognized are the followings:

Laminated fine-grained (facies Fl; Fig. 96)

Consist in mudstones and shales horizontally laminated as individual beds or as part of graded beds. These deposits are interpreted as distal diluted turbidites.

Graded sandstones (facies Sg; Fig. 96)

Correspond to normally graded beds from fine-very fine-grained sandstones to mudstones. The thickness of the layers varies from 2 cm to 20 cm and is common find repeated sequences of facies such Sm, Sr and Fl. This facies is interpreted as deposit by turbidity currents.

Deformed sandstones (facies Sd; Fig. 96)

The facies consist in distorted beds of massive sandstones with loading structures that deformed the bed. This is interpreted as rapid deposition in subaqueous environment.

Massive sandstones (facies Sm; Fig. 96)

Occur as individual beds or as part of the turbidite deposits. Consist of fine-grained sandstones without sedimentary structures. Basal marks such loading, grooves, flute casts, are common and indicate NW-NE flow direction (see fig. 14). These facies represent massive Bouma A turbidites.

Wave Rippled sandstones (facies Sr; Fig. 96 and 97)

Rippled sandstones facies is present as part of a turbidite facies association. This facies occurs in fine-grained sandstones, sometimes associated whit flaser laminatiton. The palaeocurrents analysis of the ripples shows random direction, see fig. 14, indicating possibly storm wave action.

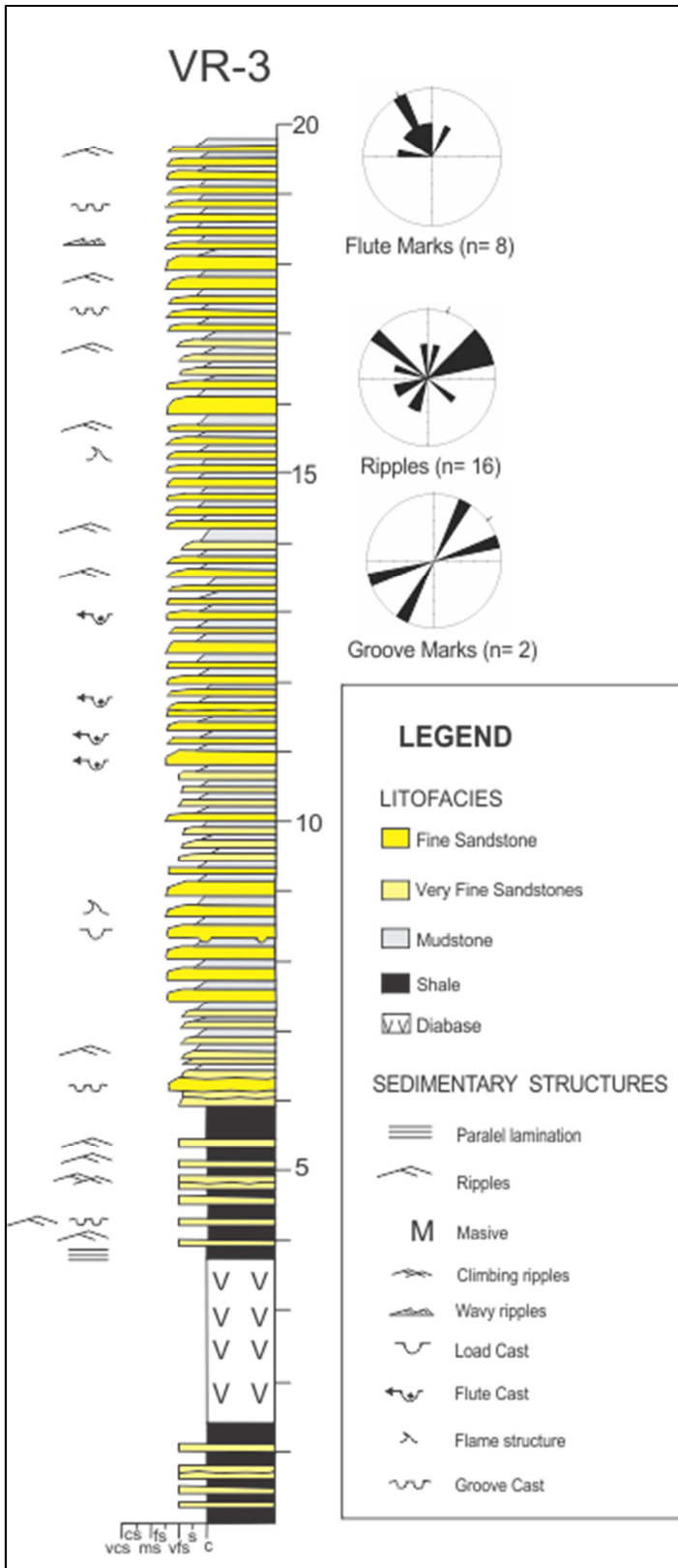


Fig. 95: Sedimentary log of Deltaic Unit at the central east part of study area. The palaeocurrents are represented in the rose diagrams for each sedimentary structure, in bracket are indicated the number of measure.

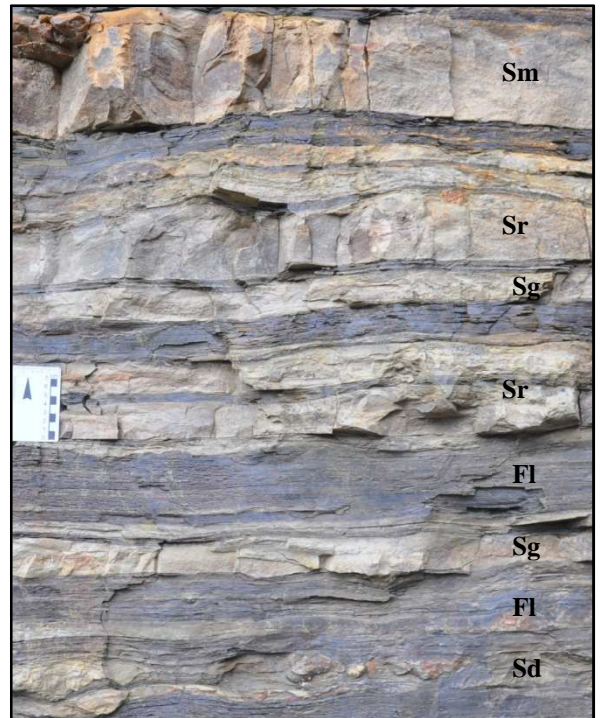


Fig. 96: Example of the different sedimentary facies presented in this log. (Sd= deformed sandstones; Fl= laminated fine grained; Sg= graded sandstones; Sr= rippled sandstones and Sm= massive sandstones)

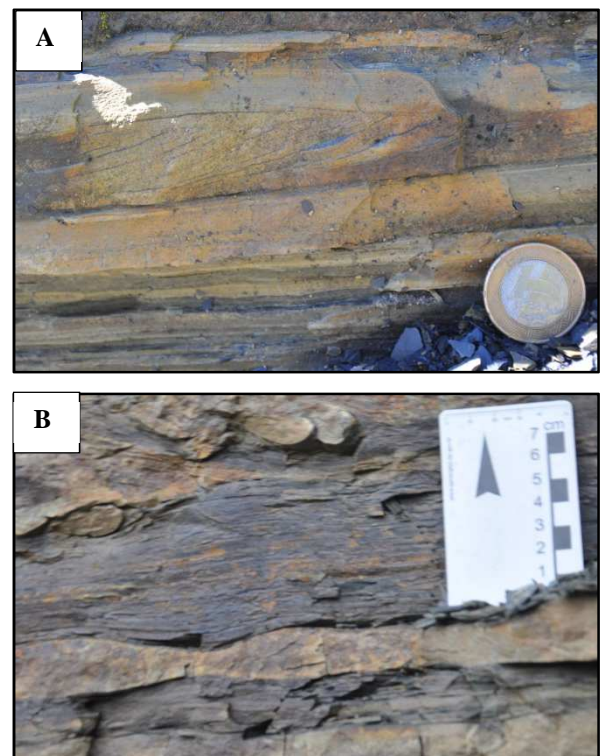


Fig. 97: Rippled sandstones, in (A) climbing ripple with flaser lamination. (B) Wavy ripple in fine grained sandstones.

VR- 4 Log

Located at the northwest of the geological map (fig. 1), this section recorded almost 20 m of deltaic sandstones (fig. 17). In this place the entire Unit is uplifted by a fault located at the East, so the Deltaic Unit is founded at 800 m.s.l. when usually appears 200 m bellow. The sedimentary facies are the followings:

Fine grained deformed (facies Fl; Fig. 98)

These facies is founded at the bottom of the log, consists of chaotic mudstones with slump features. It is interpreted as deposition in a subaqueous setting by decantation and subsequent slumping downslope.

Graded sandstones (facies Sg; Fig. 99)

These facies appears at the first 5 metres of the log, consists of fine and very fine-grained sandstones grading upward to mudstones. Associations with facies Sm, Sl and Fl are frequent indicating deposition from turbidity currents.

Horizontal laminated sandstones (facies Sl; Fig. 100)

This facies is a common component of the turbiditic facies association and occurs as fine to very fine-grained units. It indicates deposition from traction currents in upper flow regime.

Current rippled sandstones (facies Sr; Fig 101)

Correspond to fine grained sandstones with climbing ripples across the entire bed; the thickness varies from 50 cm to 3 m. Sometimes it was observed flaser lamination and cross stratification. The palaeocurrents analysis indicated NW flow direction (see fig. 17). The dominance of climbing ripples facies through the bed suggest deposition from continues flows with abundant suspended material.

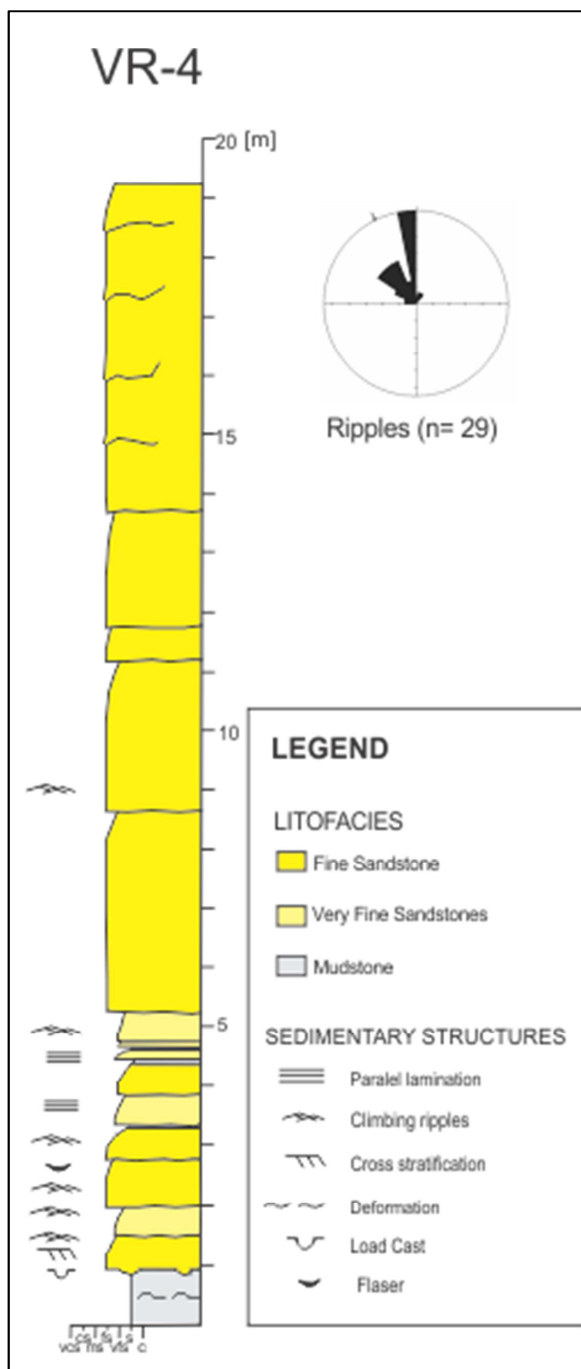


Fig. 98: Sedimentary Log recording 20 m of the Deltaic Unit. The palaeocurrents measures are represented at the rose diagram.



Fig. 99: Chaotic mudstones of the facies Fd (deformed fine-grained deposits). Note the slumps features and the erosive contact with the overlying sandstones bed.



Fig. 100: Example of the laminated sandstones facies (SI). These facies appears usually at the top of graded beds.

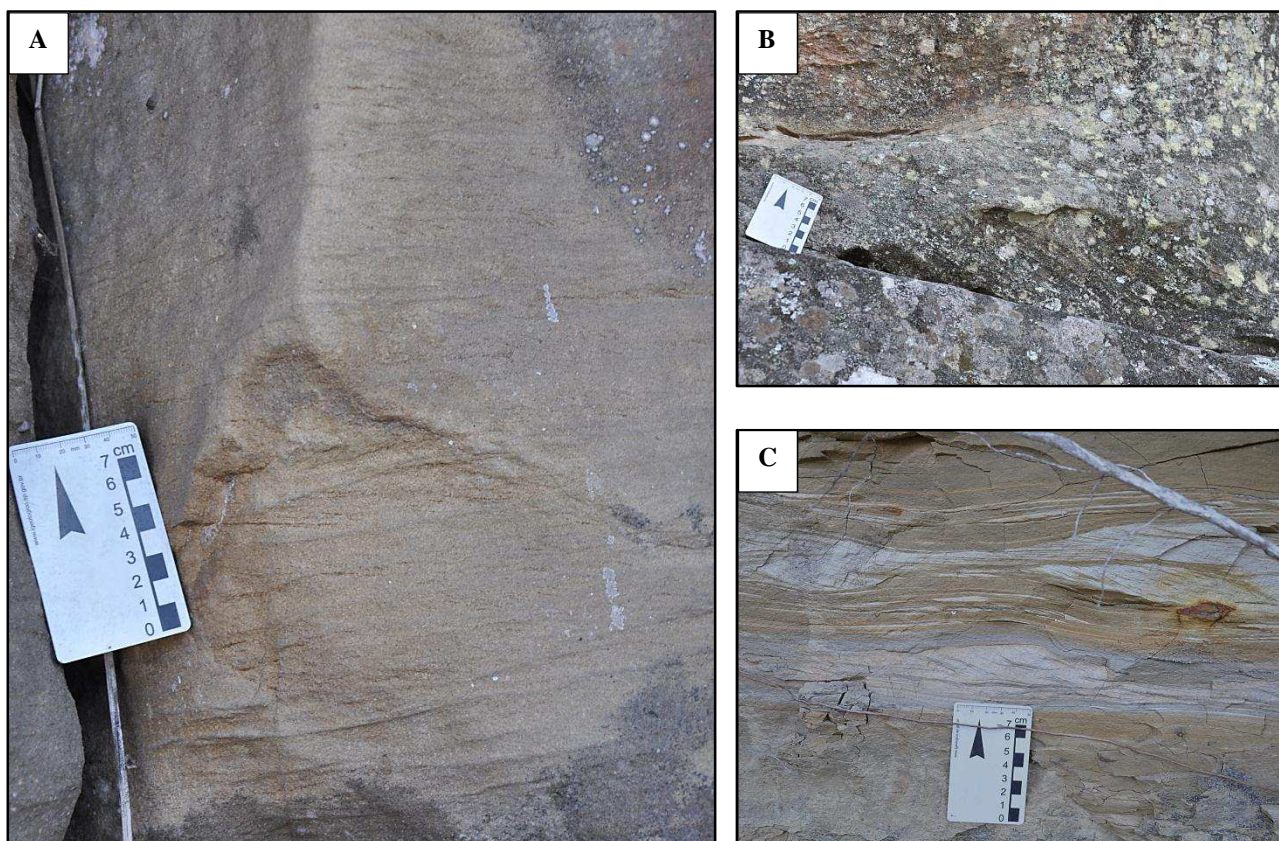


Fig. 101: Photos showing the facies Sr (rippled sandstones). (A) Climbing ripples across the entire bed. (B) Cross stratification at the bottom of a lenticular sandstone body. (C) Flaser lamination in very fine-grained sandstones.

5.2.2 TOC ANALYSIS

In order to determine the hydrocarbon potential of the Rio do Sul Fm. four mudstones samples (Fig. 102) were taken and analysed for Total Organic Carbon (TOC) using Leco SC-144DR equipment. The results are shown in Table 4; the TOC quantity indicated a fair resource potential.

Sample	Weight	Sulfur	Carbon	Method
VR Bubi	0.2346	0.046181	1.1991	Mid Carbon
VR 14-12	0.2346	0.041412	1.1745	Mid Carbon
VR 15-1	0.1447	0.035940	1.6358	Mid Carbon
VR 23-24	0.1816	0.0087791	0.67389	Mid Carbon

Table 4: Results of TOC analysis applied to 4 samples, two belong to Mafra Shale and two to Thin-bedded Turbidites/MTD Unit.

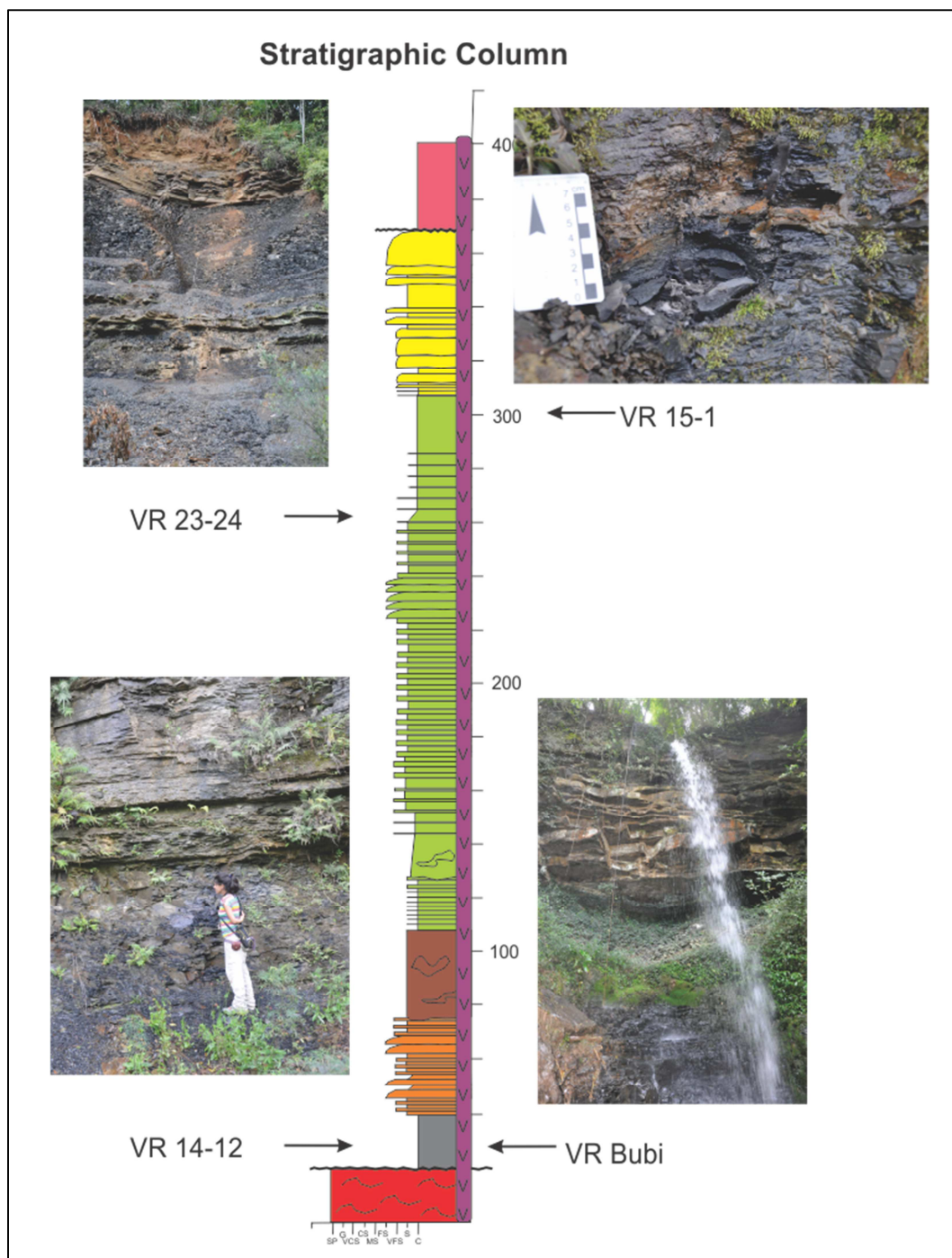


Fig. 102: Stratigraphic location of the samples analysed for TOC (see Fig. 83 for the legend of the Stratigraphy column)

5.2.3 DEPOSITIONAL MODEL

After correlate (Fig. 103) and analyse the facies identified in the Deltaic Unit at different localities, the sediments characteristics suggest a depositional setting dominate by gravity flows at the beginning. This gravity flows consists of slumps (observed at Log VR- 1) that transform into turbidity currents to the North, like we see in VR- 2 and VR- 3 logs (see Fig. 104). The evidences of wave reworking in the sediments indicate shallower water at this time.

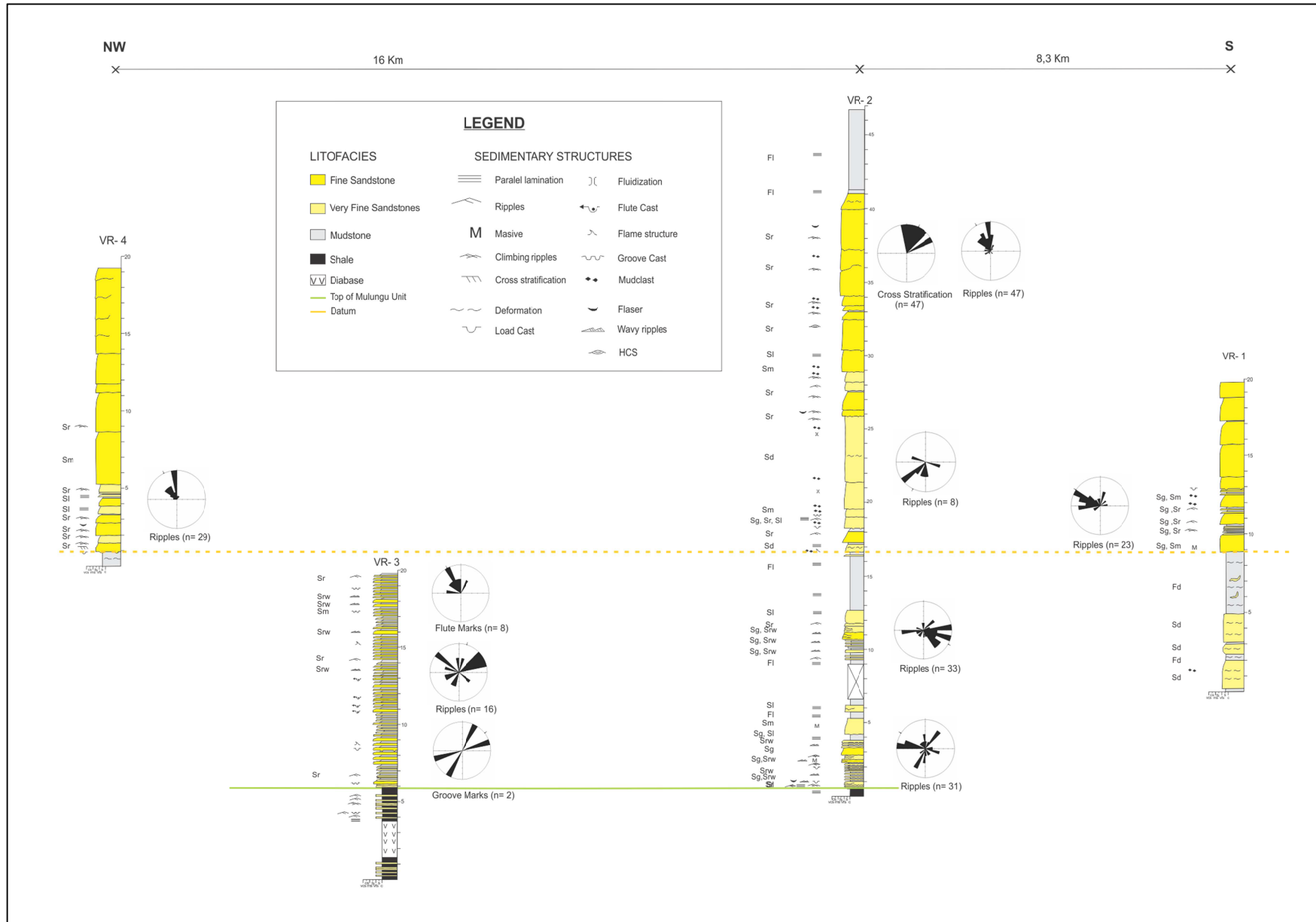


Fig. 103: Correlation panel from South to Northwest of the Deltaic Unit logs. The palaeocurrents analysis is show in the rose diagrams. The yellow dashed line indicated the datum chosen and the green line the contact with the underlying Mulungu Unit.

The predominance of resedimented facies suggest a depositional environment characterized by slope instability. The cause of this features could be related to many reasons like seismic activity; rapid sediment accumulation at river mouth, resulting in widespread sedimentary loading on the upper delta-front slope; deposition of coarser sands and silts on unconsolidated prodelta clays; or rapid biochemical of organic material leading to formation of large volumes of methane gas, that generate excess pore pressure within the sediments (Whelan et al., 1975).

The deposits shown a progradation of the delta systems reflected by the increase of sand toward the top; followed by a retrogradation attributed to a rise of the sea level and the deposition of mudstones (3 m thick) observed in the VR- 2 log.

Overlaying the mudstones appears, in sharp contact, a thickening upward package of rippled sandstones interpreted as delta front deposits (see VR- 2 and VR- 3 logs). This indicates a rapid normal progradation of the delta systems related to high rates of sediment supply.

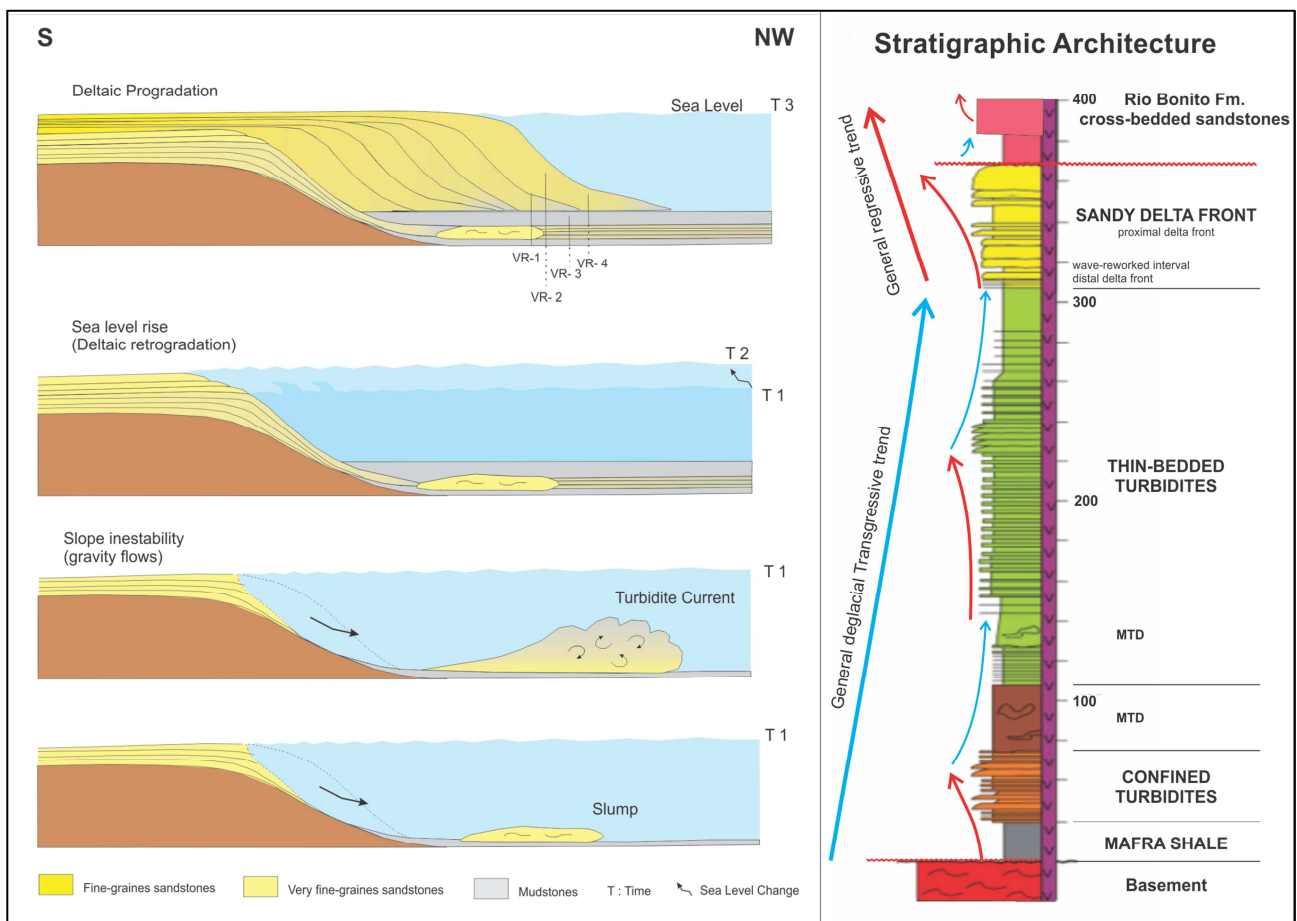


Fig. 104: Left: schematic model of the deposition of the Deltaic Unit. VR-1 to VR-4: measured logs presented in Fig. 12. Right: general interpretation of the stratigraphic evolution of Itararé Group, marked by advances of the delta systems related to phases of increased sediment supply.

6. CONCLUSIONS

The results presented in this research reflect that even if both areas present similar climatic condition (de-glacial period) the type and morphology of the basin strongly influenced the distinct sedimentary processes, sand transportation and accumulation basinward.

The Paganzo Basin, as was described before, corresponds to a foreland basin. This characteristic determinate that in the area of Cerro Bola the changes in sediment supply was mainly related to the tectonic activity. The result is the generation of high density turbidite currents and the deposition of ~165 m thick sand-rich regular curved coalescing sand-rich submarine fans with a restricted lateral extension. Unfortunately further studies have to be made to investigate if these deposits are related or not to a delta, that was the aim of this research.

By the other hand, Paraná Basin corresponds to intracratonic basin in which the deposition was controlled mostly by sea-level changes and sediment supply. Under this conditions thinner (~60 m thick) but with big areal distribution sandy delta systems could be formed as was observed in Vidal Ramos. In this setting the transport of sediment to distal areas basinward is product of the collapse of delta front deposits that generated gravity flows and turbidites in the distal delta front/prodelta regions.

Besides this general comparison, specific conclusions for each area are presented below:

Cerro Bola outcrops

- The differences in thickness and sand proportion between Stages IV and V of the Upper Turbidites correspond to variations of sand supplied to the basin attributed to changes in the sea level.
- The sharp contact between the Upper Turbidites and "Fluiodeltaic 3" is attributed to a tectonic reactivation of the basin.
- The "Fluiodeltaic 3" is re-interpreted as coalescing regular curved sand-rich submarine fans based in his sedimentological features, reason why the author proposes the change of the name to Submarine Fan.

- The submarine fan deposits can be subdivided into 4 units. The Unit 1 correspond to outer fan deposits; Unit 2 and 3 represent middle fan deposits including distributaries channels; and inner fan deposits correspond to Unit 4.
- The contact with the overlying Green Unit is not clear and could be an erosion surface result by a glacial advance, but further investigations have to make.
- The Green Unit deposits consists of a silty-sandy matrix with dropstones, mostly of metamorphic rocks and granites, structureless, deformed or with incipient lamination interpreted as deglacial sediment, locally resedimented.
- The palaeocurrents analysis of the Upper Turbidites and Submarine fan (Fluviodeltaic 3) indicates a NW-NE main flow direction.
- Provenances analysis of the both sequences reveals the Sierras Pampeanas as source rock, in agreement with the palaeocurrents.
- The Upper Turbidites are bad hydrocarbon reservoir for not present porosity.
- The samples analysed of Submarine Fan unit shows good reservoir condition at the north of Cerro Bola, but bad quality at south due compaction.

Vidal Ramos

- The upper part of Rio do Sul Fm. corresponds to deltaic deposits.
- The Deltaic Unit presents high frequency of progradation and retrogradation of the delta, influenced by changes in the sea level. The lower part of the unit is wave reworked differently of the upper succession that is river dominated.
- The palaeocurrents analysis of asymmetric ripples indicated flow direction towards NW.
- TOC analysis applied to the rock of Rio do Sul Fm., not show good potential for hydrocarbon generation.

As a final remark, the re-interpretation of the thick sandy deposits in Cerro Bola as submarine fan does not allow a direct comparison with the sandy progradational deltaic deposits of Vidal Ramos, due to the distinct record of depositional processes and paleogeographic configurations.

7. References

- Azcuy C.L., Morelli J.R., 1970a. The Paganzo Basin. Tectonic and sedimentary characteristics of the Gondwana sequences in Northwest Argentina. II Gondwana Symposium, pp. 241–247.
- Azcuy C.L., Morelli J.R., 1970b. Geología de la comarca Paganzo- Amana', el Grupo Paganzo. Formaciones que lo componen y sus relaciones. Revista de la Asociación Geológica Argentina 25, 405–429.
- Bouma, A.H., 2000a. Coarse-grained and fine-grained turbidite systems as end member models: applicability and dangers. Mar.Pet. Geol. 17, 137–143.
- Bouma, A.H., 2000b. Fine-grained, mud-rich turbidite system: model and comparison with coarse-grained, sand-rich systems. In: Bouma, A.H., Stone, C.G. (Eds.), Fine-Grained Turbidite Systems. Am. Assoc. Pet. Geol. Bull., vol. 68, pp. 9– 19.
- Buatois, L., Mángano, M.G., 1995. Post glacial lacustrine event sedimentation in an ancient mountain setting: Carboniferous lake Malanzán (Western Argentina). Journal of Paleolimnology 14, 1–22.
- Buatois L.A., Netto R.G., Mángano M.G., Balistieri P.R.M.N., 2006. Extreme freshwater release during the late Paleozoic Gondwana deglaciation and its impact on coastal ecosystems. Geological Society of America Bulletin, 34, 1021-1024 p.
- Buatois L.A., Netto R.G., Mángano M.G., 2010. Ichnology of late Paleozoic postglacial transgressive deposits in Gondwana: Reconstructing salinity conditions in coastal ecosystems affected by strong meltwater discharge. Geological Society of America Bulletin. Special Paper 468, 149-173.

- Canuto J. R., 1993. Facies e ambientes de sedimentação da Formação Rio do Sul (Permiano), Bacia de Paraná, na região de Rio do Sul, Estado de Santa Catarina. Tese de doutoramento. Universidade de São Paulo Instituto de Geociências.
- Caputo M.V., Crowell J.C., 1985. Migration of glacial centres across Gondwana during Paleozoic Era. *Geological Society of America Bulletin* 96, 1020–1036.
- Caputo M.V., de Melo J.H.G., Streel M., Isbell J.L., 2008. Late Devonian and Early Carboniferous glacial records of South America. In: Fielding, C.R., Frank, T.D., Isbell, J.L. (Eds.), *Resolving the Late Paleozoic Ice Age in Time and Space*. Geological Society of America Special Publication., Boulder, CO, pp. 161–173.
- Carvalho B., 2013. The Geometry, Evolution and Sedimentology of Confined Turbidite Sand-Sheets and their Impact on Reservoir Prediction, Paganzo Basin and Paraná Basin. Msc Dissertation. Universidade do Vale do Rio dos Sinos, Brasil.
- Carvalho B., Puigdomenech C., Rodriguez F., Paim P., Faccini U., 2013. Glacial/deglacial deposit of Itararé Group in Vidal Ramos, Santa Catarina-Brazil. (in prep.)
- Césari S.N., Gutiérrez P.R., 2000. Palynostratigraphy of Upper Paleozoic sequences in Central-Western Argentina. *Palynology* 24, 113–146.
- Crastrós J.C., Bortoluzzi C.A., Caruso F.Jr., Krebs A.S., 1994. Coluna White: Estratigrafia da Bacia do Paraná no Sul do Estado de Santa Catarina-Brasil: Florianópolis. Secretaria de estado de Tecnologia, Energia e Meio Ambiente. Série Textos básicos de geologia e Recursos Minerais de Santa Catarina, v. I. 67p.
- Crowell J.C., Frakes, L.A., 1970. Phanerozoic glaciation and the causes of ice ages. *American Journal of Science* 268, 193–224.
- Dickins J.M., 1997. Some problems of the Permian (Asselian) glaciation and the subsequent climate in the Permian. In: Martini, I.P. (Ed.), *Late Glacial and Postglacial Environmental Changes: Quaternary, Carboniferous–Permian, and Proterozoic*. U.K., Oxford University Press, Oxford, pp. 243–245.

- Dickinson W.R., 1970. Interpreting detrital modes of graywacke and arkose. *Journal of Sedimentary Petrology* 40, 695-707.
- Dickinson, W., Beard, L., Brakenridge, G., Erjavec, J., Ferguson, R., Inman, K., Knepp, R., Lindberg, A., Ryberg, P., 1983. Provenance of North American Phanerozoic sandstones in relation to tectonic setting. *Geologic Society of America Bulletin*, 222–235.
- Dykstra M., Kneller B., Milana J.P., 2006. Deglacial and postglacial sedimentary architecture in a deeply incised paleovalley–paleofjord — the Pennsylvanian (late Carboniferous) Jejenes Formation, San Juan, Argentina. *GSA Bulletin* 118, 913–937.
- Dykstra M., Garyfalou K., Kertznus V., Kneller B., Milana J.P., Molinaro M., Szuman M. and Thompson P., 2011. Mass-transport deposits: combining outcrop studies and seismic forward modeling to understand lithofacies distributions, deformation, and their seismic expression. In: *Mass-Transport Deposits* (Eds. C. Shipp, P. Weimer and H. Posamentier). SEPM, Tulsa.
- Eyles C.H., Eyles N., França A.B., 1993. Glaciation and tectonics in an active intracratonic basin: the Late Palaeozoic Itararé Group, Paraná basin, Brazil. *Sedimentology* 40, 1-25.
- Faiweather L., 2013. Mechanisms of supra-MTD topography formation and the interaction of turbidity currents with such deposits. Unpublished PhD thesis, University of Aberdeen.
- Fallgatter C., Kneller B., Paim S., 2013. High resolution and reservoir prediction of a normal to forced regression turbidites system in the Paganzo basin (Cerro Bola area, La Rioja-Argentina). 6th Latinamerican Congress of Sedimentology. São Paulo- Brazil
- Fernández Seveso, F., and Tankard, A.J., 1995. Tectonics and stratigraphy of the Late Paleozoic Paganzo Basin of Western Argentina and its Regional Implications, in Tankard, A.J., Suarez, S., and Welsink, H.J., eds., *Petroleum Basins of South America*, Volume 62: AAPG Memoir, AAPG, p. 285-301.
- Fielding C.R., Frank T.D., Birgenheier L.P., Rygel M.C., Jones A.T., Roberts J., 2008a. Stratigraphic imprint of the Late Paleozoic Ice Age in eastern Australia: a record of

alternating glacial and nonglacial climate regime. *Journal of the Geological Society of London* 165, 129–140.

Fielding C.R., Frank T.D., Isbell J.L., 2008b. The late Paleozoic ice age — a review of current understanding and synthesis of global climate patterns. In: Fielding, C.R., Frank, T.D., Isbell, J.L. (Eds.), *Resolving the Late Paleozoic Ice Age in Time and Space: Geological Society of America Special Paper*, 441, pp. 343–354. *Resolving the Late Paleozoic Ice Age in Time and Space*. In: Fielding, C.R., Frank, T.D., Isbell, J.L. (Eds.), *Geological Society of America Special Publication*, 441. Boulder, CO.

Fielding C.R., Frank T. D., Isbell J. L., 2008c. *Resolving the Late Paleozoic Ice Age in Time and Space*. Geological Society of America. Special Publication 441

Fielding C.R., Frank T.D., Birgenheier L.P., Rygel M.C., Jones A.T., Roberts J., 2008d. Stratigraphic record and facies associations of the late Paleozoic ice age in Eastern Australia (New South Wales and Queensland). In: Fielding, C.R., Frank, T.D., Isbell, J.L. (Eds.), *Resolving the Late Paleozoic Ice Age in Time and Space: Geological Society of America Special Paper*, 441, pp. 41–57.

Folk, R. L., Andrews, P. B. y Lewis, D. W., 1970. Detrital sedimentary rock classification and nomenclature for use in New Zealand. *New Zealand Journal of Geology and Geophysics* 13: 937-968.

França A.B., 1987. *Stratigraphy, Depositional Environment and Reservoir Analysis of the Itararé Group (Permo-Carboniferous), Paraná basin, Brazil*. PhD Thesis, University of Cincinnati, Ohio.

França A.B., Potter P.E., 1988. Estratigrafia, ambiente deposicional e análise de reservatório do Grupo Itararé (Permocarbonífero), Bacia do Paraná (Parte 1). *Boletim de Geociências da Petrobrás*, v. 2, n.2/4, p.147-191.

- França A.B., Potter P.E., 1991. Stratigraphy and reservoir potential of glacial deposits of Itararé Group (Carboniferous-Permian), Paraná Basin, Brazil. *Bull. Am. Ass. Petrol. Geol.*, 75, 62-85.
- Frakes L.A., Francis J.E., Syktus J.I., 1992. Climate modes of the Phanerozoic. *The History of the Earth's Climate over the Past 600 Million Years*. Cambridge University Press, Cambridge.
- Gazzi P., 1966. Le arenarie del flysch sopracretaceo dell'Appennino modenese; correlazioni con il flysch di Monghidoro. *Mineralogica et Petrographica Acta* 12, 69-97.
- Gordon J.M., 1947. Classificação das formações gondwânicas do Paraná, Santa Catarina e Rio Grande do Sul. Rio de Janeiro, Departamento Nacional da Produção Mineral. (DNPM. *Notas Preliminares e Estudos*, 38). p. 1-20.
- Holz M., Küchle, J., Philipp, R.P., Bischoff, A.P. y Arima, N., 2006. Hierarchy of tectonic control on stratigraphic signatures: Base-level changes during the Early Permian in the Paraná Basin, southernmost Brazil. *Journal of South American Earth Sciences*, 22:134-155.
- Holz M., 2003. Sequence stratigraphic of a lagoonal estuarine system- an example from the lower Permian Rio Bonito Formation, Paraná Basin, Brazil. *Sedimentary Geology*, 162:305-331.
- Howell D.G., Normark W.R., 1982. Sedimentology of submarine fans. In: Scholle, P.A., Spearing, D. (Eds.), *Sandstone Depositional Environments*. *Mem. Am. Assoc. Pet. Geol.* 31, 365-404.
- Ingersoll, R.V., Kretchmer, A.G., Valles, P.K., 1993. The effect of sampling scale on actualistic sandstone petrofacies. *Sedimentology* 40, 937-953.
- Isbell J.L., Miller M.F., Wolfe K.L., Lenaker P.A., 2003a. Timing of late Paleozoic glaciations in Gondwana: was glaciation responsible for the development of northern hemisphere cyclothem? In: Chan, M.A., Archer, A.W. (Eds.), *Extreme depositional environments: mega end members in geologic time*: Geological Society of America Special Paper, 370, pp. 5-24.

- Isbell J.L., Cole D.I., Catunaenu O., 2008b. Carboniferous–Permian glaciation in the main Karoo Basin, South Africa: stratigraphy, depositional controls, and glacial dynamics. In: Fielding, C.R., Frank, T.D., Isbell, J.L. (Eds.), *Resolving the late Paleozoic ice age in time and space: Geological Society of America Special Paper, 441*, pp. 71–82.
- Isbell, J.L., Lenaker P.A., Askin R.A., Miller M.F., Babcock L.E., 2003b. Reevaluation of the timing and extent of late Paleozoic glaciation in Gondwana: role of the Transantarctic Mountains. *Geology* 31, 977–980.
- Isbell J.L., Fraiser M.L., Henry L.C., 2008a. Examining the complexity of environmental change during the Late Paleozoic and Early Mesozoic. *Palaios* 23, 267–269.
- Isbell J.L., Taboada A.C., Koch Z.J., Limarino C.O., Fraiser M.L., Pagani M.A., Gulbranson E.L., Ciccioi P.L., Dineen A.A., 2011a. Emerging polar view of the late Paleozoic ice age as interpreted from deep-water distal, glacimarine deposits in the Tepuel– Genoa Basin, Patagonia, Argentina. In: Hakansson, E., Trotter, J. (Eds.), *Programme & Abstracts, XVII International Congress on the Carboniferous and Permian Perth 3–8, July 2011: Geological Survey of Western Australia, 2011/20*, p. 74.
- Isbell J.L., Henry L.C., Limarino C.O., Koch Z.J., Ciccioi P.L., Fraiser M.L., 2011b. The equilibrium line altitude as a control on Godwana Glaciation during the late Paleozoic Ice Age. In: Hakansson, E., Trotter, J. (Eds.), *Programme & Abstracts, XVII International Congress on the Carboniferous and Permian Perth 3–8, July 2011: Geological Survey of Western Australia, 2011/20*, p. 74.
- Isbell J.L., Henry L.C., Gulbranson E.L., Limarino, C.O., Fraiser, M.L., Koch, Z.J., Ciccioi, P.L., Dineen, A.A., 2012. Evaluations of glacial paradoxes during the late Paleozoic Ice Age using the concept of the equilibrium line altitude (ELA) as a control on glaciations. *Gondwana Research* 22, 1–19.

- Jordan T.E., Schlunegger F., Cardozo N. 2001. Unsteady and spatially variable evolution of the Neogene Andean Bermejo forelandbasin, Argentina. *Journal of South American Earth Sciences*, 14, 775-798.
- Kneller, B., Milana, J.P., Buckee, C., Al Ja'aidi, O.S., 2004. A depositional record of deglaciation in a paleofjord (Late Carboniferous [Pennsylvanian] of San Juan Province, Argentina): the role of catastrophic sedimentation. *Geological Society of America Bulletin* 116, 348–367.
- Limarino, C.O., and Spalletti, L.A., 1986, Eolian Permian deposits in west and northwest Argentina: *Sedimentary Geology*, v. 49, p. 109–127.
- Limarino C., Césari S., 1988. Paleoclimatic significance of the lacustrine Carboniferous deposits in northwest Argentina. *Palaeogeography, Palaeoclimatology and Palaeoecology* 65, 115–131.
- Limarino, C., Gutiérrez, P., 1990. Diamictites in the Agua Colorada Formation. New evidence of Carboniferous glaciation in South America. *Journal of South American Earth Sciences* 3, 9–20.
- Limarino C. O., Césari S. N., Net L. I., Marensis S. A., Gutierrez R. P., Tripaldia A., 2002. The Upper Carboniferous postglacial transgression in the Paganzo and Río Blanco basins (northwestern Argentina): facies and stratigraphic significance. *Journal of South American Earth Sciences* 15 : 445–460.
- Limarino, C.O., Spalletti, L.A., 2006. Paleogeography of the Upper Paleozoic basins of southern South America: an overview. *Journal of South American Earth Sciences* 22, 134–155.
- Limarino C., Tripaldi A., Marensi S., Fauqué L., 2006. Tectonic, sea-level, and climatic controls on Late Paleozoic sedimentation in the western basins of Argentina. *Journal of South American Earth Sciences* 22, 205–226.
- Limarino C.O., Césari S.N., Spalletti L.A., Taboada A.C., Isbell J.L., Geuna S., Gulbranson E.L., 2013. A paleoclimatic review of southern South America during the late Paleozoic: A record from icehouse to extreme greenhouse conditions. *Gondwana Research*.

- López-Gamundí, O.R., Limarino, C.O., and Cesari, S.N., 1992, Late Paleozoic paleoclimatology of central west Argentina: *Palaeogeography, Palaeoclimatology, Palaeoecology*, v. 91, p. 305-329.
- López-Gamundí, O.R., 1997. Glacial–postglacial transition in the late Paleozoic basins of Southern South America. In: Martini, I.P. (Ed.), *Late Glacial and Postglacial Environmental Changes: Quaternary Carboniferous–Permian, and Proterozoic*. Oxford University Press, Oxford U.K., pp. 147–168.
- López Gamundí O., Martínez M., 2000. Evidence of glacial abrasion in the Calingasta-Uspallata and western Paganzo basins, mid-Carboniferous of western Argentina. *Palaeogeography, Palaeoclimatology and Palaeoecology* 159, 145–165.
- Marensi, S.A., Tripaldi, A., Limarino, C.O., Caselli, A.T., 2005. Facies and architecture of a Carboniferous grounding-line system from the Guandacol Formation, Paganzo Basin, northwestern Argentina. *Gondwana Research* 8 (2), 187–202.
- Mattern F., 2005. Ancient sand-rich fans: depositional systems, models, identification, and analysis. *Earth Science Reviews* 70, 167-202.
- Miall, A.D., 1977. A review of the braided river depositional environment. *Earth Science Reviews*, 13(4), p. 1-62.
- Milana J.P. & Kneller B, 2011; “A Field Guide For Glacial and Post-Glacial Carboniferous Deposits (Paganzo And Calingasta Basins) Of Western Argentina”. (Inédito)
- Milani, E.J. & Zalán, P.V., 1999. An outline of the geology and petroleum systems of the Paleozoic interior basins of South America. *Episodes*, 22:199-205.
- Nelson, C.H., 1983. Modern submarine fans and debris aprons: an update of the first half century. In: Boardman, S.J. (Ed.), *Revolution in the Earth Sciences*. Kendall/Hunt, Dubuque, Iowa, pp. 148–165.

- Net, L.I., Alonso, M.S., Limarino, C.O., 2002. Source rock and environmental control on clay mineral associations, lower section of Paganzo group (Carboniferous), northwest Argentina. *Sedimentary Geology* 152, 183–199.
- Net L.I., Limarino C.O., 2006. Applying sandstone petrofacies to unravel the Upper Carboniferous evolution of the Paganzo Basin, northwest Argentina. *Journal of South American Earth Sciences* 22, 239–254.
- Oliveira, G. P., 1927. Geologia de recursos minerais do Estado do Paraná. Rio de Janeiro, SGM. (SGM, Monografia,6).
- Paim G. P. S., D'Avila S. R. F., Santos da Silveira A., Bidónia R., Missiagia J., Faccion J. E., Santos S. F., 2004. Estudo de depósitos turbidíticos da Bacia de Paraná/Grupo Itararé e sua comparação com os turbiditos da Bacia do Itajaí (ITA-ITA). Informe interno. Universidade do Vale do Rio dos Sinos.
- Pazos P.J., 2002a, Palaeoenvironmental framework of the glacial-postglacial transition (late Paleozoic) in the Paganzo-Calingasta Basin (southern South America) and the Great Karoo–Kalahari Basin (southern Africa): Ichnological implications: *Gondwana Research*, v. 5, p. 619–640.
- Pérez Loinaze V.S., Limarino C.O., Césari S.N., 2010. Glacial events in Carboniferous sequences from Paganzo and Río Blanco Basins (Northwest Argentina): palynology and depositional setting. *Geologica Acta* 8, 399–418.
- Ramos V.A., 1988. The tectonics of central Andes; 30°-33° S latitude, in Clark, S., and Burchfiel, D., eds., *Processes in continental lithosphere deformation*, Volume 218: GSA Special Paper, GSA, p. 31-54.
- Reading H. G., 1996. *Sedimentary Environments: process, facies and stratigraphy*. Department of Earth Sciences, university of Oxford, 432-435 p.
- Reading H.G., Richards, M., 1994. Turbidite systems in deep-water basin margins classified by grain size and feeder system. *Am. Assoc. Pet. Geol. Bull.* 78, 792– 822.

- Richards M. & Bowman M., 1998. Submarine fans and related depositional systems II: variability in reservoir architecture and wireline log character. *Marine and Petroleum Geology* 15, 821-839.
- Rocha-Campos A.C., dos Santos P.R., Canuto J.R., 2008. Late Paleozoic glacial deposits of Brazil: Paraná Basin. In: Fielding, C.R., Frank, T.D., Isbell, J.L. (Eds.), *Resolving the Late Paleozoic Ice Age in Time and Space: Geological Society of America Special Paper*, 441, pp. 97-114.
- Salfity J.A., Gorustovich S.A., 1983. Paleogeografía de la cuenca del Grupo Paganzo (Paleozoico Superior). *Revista de la Asociación Geológica Argentina* 38, 437-453.
- Schneider R.L., Muhlmann H., Tommasi E., Medeiros R.A., Daemon R.A. & Nogueira A.A. 1974. Revisão estratiográfica da Bacia do Paraná. In: SBG, 28 Congresso Brasileiro de Geologia, Porto Alegre, 1: 41-65.
- Schwalbach, J.R., Edwards, B.E., Gorsline, D.S., 1996. Contemporary channel-levee systems in active borderland basin plains, California Continental Borderland. *Sediment. Geol.* 104, 53-72.
- Sempere T., 1996. Phanerozoic evolution of Bolivia and adjacent regions. In: Tankard, A.J., Suárez, S.R., Welsink, H.J. (Eds.), *Petroleum Basins of South America: American Association of Petroleum Geologists Memoir*, 62, pp. 231-249.
- Valdez B.V., 2011. Arquitectura estratiográfica de los megadepósitos de transporte en masa de la Formación Guandacol, Sierra de Maz, Provincia de la rioja. Trabajo Final de Licenciatura. UNSJ.
- Valdez B.V., Paim G.P. S., Souza P.A., di Pascuo M., 2013. Carboniferous deglacial record in Paraná Basin (Brazil) and its analog in paganzo Basin (Argentina): A comparison Between pennsylvanian and permian sections. 6th Latinamerican Congress of Sedimentology. São Paulo- Brazil.

- Valdez B. V., 2013. Intra-Paganzo and Paganzo-Paraná regional correlation. MsC Dissertation. Universidade do Vale do Rio dos Sinos.
- Vesely F.F. & Assine, M.L. 2006. Deglaciation sequences in the Permo- Carboniferous Itararé Group, Paraná Basin, southern Brazil. *Journal of South American*
- Visser J.N.J., 1997a. b. A review of the Permo-Carboniferous glaciation in Africa. In: Martini, I.P. (Ed.), *Late Glacial and Postglacial Environmental Changes: Quaternary, Carboniferous– Permian, and Proterozoic*. Oxford University Press, Oxford, U.K., pp. 169–191.
- Visser J.N.J., 1997b. Deglaciation sequences in the Permo-Carboniferous Karoo and Kalahari basins of southern Africa: a tool in the analysis of cyclic glaciomarine basin fills. *Sedimentology* 44, 507–521.
- Walker R.G., 1978. Deep-water sandstone facies and ancient submarine fans: models for exploration for stratigraphic traps. *Am. Assoc. Pet. Geol. Bull.* 62, 932– 966.
- Weinschütz L.C.& Castro J.C., 2004. Arcabouço cronoestratigráfico da Formação Mafra (intervalo médio) na região de Rio Negro/PR- Mafra/SC, borda leste da Bacia do Paraná. *Revista Escola de Minas, Ouro Petro*, 54(3): 151-156.
- Whelan Thomas III, Coleman J.M., Suhayda J.N., Garrison L.E., 1975. The geochemistry of Recent Mississippi River delta sediments: Gas concentration and sediment stability. 7th Offshore Technology Conference, Houston, Texas, p. 71-84.
- Zapata T.R. & Allmendinger R.W. (1996) Growth stratal records of instantaneous and progressive limb rotation in the Precordillera thrust belt and Bermejo basin, Argentina. *Tectonics*, 15, 1065–1083.

ATTACH 1

ATTACH 2